8-3-2022 7:00 AM

Feasibility and Clinical Value of 3-Dimensional Myocardial Deformation Analysis by Computed Tomography in Transcatheter Aortic Valve Replacement Patients

Mohamad Rabbani, *The University of Western Ontario*

Supervisor: Dr. Michael W.A. Chu, *The University of Western Ontario*

A thesis submitted in partial fulfillment of the requirements for the Master of Science degree in Surgery

Abstract

Purpose: Multi-phase computed tomography angiography (CTA) for the pre-procedural planning of TAVR presents a unique opportunity to assess 3D myocardial biomechanics. This study aimed to assess the feasibility and predictive utility of 3D myocardial deformation analysis (3D-MDA) based principal strain to predict heart failure or death following TAVR using pre-procedural, multi-phase computed tomography angiography (CTA) datasets.

Methods: Two hundred and five patients undergoing pre-TAVR multi-phase gated CTA followed by successful TAVR were retrospectively identified. Whole heart 3D mesh chamber models were generated followed by 3D-MDA of the left ventricle (LV) to determine global LV minimum principal strain (minPS) for endocardial, epicardial and transmural layers.

Results: Of the 205 patients, 196 (96%) had analyzable CTA data for 3D-MDA [median (IQR) age of 85 (79.5−88) years (55% male); STS-PROM score: 3.10 (2.10−4.55); and echocardiographic LVEF 60.0 (55.9−65.0)%]. At a median 25 (11–36) months following TAVR, 55 patients (28%) experienced a composite clinical outcome of heart failure hospitalization or death. Patients with a global minPS below a −23.7% experienced a 3-fold higher rate of the primary outcome ($p<0.001$). This remained significant following adjustment for all baseline clinical and echocardiographic characteristics, with endocardial layer minPS providing highest prognostic value (C-index: 0.76) with a HR of 1.09 ($p<0.001$) for each 1% change.

Conclusions: CT derived 3D-MDA is feasible and delivers novel deformation markers strongly and independently predictive of future cardiovascular outcomes in patients undergoing TAVR.

KEYWORDS

Three Dimensional; Principal Strain; Left Ventricle, Computed Tomography; Mesh Models

Summary for Lay Audience

Transcatheter aortic valve replacement (TAVR) represents one of the most impactful technical advancements for patients with aortic valve disease. As a minimally invasive therapeutic alternative to open heart surgery, this technique has established an important role in the management of severe aortic stenosis: being initially reserved only for high-risk elderly patients unable to undergo surgical care, and now expanding to meet the needs of broader referral populations. This procedure inherently developed early dependency on advanced imaging for pre-procedural planning and intra-procedural guidance given need to select delivery paths, feasibility and to place valve devices without direct visualization.

This as a result has led to the ubiquitous use of multi-phase, ECG-gated computed tomography for pre-procedural evaluation in these patients. To date this imaging data has been used to confirm procedural eligibility and determine optimal deployment strategies (sizing and position) for the valve device. Despite this, tremendous value from these imaging datasets is currently disregarded. Our team is researching if images routinely obtained from CT scans prior to TAVR can be used to construct 3D "beating heart" models that predict benefit from this procedure. Specifically, our aim is to predict from these images how much undergoing a TAVR procedure will reduce the chances that patients experience future hospitalization or death.

In the second part of this research study, we are asking twenty patients referred for TAVR if they would agree to undergo an additional imaging test called a cardiac MRI (magnetic resonance imaging). This non-invasive test can assess the heart muscle's health by measuring how much scarring or "fibrosis" is present, an important influence on how the heart will function following TAVR. By measuring this we can better understand how information from the CT scan is allowing

artificial intelligence to predict future risk of heart failure and death, an important part of building trust in this technology.

Co-Authorship Statement

Chapter 1 and 2: The introduction and literature review in the present document were designed and written by Dr. Mohamad Rabbani and reviewed by Dr. James White and Dr. Michael Chu.

Chapter 3:
Study Design: Dr. Mohamad Rabbani, Dr. James White, Dr. Michael Chu
Data Collection: Dr. Mohamad Rabbani
Data analysis: Dr. Mohamad Rabbani, Dr. James White, Dr. Michael Chu
Statistical analysis was carried in collaboration with Zhiying Liang.
The 3D Myocardial Deformation Software (3D-MDA) was developed by Dr. Alessandro Satariano.
Manuscript preparation: Dr. Mohamad Rabbani
Manuscript Review: Dr. James White and Dr. Michael Chu

Chapter 4:
Project Design: Dr. Mohamad Rabbani, Dr. James White, Dr. Michael Chu
Patient Referral: Dr. Anna Bizios
Patient Recruitment: Dr. Mohamad Rabbani
Data Collection: Dr. Mohamad Rabbani
Ethics Communications: Dr. Mohamad Rabbani, Dr. James White, Dr. Michael Chu

Table of Contents

Abstract ---- *ii*

Summary for Lay Audience ---- *iv*

Co-Authorship Statement ---- *vi*

Acknowledgment ---- *x*

List of Tables by Chapter ---- *xi*

List of Figures by Chapter ---- *xii*

Abbreviations ---- *xiii*

Chapter 1: Introduction ---- *1*

1.1 Natural History and Pathophysiology of Aortic Stenosis ---- 1

1.2 Treatment options for Aortic Stenosis ---- 3

1.2.1 Indication for Aortic Valve Replacement ---- 3

1.2.2 Suitability for SAVR vs. TAVR Explained ---- 4

1.3 The TAVR Procedure ---- 5

1.3.1 History of TAVR ---- 5

1.3.2 Access Route, Approach and Techniques Used ---- 8

a) Transfemoral Access ---- 8

b) Transapical Access ---- 10

c) Subclavian/axillary Access ---- 11

d) Direct Aortic Route ---- 11

1.4 Reliance of TAVR on Multi-modality Imaging ---- 12

1.4.1 Pre-procedural Anatomical Assessment of TAVR Patients Using CT Imaging ---- 13

a) Annular sizing ---- 14

b) Coronary Ostia and the Hinge Point ---- 15

c) Vascular Tree ---- 16

d) Projection Angle ---- 17

1.5 General Principles of Strain ---- 19

1.6 References ---- 20

Chapter 2 - Literature Review: The Prognostic Value of Multimodality Derived Left Ventricular Myocardial Strain in Transcatheter Aortic Valve Replacement ---- *24*

2.1 INTRODUCTION ---- 24

2.2 PROGNOSTIC VALUE OF ECHOCARDIOGRAPHY DERIVED LV STRAIN ---- 26

2.3 PROGNOSTIC VALUE OF COMPUTED TOMOGRAPHY DERIVED LV STRAIN - 32

2.4 PROGNOSTIC VALUE OF MAGNETIC RESONANCE IMAGING DERIVED LV STRAIN ---- 36

2.5 CONCLUSION ---- 40

2.6 REFERENCE ---- 41

Chapter 3: Feasibility and Clinical Value of 3-Dimensional Myocardial Deformation Analysis by Computed Tomography in Transcatheter Aortic Valve Replacement Patients ---------- *45*

3.1 INTRODUCTION ---------- **45**
3.1.1 Research Questions ---------- 47

3.2 METHODS ---------- **48**
3.2.1 Study Population ---------- 48
Inclusion criteria ---------- 48
Exclusion criteria ---------- 49
3.2.2 Ethics Approval ---------- 49
3.2.3 Clinical Characteristics ---------- 50
3.2.4 Outcomes ---------- 51
3.2.5 Echocardiography Imaging Acquisition ---------- 51
3.2.6 Computed Tomography Imaging Acquisition ---------- 52
3.2.7 Multi-chamber CT Whole Heart Segmentation and Meshing ---------- 53
3.2.8 3D Myocardial Deformation Analysis (3D-MDA) ---------- 56

3.3 STATISTICAL ANALYSIS ---------- **57**

3.4 RESULTS ---------- **58**
3.4.1 Baseline Clinical and Non-CTA Imaging Characteristics ---------- 58
3.4.2 Intra-observer and Inter-observer Variability ---------- 62
3.4.3 Primary Composite Clinical Outcome ---------- 62
3.4.4 CT 3D-MDA and Associations with the Composite Clinical Outcome ---------- 63
3.4.5 Survival Free of Composite Outcome Based on Principal Strain Threshold ---------- 66

3.5 DISCUSSION ---------- **68**
3.5.1 Three-dimensional Myocardial Deformation Analysis Highly Feasible in TAVR ---------- 68
3.5.2 Left Ventricle Minimum Principal Strain is Highly Predictive of Clinical Outcomes ---------- 69
3.5.3 Prognostic Value of 3D Left Ventricle Principal Strain ---------- 70
3.5.4 Transition to Using Novel CT Derived 3D Axis Independent Markers of Tissue Deformation - 71
3.5.5 Left Atrial Contribution to Clinical Outcomes ---------- 72
3.5.6 Clinical Implications ---------- 72

3.6 LIMITATIONS ---------- **73**

3.7 CONCLUSITONS ---------- **74**

3.8 REFERENCE ---------- **77**

Chapter 4: Proposal for Validation study ---------- *82*

4.1 INTRODUCTION ---------- **82**

4.2 STUDY OBJECTIVES ---------- **83**
- **Primary objectives** ---------- 83
- **Secondary objectives** ---------- 83

4.3 METHODS ---------- **83**
4.3.1 Study Population ---------- 85
- **Inclusion Criteria:** ---------- 85
- **Exclusion Criteria** ---------- 85

4.3.2 Study Subject Recruitment ---------- 86
4.3.3 Imaging Protocols ---------- 86
- **Echocardiography 3D-STE Protocol** ---------- 86
- **Cardiac MRI Protocol** ---------- 87

4.4 PLANNED ANALYSIS ---- **87**
4.4.1 Cardiac MRI Analysis ---- 87
4.4.2 3D-MDA ---- 88
4.4.3 4D Flow Analysis ---- 88
4.4.4 Tissue Mapping Analysis ---- 89
4.4.5 Sample Size ---- 90
4.5 STATISTICAL ANALYSIS ---- **90**
4.6 EXPECTED RESULTS AND SIGNIFICANCE ---- **90**
4.7 REFERENCES ---- **92**
Chapter 5: Future Prospective from a Cardiac Surgery Point of View ---- ***93***
Appendix ---- ***96***
Curriculum Vitae ---- ***99***

Acknowledgment

I would like to first and foremost acknowledge the support and guidance of Dr. James White and Dr. Michael Chu for their supervision and their feedback in the conduct of this project.

I would like to thank Dr. Mathew Valdis and Dr. Pentelis Diamantouros for sitting on the supervisory committee and giving valuable recommendations throughout. I would like to thank our cardiac surgery program director, Dr. ML Myers, for her support and commitment to provide the best learning environment.

I would like to thank Dr. Michael Bristow, Dr. Carmen Lydell, and Dr. Bizios for their incredible support and teaching. I would like to thank Dr. Alessandro Satriano for his incredible commitment.

This project would not have been possible without the help of our incredible research team, Jacqueline Flewitt, Sandra Rivest, and Carrie Smart and I would like to thank them for their contribution.

Last and not least, I would like to recognize the indefinite support of my family.

List of Tables by Chapter

Chapter 1: None

Chapter 2:

- **Table 1**: Predictive value of LV longitudinal strain in Echocardiography
- **Table 2**: Predictive value of LV longitudinal strain in Computed Tomography
- **Table 3**: Predictive value of LV longitudinal strain in Magnetic Resonance Imaging

Chapter 3:

- **Table 1:** Demographic and baseline characteristics of all TAVR patients, patients with and patients without occurrence of composite outcome.
- **Table 2:** Baseline and post procedural Echocardiography and multiphase CTA derived 3-Dimensional Myocardial Deformation (3D-MDA) values of all TAVR patients, patients with and patients without occurrence of composite outcome.
- **Table 3:** Cox regression analysis for a composite outcome of all-cause mortality or heart failure hospitalization
- **Table 4:** Prognostic value of 3D CT- derived minimum principal strain
- **Table 5:** Intra-observer repeatability and inter-observer reliability among

Chapter 4: None

Chapter 5: None

List of Figures by Chapter

Chapter 1

- **Figure 1:** A) Aortic annular plane marked by the dashed lines. B) Post-implantation CT of the same patient showing the circular deployment of the prosthesis.
- **Figure 2:** A) Measurement of the distance between the coronary ostia and the aortic annulus plane. B) Severely calcified left coronary cusp with close relationship between annular plane and ostium of the left main coronary artery (red arrow).
- **Figure 3:** A) Multiplanar reconstruction showing minimal calcification of the peripheral vessels. B) a 3D reconstruction of the same patient showing severe kinking of the ileo-femoral access.

Chapter 2:

- **Figure 1.** Representative Cases of 3D Speckle-Tracking Analysis

Chapter 3:

- **Figure 1:** Study flow chart.
- **Figure 2:** Methodology explained – from multiphase CTA image to whole heart mesh generation
- **Figure 3:** Contour modification of the endocardial layer
- **Figure 4:** Relative hazard of death or heart failure hospitalization by baseline 3D CT endocardial minPS.
- **Figure 4:** Survival curve based on endocardial minPS threshold
- **Supplementary figure 1:** Relative hazard of death or heart failure hospitalization by baseline 3D CT minPS (epicardial and transmural)
- **Supplementary figure 2:** Survival curve based on epicardial and transmural minPS thresholds

Abbreviations

AS: Aortic Stenosis

TAVR: Transcatheter Aortic Valve Replacement

SAVR: Surgical Aortic Valve Replacement

CTA: Computed Tomography Angiography

EuroSCORE: European System for Cardiac Operative Risk Evaluation

STS-PROM: Society of Thoracic Surgeons Predicted Risk of Mortality

NYHA: New York Heart Association

CCS: Canadian Cardiovascular Society

LV EF: Left Ventricle Ejection Fraction

3D MDA: Three-dimensional Myocardial Deformation Analysis

2D: Two-Dimensional

minPS: Minimum Principal Strain

GLS: Global Longitudinal Strain

ICD-10: International Classification of Disease-10

AHA: American Heart Association

ESC: European Society of Cardiology

HFpEF: Heart Failure with preserved Ejection Fraction

Chapter 1: Introduction

The purpose of this thesis is to assess the feasibility and predictive utility of 3D myocardial deformation analysis (3D-MDA) to deliver principal strain (PS) based markers of left ventricular (LV) health for the prediction of time to heart failure hospitalization or death following TAVR. However, before delving into our topic, a solid foundation about the history of aortic stenosis, treatment options and reliance of cardiac surgery on medical imaging needs to be addressed. This chapter focuses on providing the foundational knowledge to which this thesis will build on.

1.1 Natural History and Pathophysiology of Aortic Stenosis

Aortic stenosis (AS) is the most common valvular heart disease globally[1]. With a reported prevalence of 0.2% among adults aged 50–59 years, this increases to approximately 10% in adults 80 years of age or older[2]. Importantly, it is therefore associated with significant comorbidities in more than one-third of the cases[3]. Aortic stenosis in a population aged 70 years and older is usually associated with age-related calcification. However, in younger populations, congenital bicuspid aortic valve, and disorders of calcium metabolism, such as renal failure are the primary causes[4].

Its pathology seems to be mediated by an inflammatory process, similar to that of atherosclerosis, including accumulation, inflammation, and calcification[5]. The progression of deposits and valvular thickening results in the obstruction of the LV outflow tract. Initially, the LV remodels and hypertrophies to overcome this. Increased chamber filling pressures and reduced cardiac output leads to dyspnea, which is the most common symptom of aortic stenosis.

Angina is common in severe disease and may occur because of increased LV mass, poor coronary filling and reduced coronary flow reserve[6]. At times of increased demand such as exercise, pre-syncope and syncope may occur due to the fixed cardiac output and vasodilation or arrythmia. Unsurprisingly, the risk of suffering a cardiac death increases with the severity of the disease. Over time, the myocardium becomes less compliant. Impaired systolic function alone or in combination with impairment of relaxation (diastolic dysfunction), may lead to clinical heart failure. Similar symptoms may occur if the atrial kick is lost and diastolic filling shortens, such as in atrial fibrillation with rapid ventricular response.

Heart failure is a serious co-morbidity and a leading cause of hospitalization in people older than 65 with the average annual mortality rate of 33% in Canada[7]. The increase in prevalence of heart failure is partly due to the improved medical therapies post cardiac arrest and other cardiac conditions allowing patients to survive longer. It is vital to understand the significant economic burden that heart failure places on Canadians with an estimated annual healthcare cost to be $1.18 billion, and $108 billion per year worldwide[8].

Without intervention, the prognosis of patients with symptomatic severe aortic stenosis is poor. The onset of symptom carries a rapid decline and mortality in patients with heart failure symptoms is around 50% in the first year[9]. Patients with other symptoms do slightly better, with 50% survival up to 3 years once syncope occurs and up to 5 years following presentation with angina[10]. The presence or absence of symptoms, severity of aortic valve obstruction, and LV response to pressure overload are the primary drivers for clinical decision making in patients with aortic stenosis. Classic symptoms of aortic stenosis accompanied by echocardiographic

findings consistent with severe stenosis should prompt a cardiology consultation to consider treatment options.

1.2 Treatment options for Aortic Stenosis

1.2.1 Indication for Aortic Valve Replacement

It is essential to take proper history and risk stratify patients in clinic. Although the outcomes in asymptomatic patients with aortic stenosis are similar to those in age matched control patients, survival is extremely poor once even subtle symptoms are present in patients who did not undergo surgical treatment[11-13].

Aortic valve replacement (AVR) is the only effective treatment for symptomatic, hemodynamic severe aortic stenosis. Surgical replacement (SAVR) leads to significant improvement in survival and symptoms[13-15]. In the United Stated, the 10 year survival rate in Medicare-aged patients after aortic valve replacement is almost identical to that in age- and sex-matched individuals who do not have aortic stenosis[16].

There are multiple scenarios in which a cardiology referral is appropriate. The first is a symptomatic patient who is found to have moderate stenosis because in those patients further assessments may lead to the identification of low-flow, low gradient severe aortic stenosis despite having a normal EF (due to a small stoke volume in a patient with a small ventricular cavity). Alternatively, if the EF is less that 50%, then a dobutamine stress echocardiography is warranted and may reveal severe aortic stenosis. The second scenario where a cardiology consult is prompted is when a patient is asymptomatic with severe stenosis accompanied with LV systolic dysfunction (EF less than 50%). When severe aortic stenosis is found to be the primary

pathology in this setting, aortic valve replacement is lifesaving and should not be delayed as it improves LV function[17]. The third scenario is a patient who is asymptomatic with severe or even moderate stenosis who is undergoing cardiac surgery for another indication. In this case, aortic valve replacement is indicated to avoid repeat surgery once the valve disease inevitably progresses.

1.2.2 Suitability for SAVR vs. TAVR Explained

The European Society of Cardiology recommends that transcatheter aortic valve replacement (TAVR) be offered to patients who are unsuitable for conventional surgery on the bases of comorbidities rather than age[18]. This recommendation was based on the realization that even elderly patients surprisingly do well following surgical aortic valve replacement (SAVR) with a survival in one population of patients older than 80 years at 89% and 69% after 1 and 5 years respectively[19].

There are many factors that contribute to poorer outcomes in aortic valve surgery and those include moderate to severe heart failure (New York Heart Association Stage III or IV), concomitant coronary artery disease, and pre-operative atrial fibrillation. It has been reported that 30% to 50% of the patients with severe aortic stenosis (AS) are not offered surgery, primarily because of the perception that the risk of surgical aortic valve replacement (SAVR), due to age and/or other comorbidities, is high relative to the potential benefit [20-22]. Such patients have been labeled as “high risk” or “inoperable” with respect to their suitability for surgery. The availability of TAVR affords a new treatment option for patients previously not felt to be optimal candidates for surgical valve replacement and allows for the opportunity to re-examine the methods for assessing operative risk in the context of more than one available treatment.

Surgical aortic valve replacement is the standard of care in patients with low or intermediate surgical risk[23]. Overall, 30-day surgical mortality for isolated valve replacement is 3% and approximately 4.5% for valve replacement with coronary artery bypass grafting. TAVR brings another treatment option for patients who have indications for valve replacement but are high risk patients. There is a spectrum of operative risk at play when deciding between the two treatment options. A multidisciplinary team composed at minimum of a clinical cardiologist and a cardiac surgeon, and usually including subspecialists in interventional cardiology, cardiovascular imaging, anesthesiology, and heart failure management must be involved in determining the best treatment course. At the far end of the risk spectrum, are those patients who are in-operatable and denied surgery on the basis of clinical, anatomical, and/or technical parameters. There is a likely probability that they are unlikely to survive operation and if they do survive surgery they will be left with irreversible morbidity. Those patients are often referred to undergo TAVR.

1.3 The TAVR Procedure

1.3.1 History of TAVR

The concept of permanent "stent valve" has been around for a quarter of a century with preliminary animal studies and temporary palliative devices being developed as early as the 1960s and 1970s[24]. In 2002, Cribier *et. al.* demonstrated for the first time the feasibility of a percutaneous valve implantation in a patient with aortic stenosis, providing a promising less invasive alternative treatment for valvular heart disease[25]. Since then, a great effort has been made to address the limitations of TAVR technology and broaden its use. New valve technology has been developed and TAVR deployment devices have reduced the risk of complications,

simplified the procedure, and allowed for the treatment of complex anomalies. This was also backed up with registries and randomized control trials which provided a robust database on which clinicians and surgeons alike can rely on in their decision making.

It was a decade into experimentation before the first human received a TAVR in 2002. Since then, the rate of TAVR has risen enormously. In 2019 TAVR exceeded all forms of surgical aortic valve replacement (SAVR) for the first time. It all started in 1965, when Davies *et. al.* described a catheter mounted cone shaped valve that has a parachute configuration which allowed blood to flow towards the peripheral circulation and prevented aortic regurgitation[24]. The device at the time was designed to treat aortic regurgitation, where it is inserted in the ascending aorta through the carotids and its feasibility tested in animals. Two other prototypes a few years later were introduced by Moulopoulos *et. al.* and they relied on a catheter mounted valve design similar to what is use today, but indicated to treat AR[26]. It was inflated during diastole to prevent AR, and deflated during systole to allow forward flow. The limitation of those prototypes, however, was the risk of balloon rupture and the need for an external system to regulate the inflation and deflation of the balloon.

This paved the way for a third catheter mounted valve which had a more promising clinical application as it relied on an umbrella shaped design that was able to passively close during systole allowing blood to flow freely during the systolic phase. Following this concept, Matsubara *et. al.* designed another prototype that consisted of a balloon catheter which utilizes 2 latex check valves that prevented the backflow of blood during diastole[27].

Anderson *et. al.* was the first to develop an artificial valve that is suitable for percutaneous implantation. The system used consisted of a porcine valve that was mounted on a stainless steel

frame constructed of 2 wires[28]. The device was compressed and then mounted into a deflated 3 foiled balloon catheter (diameter, 41F). This device was then tested in vivo on 7 pig models, where a laparotomy was made and the abdominal aorta was revealed and used as the route. Two pigs had obstructed coronaries, and the rest exhibited excellent hemodynamic gradients across the valve. However, despite the promise, the large size of the introducing device did not help in its clinical implementation.

This required the introduction of a different design by Bonhoeffer *et. al.* that relied on a vein valve which was sutured to a platinum/iridium stent[29]. This was tested in a sheep model, and the device successfully was used in humans with pulmonary stenosis. However, the design couldn't be used in the treatment of AS because of the fragile venous valve that couldn't withstand high pressures. A different design was introduced by Cribier *et. al.* that consisted of 3 polyurethane and later of 3 bovine pericardial leaflets which were mounted into a tubular slotted stainless steel balloon expandable stent[30]. This was tested in a sheep model through a 24F sheath, and long-term performance was tested in vitro in a pulse duplicator models.

Around the same time, Paniague *et. al.* was designing a valve that consisted of porcine pericardial leaflets and had a small diameter (11F-16F) allowing its percutaneous implantation through the antegrade approach[31]. The device was tested in 15 animals and the histological examination at 3, 6, and 9 months showed good acceptance with endothelization and no inflammation.

Finally, on April 16, 2002, the first TAVR procedure was performed by Caribier *et. al.*[25] and it had opened a new landscape in the treatment of aortic valve stenosis. The first patient was a 57-year-old inoperable patient with severe symptomatic AS who had an initial unsuccessful balloon

aortic valvuloplasty and deteriorated. In view of his life-threatening condition, the TAVR procedure was offered through the antegrade approach. Patient status improved considerably and was able to return to activity within few hours after TAVR. The device has shown good durability at the first 9 weeks of follow up. The patient died at 4 months because of non-cardiac or procedure related causes.

1.3.2 Access Route, Approach and Techniques Used

TAVR has offered a less invasive approach and an alternative treatment for symptomatic severe aortic stenosis. Depending on the institution, the procedure is being performed in a standard catheterization laboratory, an operating theatre, or a dedicated hybrid room. The same rules for an open approach apply. The field must be sterile to avoid complication of wound infection and endocarditis. The cardiopulmonary bypass assist device and surgical instruments are all ready for immediate access in case an open approach becomes required. Most environments today rely on hybrid rooms as it is the ideal setting for the TAVR procedure. The room is equipped with high resolution imaging and user interface, which is friendly with enough space to maneuver during the procedure. There are four main access routes used each with certain variability in surgical technique:

a) Transfemoral Access

In up to 80% of cases today, the retrograde transfemoral access route is the least invasive and most frequently used. Initially, due to the large size of the sheath (up to 24Fr) the procedure was performed through a surgical cut-down on the femoral artery. Technology has improved since then and the sheath size profiles are much smaller which allows for a purely percutaneous access via the common femoral artery. This was also coupled with the help of percutaneous closure

devices that have pushed the transfemoral TAVR to become the default access route in many centres irrespective of the device used.

There are many complications that may occur and therefore a systematic step-by-step approach must be followed to minimize the risks. The first step is to identify the puncture side, which is above the femoral bifurcation in a segment without or only little calcification. Then, the femoral artery in punctured under fluoroscopic or ultrasound guidance and a wire is introduced retrogradely into the femoral artery. A skin incision of 1cm is made beside the wire exit point and bluntly dissection of the subcutaneous tissue performed with a surgical clamp. The femoral artery is predilated in order to accommodate a PerClose suture device. After placing the PerClose suture, a 9-10 Fr sheath is re-inserted over the guidewire to minimize bleeding. The standard guidewire is then exchanged to a stiff wire through a pigtail catheter to minimize injury keeping in mind that the wire of choice may change depending on many factors such as tortuosity, calcification, and type of prothesis. This is followed with inserting the valve delivery sheath which is done under fluoroscopic control with careful attention to any resistance. A weight adjusted (70-100 IU/Kg) intravenous bolus of unfractionated heparin is then administered. The native aortic valve is retrogradely crossed with a straight tip, hydrophilic wire through a JR4 or AL1 catheter. The valve is then crossed with the catheter and exchanged for a pigtail catheter over a long J tipped exchange wire. The catheter is then replaced by a stiff wire, with the tip pre-shaped into a pigtail curve.

During that time, the transcatheter aortic valve prothesis is being prepared, which should be finished before pre-dilatation of the stenosed valve if this to be performed. The pacemaker is inserted via the jugular vein or femoral vein and positioned in the right ventricle. Rapid

ventricular pacing at 160 – 200 bpm is performed and the aortic valvuloplasty balloon is inflated with careful attention to avoid dislodgment in to the left ventricle cavity or ascending aorta to avoid perforation or aortic dissection. The transcatheter aortic valve is brought through the sheath, across the aortic arch into the aortic annulus on the delivery system and is deployed with or without additional rapid pacing, depending on prosthetic valve system. After successful deployment of the prosthesis, the delivery catheter is withdrawn, and a hemodynamic assessment is performed with the help of echocardiography. Once happy with the results, the vascular access sheath are removed and the PerClose sutures are tightened.

b) Transapical Access

The transapical approach provides antegrade access to the aortic valve via a left antero-lateral wall, without the need for peripheral circulation access. This approach requires orotracheal intubation with general anesthesia and is more invasive, therefore it is mainly performed in patients with severe peripheral arterial disease.

The first step is to localize the ventricular apex by echocardiography, fluoroscopy and pre-operative CT planning which will guide the location of the anterolateral mini-thoracotomy at the fifth or sixth intercostal space with a small incision in the sub-mammary fold. Any adhesions are released from the pericardium and a pericardiotomy is performed. Temporary epicardial pacemaker electrodes are sutured in place. The puncture site on the LV is identified and two circular purse-string sutures are places at the anterolateral wall. A guidewire is advanced antegrade across the degenerated aortic valve, with paying close attention to the chordae of the mitral valve. Subsequently, a long stiff wire is placed into the catheter to provide appropriate support for the delivery sheath and prosthesis positioning. The delivery sheath (21-26 Fr) is

gently advanced over the wire through the myocardium and placed just below the native aortic valve. After this step is done, the same concepts of the transfemoral approach are applied.

c) Subclavian/axillary Access

The third route is the subclavian access, which is an alternative to patients with severe peripheral artery disease. Usually, the left subclavian or axillary artery is preferred over the corresponding right side due to anatomical consideration. The subclavian artery needs to be assessed for diameter, tortuosity, and calcification. In patients who had a previous coronary artery bypass using the left internal mammary artery, one must consider that the intravascular delivery sheath may lead to obstruction and therefore ischemia during the procedure.

Once the subclavian artery is exposed, a direct puncture to the artery is performed or a vascular endograft with a side to end anastomosis is used to facilitate the insertion of the sheath. Percutaneous access to the left axillary artery is also feasible. Similar to the transfemoral approach, the delivery sheath is advanced over a stiff wire that has been place in the left ventricle. As soon as the delivery sheath is in place, the same approach for the transfemoral approach is followed. This procedure is usually performed with general anesthesia and follows a similar post operative course like in the trans-apical approach[32].

d) Direct Aortic Route

One final approach that is much less commonly used is the direct aortic route[33]. In the case of very diseased peripheral vessels combines with left ventricular anatomical consideration precluding a trans-apical approach, the direct aortic access might be the only route by direct exposure of the ascending aorta and introducing the transcatheter valve system. A small incision is made in the mid clavicular region or right parasternal region, the ascending aorta is exposed.

Two purse-string sutures are applied after identifying the correct angle of entry. After passing the stenotic aortic valve the same steps outlined in the transfemoral and subclavian access routes apply. The aorta is then closed under direct vision.

1.4 Reliance of TAVR on Multi-modality Imaging

Echocardiography remains the first imaging modality of choice when it comes to assessment of valvular function due to its high temporal and spatial resolution. However, acoustic windows are limited in evaluating the cardiovascular anatomy, particularly extra-cardiac structures which are of huge importance in planning minimally invasive cardiac surgery and endovascular interventions. Computed tomography (CT) is increasingly used in the evaluation of patients with valvular heart disease [34]. Given the endovascular nature of this technique, an inherent lack of exposure and visualization of the operative field poses challenges for deployment and therefore constructed a reliance on image guidance; both for the selection of patients and to deliver optimal procedural success. While echocardiography remains essential for the assessment of valve hemodynamics and ventricular function, multi-phase computerized tomography (CT) has emerged as a ubiquitously utilized non-invasive diagnostic tool in the pre-procedural assessment of TAVR candidates[35].

CT technology offers numerous post processing techniques, all of which have their usefulness in planning a TAVR procedure. Firstly, multi-planar reconstruction allows the data obtained from axial scans to be reconstructed in any desired plane, orthogonal or oblique relative to the body axis without a compromise in spatial resolution[36]. Secondly, volume-rendering allows the entire volume of the dataset to be used to create final 3D images. Specific structures can be interrogated and displayed, based on clinical need[37]. Thirdly, 4D rendering allows images to be

acquired in multiple cardiac phases using ECG-gated acquisitions and can be displayed as a cine loop. This allows for functional assessment of cardiac valves and chambers and a realistic simulation of the entire valvular apparatus prior to surgery. The next sections will outline the anatomical assessment of TAVR patients using CT imaging that is currently in clinical use today, followed by the functional assessment which thesis will focus and build on.

1.4.1 Pre-procedural Anatomical Assessment of TAVR Patients Using CT Imaging

At most institution, patients undergo both echocardiography and CT assessment prior to TAVR. Usually, the pre-operative CT image protocol includes a whole body prospectively ECG-triggered CT angiography covering the supra-aortic vessels as well as the peripheral vasculature up to the femoral artery. Optimal image quality for aortic root imaging is crucial for precise assessment of the aortic annulus. Therefore, imaging of the aortic root must be synchronized to the ECG either by retrospective ECG gating or through the use of prospective ECG triggering to avoid artefacts. In the rest of the aorta it is not necessary to image with ECG gating. For less advanced CT systems, non-gated acquisitions may be preferred to image the aorta and the iliac/femoral arteries as it allows for faster volume coverage and therefore less iodine contrast. Special resolution must be high especially for the aorta as the measurements and sizing of the valve will depend on accuracy. The image quality for the iliofemoral arteries should also be high as very detailed measurement are obtained to adequately plan the procedure.

There are multiple acquisition protocols that are available and used depending on the CT hardware at the site. Regardless of which protocol is used, the acquisition should allow for sub-millimetre slice reconstruction especially for the aortic root. Single source CT systems that have wide detectors or with dual source CT, it is possible to image the entire volume with an ECG-

synchronized approach. ECG triggered acquisition are advantageous as they allow for lower volumes of contrast to be used for imaging the aortic root as well as the peripheral access[38]. If the system has a limited detector width, then the area covering the heart and aortic root can be acquired ECG gated and the rest can be acquired with second non-gated acquisition. Computed Tomography is essential in the pre-procedural planning of TAVR patients today. The following section outlines the CT uses in TAVR.

a) Annular sizing

Aortic annulus assessment is essential and paramount for the success of TAVR. It relies entirely on pre and peri-procedural imaging. This is a remarkable difference compared to SAVR, where the surgeon has a direct visualization of the aortic annulus and can size the annulus using a probe[39]. The annulus is predominantly measured using transesophageal echocardiography (2 dimension or 3 dimensional), or multiplanar imaging. The disadvantage of the use of 2D is the complexity of the aortic annulus. It is often larger than it might appear in single plane imaging due to its oval shape[40]. Echocardiography underestimated the annular size in about half of all patients compared with both CT and intra-operative findings[41].

Cardiac magnetic resonance (CMR) imaging for the aortic valve is also very valuable as it permits simultaneous anatomical and functional assessment of the valve. The disadvantage in CMR is its poor delineation assessment of calcified tissue, and its accuracy in assessing TAVR is not well established[39]. Cardiac imaging has allowed the TAVR team to appreciate the accuracy at which the valve can be visualized and described anatomically in 3D space. Multiple reconstruction images are done through the outflow tract in order to be able to measure the annulus[42].

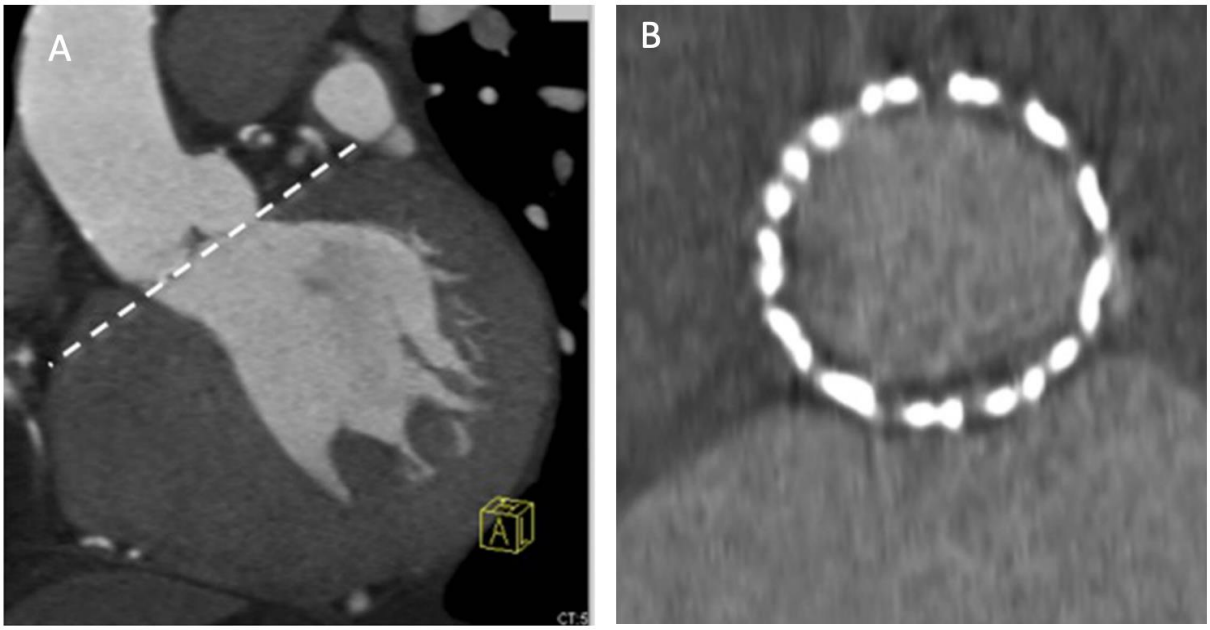

Figure 1: A) Aortic annular plane marked by the dashed lines. B) Post-implantation CT of the same patient showing the circular deployment of the prosthesis. (Reused with permission from Springer Nature publishing. Mohamed Marwan et al, Role of Cardiac CT Before Transcatheter Aortic Valve Implantation (TAVI). Curr Cardiol Rep. 2016 Feb;18(2):21. doi: 10.1007/s11886-015-0696-3)[43].

b) Coronary Ostia and the Hinge Point

It is essential to know the height of the coronary ostia from the aortic annulus as this may present further problems for surgeons, particularly if taller profile transcatheter prostheses are used. The procedure has to be planned carefully and ensuring that the coronaries are protected. Obstructing the coronaries with a prosthesis is a life-threatening complication. The calcified coronary cusps as they are pushed to the side must be considered as this might also cause coronary obstruction[44]. A distance of 14mm between the cusp hinge point and the coronary ostium has been recommended, and some TAVR operators go further than this measuring the cusp length and degree of calcification.

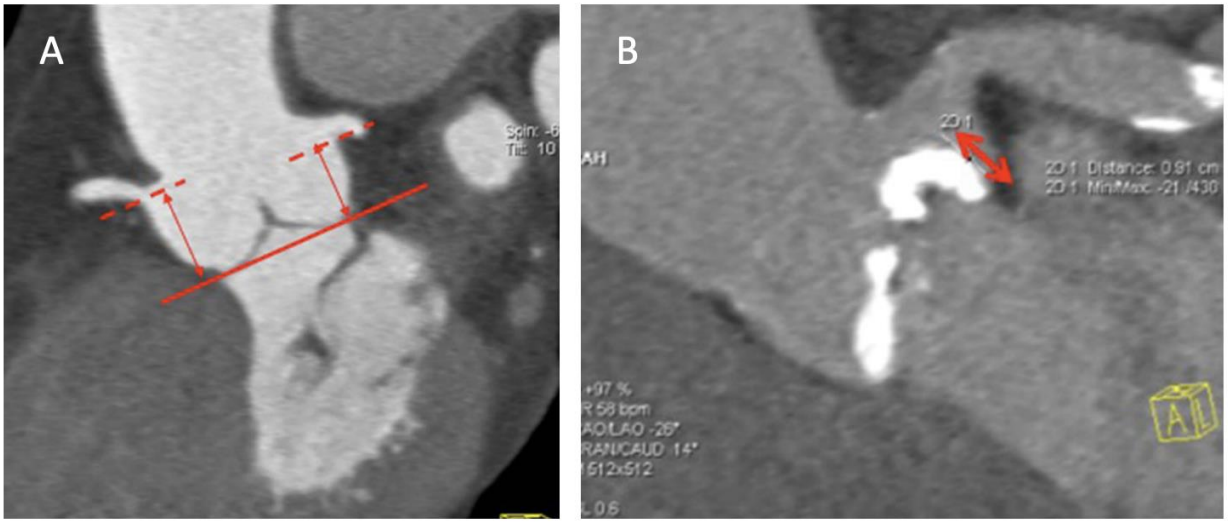

Figure 2: A) Measurement of the distance between the coronary ostia and the aortic annulus plane. B) Severely calcified left coronary cusp with close relationship between annular plane and ostium of the left main coronary artery (red arrow). (Reused with permission from Springer Nature publishing. Mohamed Marwan et al, Role of Cardiac CT Before Transcatheter Aortic Valve Implantation (TAVI). Curr Cardiol Rep. 2016 Feb;18(2):21. doi: 10.1007/s11886-015-0696-3)[43].

c) Vascular Tree

Detailed knowledge on the assessment of the peripheral vessels is a highly relevant aspect in planning of TAVR. In the old days, the vascular anatomy was assessed angiographically at the time of the coronary evaluation, today with the advent of multidetector CT (MDCT) imaging, every patient is evaluated in this way. The assessment is not just luminal anymore, but also assessment of tortuosity and calcification in made. It is important to know this information, as circumferential calcification has been implicated with an increased risk of vessel dissection and catheterization failure[45]. MDCT provides 3D volume rendered images that make it easy to visualize the anatomy and plan for the procedure. Finally, the entire anatomy of the aorta must be precisely evaluated to exclude relevant vascular disease and variation, such as dissection,

elongation, kinking, or intraluminal thrombi as those factors contraindicate doing the procedure[46].

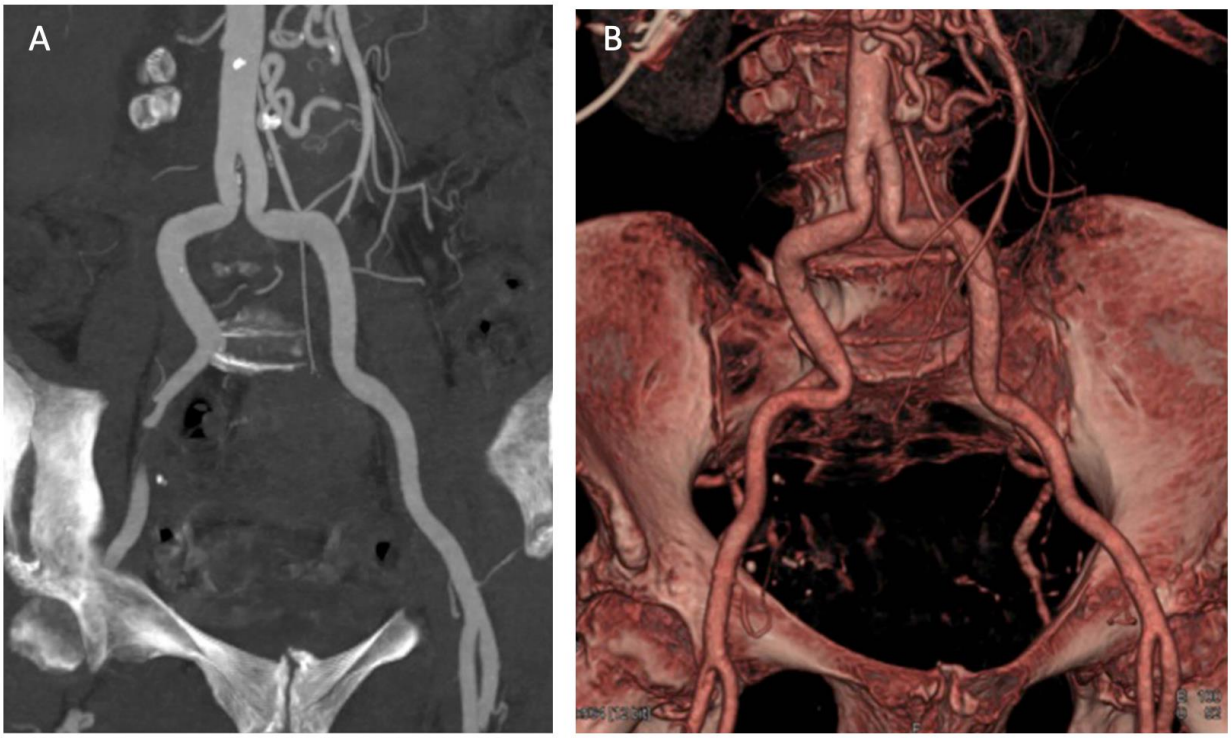

Figure 3: A) Multiplanar reconstruction showing minimal calcification of the peripheral vessels. B) a 3D reconstruction of the same patient showing severe kinking of the ileo-femoral access. (Reused with permission from Springer Nature publishing. Mohamed Marwan et al, Role of Cardiac CT Before Transcatheter Aortic Valve Implantation (TAVI). Curr Cardiol Rep. 2016 Feb;18(2):21. doi: 10.1007/s11886-015-0696-3)[43].

d) Projection Angle

One important factor to consider when deploying the aortic prothesis is the projection angle. The valve must be deployed coaxially to the centreline of the aorta, perpendicular to the annulus to minimize a number of life threatening complication. MDCT allows for the evaluation of the aortic root projection or axis, relative to the body. It also allows for the assessment of the optimal C-arm angle to achieve optimal visualization for valve deployment.

1.4.2 Pre-procedural Functional Assessment of TAVR Patients

Assessment of cardiac contractile function remains a challenge today. The well known metric used to assess cardiac contractility, ejection fraction, is a traditional parameter that described left ventricular (LV) function and presents significant limitations[47]. Most standing limitation is its sub-optimal reproducibility, inability to reflect regional function and its volumetric nature. This has prompted many to start looking at a more in-depth metric that characterizes LV mechanics through a non-invasive evaluation of myocardial deformation. This metric is called strain[48]. Strain is the deformation produced by the application of force and myocardial strain represented percent change in myocardial length from the relaxed to the contractile state.

In comparison to EF, strain allows for studying the special components of contraction in either the longitudinal strain (LS), circumferential strain (CS), or radial strain (RS) directions, both globally and regionally. Assessment of LV deformation through quantifying strain has reached many imaging modalities and the field has witnessed considerable development. Today strain is being applied to echocardiography in determining circumferential fibre shortening[49], tissue doppler echocardiography and current speckle tracking echocardiography (STE)[50], cardiac magnetic resonance (CMR) tissue tagging[51], and many feature tracking approaches[52-54].

Analyzing alterations in strain has been reported to provide additional prognostic value over EF even when EF is maintained[55]. Strain analysis has been applied to a multitude of clinical scenarios, ranging from asymptomatic adults with previous cardiac pathology[56], to valvular heart disease (in particular aortic stenosis)[55], cardiac oncology and heart failure with preserved or reduced EF[57,58]. As a result, numerous work has been done in relation to myocardial strain and today there is an extensive number of published articles, with “myocardial strain” keyword

search hitting 21,700 results on PubMed alone. The enthusiasm is pronounced; however, the field has only partly breached the clinical setting due to many challenges.

1.5 General Principles of Strain

The tools for measuring myocardial strain have evolved over the last decade, but the main principal is the same. It started in 1990 with tissue Doppler echocardiography[59]. The term strain described the local shortening, thickening and lengthening of the myocardium as a measure of regional LV function. The term strain is used to describe the deformation of a small cube during a short time interval. The strain tensor has six components, three of them refer to the shortening along three orthogonal axes (x, y, z) in an external coordinate and the other three share strain numbers giving the skew in the x-y, x-z, y-z planes. This however, is very detailed for translation into clinical practice. Therefore, an internal coordinate system that aligned with the three cardiac axis: longitudinal, circumferential, and radial is used to measure the shortening and elongation in the three directions through the cardiac cycle.

Mathematically speaking, if $L(t)$ is the length of a segment along one of the directions above at a time t in the cardiac cycle and L_0 is the initial length, 1D strain is defined as $\varepsilon(t)= (L(t)-L_0)/L_0$. A positive strain value means elongation, whereas negative means shortening. It might be confusing and therefore when communication strain, it is recommended to refer an increase or decrease in the absolute value of strain[60]. The next chapter will provide a literature review of prognostic value that left ventricular strain has played in TAVR across multiple imaging modalities.

1.6 References

1. Iung B, Baron G, Butchart EG, et al. A prospective survey of patients with valvular heart disease in Europe: The Euro Heart Survey on Valvular Heart Disease. *Eur Heart J.* 2003;24(13):1231-1243.
2. Eveborn GW, Schirmer H, Heggelund G, Lunde P, Rasmussen K. The evolving epidemiology of valvular aortic stenosis. the Tromsø study. *Heart.* 2013;99(6):396-400.
3. Iung B, Baron G, Tornos P, Gohlke-Bärwolf C, Butchart EG, Vahanian A. Valvular heart disease in the community: a European experience. *Curr Probl Cardiol.* 2007;32(11):609-661.
4. Roberts WC, Ko JM. Frequency by decades of unicuspid, bicuspid, and tricuspid aortic valves in adults having isolated aortic valve replacement for aortic stenosis, with or without associated aortic regurgitation. *Circulation.* 2005;111(7):920-925.
5. Otto CM, Kuusisto J, Reichenbach DD, Gown AM, O'Brien KD. Characterization of the early lesion of 'degenerative' valvular aortic stenosis. Histological and immunohistochemical studies. *Circulation.* 1994;90(2):844-853.
6. Julius BK, Spillmann M, Vassalli G, Villari B, Eberli FR, Hess OM. Angina pectoris in patients with aortic stenosis and normal coronary arteries. Mechanisms and pathophysiological concepts. *Circulation.* 1997;95(4):892-898.
7. Braunwald E. Heart failure. *JACC Heart Fail.* 2013;1(1):1-20.
8. Cook C, Cole G, Asaria P, Jabbour R, Francis DP. The annual global economic burden of heart failure. *Int J Cardiol.* 2014;171(3):368-376.
9. Leon MB, Smith CR, Mack M, et al. Transcatheter Aortic-Valve Implantation for Aortic Stenosis in Patients Who Cannot Undergo Surgery. *New England Journal of Medicine.* 2010;363(17):1597-1607.
10. Carabello BA. Evaluation and management of patients with aortic stenosis. *Circulation.* 2002;105(15):1746-1750.
11. Pellikka PA, Sarano ME, Nishimura RA, et al. Outcome of 622 adults with asymptomatic, hemodynamically significant aortic stenosis during prolonged follow-up. *Circulation.* 2005;111(24):3290-3295.
12. Ben-Dor I, Pichard AD, Gonzalez MA, et al. Correlates and causes of death in patients with severe symptomatic aortic stenosis who are not eligible to participate in a clinical trial of transcatheter aortic valve implantation. *Circulation.* 2010;122(11 Suppl):S37-42.
13. Makkar RR, Fontana GP, Jilaihawi H, et al. Transcatheter aortic-valve replacement for inoperable severe aortic stenosis. *N Engl J Med.* 2012;366(18):1696-1704.
14. Kodali SK, Williams MR, Smith CR, et al. Two-year outcomes after transcatheter or surgical aortic-valve replacement. *N Engl J Med.* 2012;366(18):1686-1695.
15. Schwarz F, Baumann P, Manthey J, et al. The effect of aortic valve replacement on survival. *Circulation.* 1982;66(5):1105-1110.
16. Lindblom D, Lindblom U, Qvist J, Lundström H. Long-term relative survival rates after heart valve replacement. *J Am Coll Cardiol.* 1990;15(3):566-573.
17. Pellikka PA, Nishimura RA, Bailey KR, Tajik AJ. The natural history of adults with asymptomatic, hemodynamically significant aortic stenosis. *J Am Coll Cardiol.* 1990;15(5):1012-1017.
18. Vahanian A, Alfieri O, Andreotti F, et al. Guidelines on the management of valvular heart disease (version 2012). *Eur Heart J.* 2012;33(19):2451-2496.

19. Asimakopoulos G, Edwards MB, Taylor KM. Aortic valve replacement in patients 80 years of age and older: survival and cause of death based on 1100 cases: collective results from the UK Heart Valve Registry. *Circulation.* 1997;96(10):3403-3408.
20. Bach DS, Cimino N, Deeb GM. Unoperated patients with severe aortic stenosis. *J Am Coll Cardiol.* 2007;50(20):2018-2019.
21. Bach DS, Siao D, Girard SE, Duvernoy C, McCallister BD, Jr., Gualano SK. Evaluation of patients with severe symptomatic aortic stenosis who do not undergo aortic valve replacement: the potential role of subjectively overestimated operative risk. *Circ Cardiovasc Qual Outcomes.* 2009;2(6):533-539.
22. Iung B, Cachier A, Baron G, et al. Decision-making in elderly patients with severe aortic stenosis: why are so many denied surgery? *Eur Heart J.* 2005;26(24):2714-2720.
23. Nishimura RA, Otto CM, Bonow RO, et al. 2014 AHA/ACC Guideline for the Management of Patients With Valvular Heart Disease: executive summary: a report of the American College of Cardiology/American Heart Association Task Force on Practice Guidelines. *Circulation.* 2014;129(23):2440-2492.
24. Davies H. CATHETER-MOUNTED VALVE FOR TEMPORARY RELIEF OF AORTIC INSUFFICIENCY. *The Lancet.* 1965;285(7379):250.
25. Cribier A, Eltchaninoff H, Bash A, et al. Percutaneous transcatheter implantation of an aortic valve prosthesis for calcific aortic stenosis: first human case description. *Circulation.* 2002;106(24):3006-3008.
26. Moulopoulos SD, Anthopoulos L, Stamatelopoulos S, Stefadouros M. Catheter-mounted aortic valves. *Ann Thorac Surg.* 1971;11(5):423-430.
27. Bourantas CV, Serruys PW. Evolution of Transcatheter Aortic Valve Replacement. *Circulation Research.* 2014;114(6):1037-1051.
28. Andersen HR, Knudsen LL, Hasenkam JM. Transluminal implantation of artificial heart valves. Description of a new expandable aortic valve and initial results with implantation by catheter technique in closed chest pigs. *Eur Heart J.* 1992;13(5):704-708.
29. Bonhoeffer P, Boudjemline Y, Saliba Z, et al. Percutaneous replacement of pulmonary valve in a right-ventricle to pulmonary-artery prosthetic conduit with valve dysfunction. *Lancet.* 2000;356(9239):1403-1405.
30. Cribier A, Eltchaninoff H, Bash A, et al. Percutaneous Transcatheter Implantation of an Aortic Valve Prosthesis for Calcific Aortic Stenosis. *Circulation.* 2002;106(24):3006-3008.
31. Paniagua D, Induni E, Ortiz C, Mejia C, Lopez-Jimenez F, Fish RD. Percutaneous Heart Valve in the Chronic In Vitro Testing Model. *Circulation.* 2002;106(12):e51-e52.
32. Petronio AS, De Carlo M, Bedogni F, et al. Safety and efficacy of the subclavian approach for transcatheter aortic valve implantation with the CoreValve revalving system. *Circ Cardiovasc Interv.* 2010;3(4):359-366.
33. Al-Lamee R, Godino C, Colombo A. Transcatheter Aortic Valve Implantation. *Circulation: Cardiovascular Interventions.* 2011;4(4):387-395.
34. Vogel-Claussen J, Pannu H, Spevak PJ, Fishman EK, Bluemke DA. Cardiac valve assessment with MR imaging and 64-section multi-detector row CT. *Radiographics.* 2006;26(6):1769-1784.
35. Salgado RA, Leipsic JA, Shivalkar B, et al. Preprocedural CT Evaluation of Transcatheter Aortic Valve Replacement: What the Radiologist Needs to Know. *RadioGraphics.* 2014;34(6):1491-1514.

36. Schoenhagen P, Hausleiter J, Achenbach S, Desai MY, Tuzcu EM. Computed tomography in the evaluation for transcatheter aortic valve implantation (TAVI). *Cardiovasc Diagn Ther.* 2011;1(1):44-56.
37. Francone M, Budde RPJ, Bremerich J, et al. CT and MR imaging prior to transcatheter aortic valve implantation: standardisation of scanning protocols, measurements and reporting—a consensus document by the European Society of Cardiovascular Radiology (ESCR). *European Radiology.* 2020;30(5):2627-2650.
38. Wuest W, Anders K, Schuhbaeck A, et al. Dual source multidetector CT-angiography before Transcatheter Aortic Valve Implantation (TAVI) using a high-pitch spiral acquisition mode. *Eur Radiol.* 2012;22(1):51-58.
39. Bloomfield GS, Gillam LD, Hahn RT, et al. A practical guide to multimodality imaging of transcatheter aortic valve replacement. *JACC Cardiovasc Imaging.* 2012;5(4):441-455.
40. Tops LF, Wood DA, Delgado V, et al. Noninvasive evaluation of the aortic root with multislice computed tomography implications for transcatheter aortic valve replacement. *JACC Cardiovasc Imaging.* 2008;1(3):321-330.
41. Clayton B, Morgan-Hughes G, Roobottom C. Transcatheter aortic valve insertion (TAVI): a review. *Br J Radiol.* 2014;87(1033):20130595-20130595.
42. Piazza N, de Jaegere P, Schultz C, Becker AE, Serruys PW, Anderson RH. Anatomy of the aortic valvar complex and its implications for transcatheter implantation of the aortic valve. *Circ Cardiovasc Interv.* 2008;1(1):74-81.
43. Marwan M, Achenbach S. Role of Cardiac CT Before Transcatheter Aortic Valve Implantation (TAVI). *Curr Cardiol Rep.* 2016;18(2):21.
44. Masson JB, Kovac J, Schuler G, et al. Transcatheter aortic valve implantation: review of the nature, management, and avoidance of procedural complications. *JACC Cardiovasc Interv.* 2009;2(9):811-820.
45. Leipsic J, Gurvitch R, Labounty TM, et al. Multidetector computed tomography in transcatheter aortic valve implantation. *JACC Cardiovasc Imaging.* 2011;4(4):416-429.
46. Okuyama K, Jilaihawi H, Kashif M, et al. Transfemoral access assessment for transcatheter aortic valve replacement: evidence-based application of computed tomography over invasive angiography. *Circ Cardiovasc Imaging.* 2015;8(1).
47. Konstam MA, Abboud FM. Ejection Fraction: Misunderstood and Overrated (Changing the Paradigm in Categorizing Heart Failure). *Circulation.* 2017;135(8):717-719.
48. Mirsky I, Parmley WW. Assessment of passive elastic stiffness for isolated heart muscle and the intact heart. *Circ Res.* 1973;33(2):233-243.
49. Domanski MJ, Follmann D, Mirsky II. A New Approach to Assessing Regional and Global Myocardial Contractility. *Echocardiography.* 1997;14(1):1-8.
50. Sutherland GR, Stewart MJ, Groundstroem KW, et al. Color Doppler myocardial imaging: a new technique for the assessment of myocardial function. *J Am Soc Echocardiogr.* 1994;7(5):441-458.
51. Zerhouni EA, Parish DM, Rogers WJ, Yang A, Shapiro EP. Human heart: tagging with MR imaging--a method for noninvasive assessment of myocardial motion. *Radiology.* 1988;169(1):59-63.
52. Collier P, Phelan D, Klein A. A Test in Context: Myocardial Strain Measured by Speckle-Tracking Echocardiography. *J Am Coll Cardiol.* 2017;69(8):1043-1056.
53. Jasaityte R, Heyde B, D'Hooge J. Current state of three-dimensional myocardial strain estimation using echocardiography. *J Am Soc Echocardiogr.* 2013;26(1):15-28.

54. Rodríguez-Zanella H, Haugaa K, Boccalini F, et al. Physiological Determinants of Left Ventricular Mechanical Dispersion: A 2-Dimensional Speckle Tracking Echocardiographic Study in Healthy Volunteers. *JACC Cardiovasc Imaging.* 2018;11(4):650-651.
55. Delgado V, Tops LF, van Bommel RJ, et al. Strain analysis in patients with severe aortic stenosis and preserved left ventricular ejection fraction undergoing surgical valve replacement. *Eur Heart J.* 2009;30(24):3037-3047.
56. Choi EY, Rosen BD, Fernandes VR, et al. Prognostic value of myocardial circumferential strain for incident heart failure and cardiovascular events in asymptomatic individuals: the Multi-Ethnic Study of Atherosclerosis. *Eur Heart J.* 2013;34(30):2354-2361.
57. Park JJ, Park JB, Park JH, Cho GY. Global Longitudinal Strain to Predict Mortality in Patients With Acute Heart Failure. *J Am Coll Cardiol.* 2018;71(18):1947-1957.
58. Shah AM, Claggett B, Sweitzer NK, et al. Prognostic Importance of Impaired Systolic Function in Heart Failure With Preserved Ejection Fraction and the Impact of Spironolactone. *Circulation.* 2015;132(5):402-414.
59. Heimdal A, Støylen A, Torp H, Skjaerpe T. Real-time strain rate imaging of the left ventricle by ultrasound. *J Am Soc Echocardiogr.* 1998;11(11):1013-1019.
60. Smiseth OA, Torp H, Opdahl A, Haugaa KH, Urheim S. Myocardial strain imaging: how useful is it in clinical decision making? *European heart journal.* 2016;37(15):1196-1207.

Chapter 2 - Literature Review: The Prognostic Value of Multimodality Derived Left Ventricular Myocardial Strain in Transcatheter Aortic Valve Replacement

Before proceeding with the assessment of our own patient cohort for this thesis project, it is important to assess the available literature on our topic as pertaining to strain analysis. Through this literature review, I wanted to outline the currently available literature that assessed the prognostic value of left ventricular (LV) strain in TAVR patients across three imaging modalities, echocardiography, computed tomography, and cardiac magnetic resonance imaging. This section will critically assess the current knowledge on LV strain prognostication which will serve as a good transition to the thesis project presented in Chapter 3.

A version of this chapter will be submitted for publication – undetermined journal.

2.1 INTRODUCTION

In the last two decades, progress has been marked by advances in every modality used to image the heart, including echocardiography[1-3], nuclear cardiology[4,5], cardiac computed tomography (CT)[6,7], and cardiac magnetic resonance (CMR) imaging[8,9]. In addition, there has been a great deal of fusion of modalities which has leveraged the unique capabilities of two imaging modalities simultaneously[10]. These advances in the field of non-invasive medical imaging have guided management of many patients who otherwise would be deemed inoperable. Our better understanding of cardiovascular disease coupled with technological innovation has enabled the increased use of minimally invasive cardiovascular surgical approaches and trans-catheter interventions, with reduced morbidity and mortality. Unlike conventional surgical procedures done through a median sternotomy, pre-operative findings cannot be confirmed by direct

visualisation of the structures. Therefore, imaging plays an increasingly important role in the pre-procedural evaluation of patients and for peri-procedural imaging guidance.

The onset of symptoms is a major predictor of mortality in AS[11]. Within the elderly population, one-third suffer from significant comorbidity and therefore have a poor prognosis[12]. In octogenarians with comorbidities, mortality rates are between 40% and 50% at 1 year[13]. The five year mortality has been reported at 60% after the first hospitalization with a diagnosis of AS[13]. The PARTNER Cohort B study indicated standard medical treatment was associated with a cardiovascular mortality of 62.4% and repeat hospitalisation of 72.5% at two-year follow up[14]. The lack of effective medical management emphasized the importance of timing of aortic intervention to reverse the functional deterioration and remodeling; ultimately restoring prognosis.

For this reason, there is a growing body of evidence that looks at leveraging the use of multi-modality imaging in predicting the clinical outcomes of patients undergoing TAVR for severe AS[15,16]. This population is suitable for this purpose as most patients being considered for TAVR undergo echocardiography and CT imaging at a minimum to plan for the operation. Pre-procedural imaging plays an important role in assessing the anatomy of the aortic annulus, aorta, iliac and femoral arteries in these patients as we have seen in Chapter 2 of this thesis. In addition, assessment of the systolic function by ejection fraction measurement (LVEF) is considered a central parameter for timing of intervention. However, LVEF is often preserved until late in the diseases process even after symptoms occur. It might remain normal despite progression of AS severity and LV hypertrophy, which indicates that LVEF as a marker is poor at detecting subtle changes of myocardial performance[16]. On the other hand, myocardial strain

assessment has been demonstrated to detect subtle change in LV systolic function with a good correlation to symptoms and an independent prognostic value in asymptomatic and symptomatic aortic stenosis[17,18].

Despite a constant growing body of evidence that supports LV myocardial strain evaluation in the majority of cardiovascular disease, its assessment and reporting has not become part of routine echocardiography, CT, or MR imaging laboratories. The aim of this clinical review is to summarize the current literature about the predictive value of LV myocardial strain across multi-modality imaging techniques in patients undergoing TAVR to emphasize the importance of its evaluation in routine examination.

2.2 PROGNOSTIC VALUE OF ECHOCARDIOGRAPHY DERIVED LV STRAIN

Although LVEF carries an important prognostic information in the assessment of patients with aortic stenosis, it remains load dependent and confounded by the presence of left ventricle hypertrophy in the TAVR population. Therefore, LVEF may remain in the normal range until late into the disease process even when fibrosis is present[19]. Strain assessment allows for a better understanding of the progression of heart failure in aortic stenosis and earlier changes in myocardial function[20-22].

Systolic longitudinal strain parameters, assessed by Tissue Doppler Imaging (TDI) are significantly decreased in patients with AS and preserved LVEF, and their decline is related to the severity of AS[21]. However, one limitation in LV deformation by TDI is that it requires the doppler beam to be in alignment with the myocardial motion direction and therefore cannot be performed for all LV segments. Speckle tracking echocardiography (STE) has overcome these limitations, by allowing a multidirectional evaluation of myocardial deformation[23]. The lack of

angle-dependency is of great advantage because it allows for tracking the myocardium in two-dimensions, along the direction of the wall and not along the ultrasound beam[24]. This allows for the measurement of deformation in three spatial directions: a longitudinal and circumferential shortening and radial thickening[25].

An increasing body of evidence suggests the usefulness of global longitudinal strain (GLS) for risk stratification and management of asymptomatic patients with severe AS and preserved LVEF[20]. A study that included 104 asymptomatic severe AS patients with preserved LVEF investigated the influence of echocardiographic parameters on 1-year outcome and reported that 3D GLS showed the best specificity and sensitivity in the prediction of cardiovascular events, significantly better than AVA index, LVEF, LV mass index, and maximal LA volume index. AS patients with 3D GLS cut-off value of <-14.5% experienced fewer cardiovascular events than those with 3D GLS strain ≥-14.5%. Moreover, 2D GLS, 3D GLS, and 3D GRS could stratify a group of patients at high-risk of MACE and in a sub-group analysis according to the status of the mean PG demonstrated that both 2D GLS and 3D GLS could predict future MACE in low and high PG severe AS patients[26].

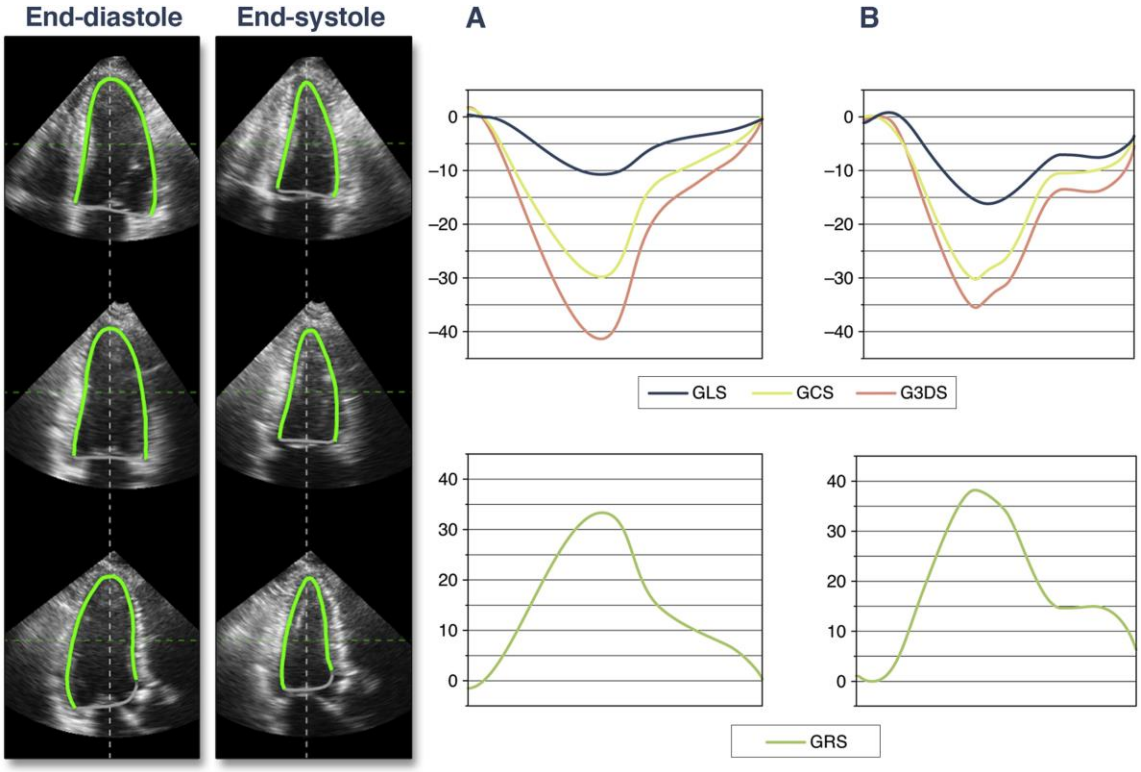

Figure 1. Representative Cases of 3D Speckle-Tracking Analysis: A) A patient who had a subsequent major adverse cardiac event (MACE). B) A patient without MACE. Global longitudinal strain (GLS) and global radial strain (GRS) were lower in patients with MACE compared with those without MACE. Note nearly the same value of global circumferential strain (GCS) and global 3-dimensional strain (G3DS) between the 2 patients. 3D = 3-dimensional. (Reused with permission from Elsevier publishing. Nagata et al. Prognostic Value of LV Deformation Parameters Using 2D and 3D Speckle-Tracking Echocardiography in Asymptomatic Patients With Severe Aortic Stenosis and Preserved LV Ejection Fraction. *JACC: Cardiovascular Imaging.* 2015;8(3):235-245. doi.org/10.1016/j.jcmg.2014.12.009)[26].

Similarly another study that included 101 patients with asymptomatic severe aortic stenosis and preserved LVEF, investigated the role of contractile reserve (CR) during exercise stress echocardiography estimated via GLS (CR-GLS) to better stratify asymptomatic AS patients who could benefit from early intervention[27]. All patients who underwent exercise stress echo with a negative result for inducible ischemia were included and divided into patients whom CR-GLS was present and patients whom CR-GLS was absent. The group reported the mean resting (GLS of -18.8) to be at the lower limit of the values considered normal. The discrepancy seen

compared to previous studies reporting a resting GLS of <-15 in predicting clinical outcomes has led to the evaluation of CR-GLS in order to unmask subclinical ventricular dysfunction. CR-GLS was shown to be an independent predictor of composite endpoint of major cardiovascular events, among which AVR was the main event. As well as this parameter was an independent predictor of long-term risk. The discrimination power of CR derived from GLS was slightly better than that of CR derived from EF. In addition, the cut-off value of -20% GLS during peak exercise predicted a higher risk of requiring AVR in patients during follow up[27]. Another study that investigated 411 patients with symptomatic severe AS treated with TAVR during a 5 year period demonstrated reduced survival with LV global longitudinal strain > -14% in the total population, but also patients with high AS gradient with preserved LVEF[28]. A strong association between severity of LV GLS impairment and mortality was noted. A risk model demonstrated additive prognostic value of LV GLS to the clinical characteristics, AVA, and LVEF. In both studied, LV GLS offered a more reliable parameter than LVEF for evaluating myocardial function and prognosis in both asymptomatic and symptomatic AS patients with a wide range of severities and ages.

Not only LV strain at baseline, but also its change during therapy and follow-up is important for prognosis of TAVR patients. In a recent study, Al-Rashid *et. al.* demonstrated that baseline LV GLS correlated significantly with the postprocedural outcome in 150 consecutive patients undergoing TAVR[29]. The speckle tracking strain analysis revealed that GLS has an ascending trend 1 week after TAVR and improved significantly 3 months after TAVR while LVEF did not show a substantial change, signaling an early recovery of LV longitudinal function after the intervention. Tsampasian *et. al.* have also demonstrated that TAVR resulted in reverse remodelling and improvement of GLS, especially in patients with impaired baseline LV

function[30]. In 303 consecutive patients with a mean follow up period of 49 days, GLS improved from -14.0% to -15.3% but not ejection fraction. The type of valve (Edwards S3 vs Evolut R valves) did not have an appreciable difference in LV function improvement or overall LV remodelling after TAVR. The findings of these two study suggest that GLS might be a more sensitive marker for left ventricular assessment after TAVR compared to EF, as it can potentially detect changes of the left ventricular function even in the short-term follow-up. The same message has been echoed by Granero et al. after studying 119 patients pre and post TAVR with a GLS improvement from -14.6 at baseline to –15.7 at discharge[31].

In a more detailed analysis by Cimino *et. al*., patients were enrolled to look at changes in longitudinal strain (LS) measured from the endocardial layer (Endo-LS), epicardial layer (Epi-LS) and full thickness of myocardium (Transmural-LS) before and after TAVR[32]. The cohort was divided further based on relative wall thickness: concentric LV hypertrophy (cLVH) vs eccentric LV hypertrophy (eLVH). The authors reported that cLVH had a less impaired LS values at baseline compared to eLVH in all layers. As well as a significant improvement of Endo-LS early after TAVR, only in cLVH. These results are in line with previous studies exploring LS behavior in different myocardial layers after TAVR. Shiino *et. al.* demonstrated a more prominent LS improvement in the sub-endocardial layer post TAVR[33]. The same behavior was observed by Kim *et. al.,* with LS improvement being greater in patients with higher grade LVH[34].

The role of echo-derived LV longitudinal strain in prediction of adverse outcomes in TAVR patients is on display across many publications. Suzuki-Eguchi *et. al.* also investigated patients with severe symptomatic aortic stenosis and found that 2-year survival in patients with LV longitudinal strain ≥ -10.6% was significantly lower than those with LV longitudinal strain < -

10.6%. Patients with events had higher LVMi, more severe aortic regurgitation, and worse GLS compared to those without events[35].

Table 1: Predictive value of LV longitudinal strain in Echocardiography

Reference	Sample Size	LV GLS cut-off	Follow up period (months)	Main findings
Magne *et al*[20]	1067	-14.7%	1.8 years median	LV global longitudinal strain <-14.7% is strongly associated with mortality. Risk of death for patients with LVGLS <14.7% was multiplied by >2.5.
Nagata *et. al.*[36]	104	-17% (2D) -14.5% (3D)	373 days media	Both 2D GLS and 3D GLS could predict future MACE in low and high PG severe AS patients. 3DGLS was only significant as independent predictor for future MACE after correcting for mean pressure gradient and left ventricular mass index
Arbucci *et. al.*[27]	101	-20	46.6 ± 3.4 months (mean)	CR-GLS was an independent predictor of major cardiovascular events. A cutoff value of 20% GLS during peak exercise predicted a higher risk of requiring AVR in patients during follow-up
Povlsen *et. al.*[28]	411	-14	762 days median	LVGLS > − 14% was an independent predictor of all-cause mortality, and survival was reduced if LVGLS > − 14%.
Al-Rashid *et. al.*[29]	150	-	3 months	GLS improves at 3 months after TAVR, while LV ejection fraction did not. GLS had a direct correlation with the postprocedural outcomes
Tsampasian *et. al.*[30]	303	-	49 ± 39 days (mean)	TAVI results in reverse remodelling and improvement of GLS, especially in patients with impaired baseline LV function. No differences in the extent of LV function improvement between Edwards S3 and Evolut R valves
Granero *et. al.*[31]	119	-	1 year	Immediate and sustained improvement in GLS was appreciated after the TAVR procedure.

Cimino *et. al.*[32]	68	-	-	Concentric LVH had better basal strain function and showed a better myocardial recovery after TAVI compared to eccentric LVH.
Shiino *et. al.*[33]	119	-	1 month	Multilayer GLS is more sensitive than conventional LVEF to detect early improvement in LV systolic function after TAVI in patients with severe AS. There is a disproportional improvement in different layers with least improvement in the endocardium.
Kim *et. al.*[34]	28	-	1 month	Longitudinal strain significantly improved in all three layers following acute pressure unloading, the most prominent of which was observed in the endocardium.
Suzuki-Eguchi *et. al.*[35]	128	-10.6%	591 days (median)	GLS was associated with MACE after TAVI, unlike LVEF, AVA, AV mean PG, LVMI.

2.3 PROGNOSTIC VALUE OF COMPUTED TOMOGRAPHY DERIVED LV STRAIN

The ubiquitous use of CT today is turning away from only being a diagnostic tool that can image general heart anatomy, the coronary arteries, the myocardium, and moving to offer an assessment of cardiac function and prediction of outcomes. The emergence of myocardial strain in CT has encouraged a trend towards cardiac CT becoming a "one stop shop" for cardiac diagnostics. This has been apparent with the most recent literature that proved the feasibility of using CT images to study myocardial health.

Vach *et. al.* aimed to assess the feasibility of measuring myocardial strain in cardiac CT in patients with advanced cardiac valve disease and compare it to strain measurement in transthoracic echocardiography. The group had studied 43 consecutive patients who received a

clinically indicated retrospectively gated CT for planning an intervention of mitral or tricuspid valve as well as evaluation of the aortic valve. The longitudinal, circumferential as well as radial systolic strain were determined in all patients utilizing a commercially available CT strain software. Short-axis views were reconstructed from transversal images. Strain measurements were feasible in all patients. CT derived longitudinal strain correlated moderately with TTE derived GLS. Also a moderate correlation between CT derived GLS and CT derived LVEF was found compared with speckle tracking TTE[15].

Benetos *et. al.* in a study of 123 consecutive TAVR patients and a mean follow up period of 875 days evaluated the impact of tricuspid annular diameters (TAD) and mitral annular diameter (MAD) from CTA datasets and demonstrated that TAD and MAD are associated with heart failure hospitalization and clinical events respectively in patients undergoing TAVR with a self-expanding valve[37]. In another investigation conducted by Gegenaca *et. al.*, the study enrolled 214 patients with severe aortic stenosis aimed at evaluating the association between feature tracking (FT) MDCT derived LV GLS and all-cause mortality in patients treated with TAVR. The authors found that a cut-off value of LV GLS ≤ -14% was associated with all-cause mortality. FT MDCT-derived LV GLS was an independent predictor of all-cause mortality in this population[38].

In a larger study, Fukui *et. al.* looked at 223 consecutive patients with pre-TAVR retrospective gated acquisition CT study to evaluate the prognostic value of CT GLS with all-cause mortality and hospitalization for heart failure after TAVR. Patients with normal LVEF (≥50%) but reduced CT GLS (> -20.5%) had higher rate of all-cause mortality and risk of composite outcome when compared to patients with normal LVEF and preserved CT GLS (≤-20.5%). The results held true even for patients with impaired LVEF. In a multi-variable Cox regression analysis, reduced CT

GLS was independently associated with all-cause mortality and the risk of composite outcome despite adjustment for multiple clinical and echocardiographic characteristics. This work demonstrated that baseline CT GLS is a sensitive marker for higher all-cause mortality and the composite outcome of all-cause death and heart failure hospitalization after TAVR despite a normal CT LVEF[39].

Changes in strain during therapy and follow up has also been studies in CT for TAVR patients. Marwan *et. al.* assessed the potential of CT strain to detect changes in myocardial function in 25 patients referred for TAVR pre- and post-intervention[40]. In this prospective analysis, the group demonstrated CT strain assessment of left ventricle is feasible. Peak global maximum principal strain was significantly higher at follow-up compared to baseline. Similarly global longitudinal strain was significantly lower compared to baseline (better contraction). Moreover, CT parameters of left ventricle strain showed significant correlation with echocardiographic determined ejection fraction pre and post intervention.

Another larger investigation that included 431 patients with aortic stenosis and undergone TAVR showed that left ventricular CT GLS strongly corelated with CT LVEF. CT GLS > -18.2 remained associated with the risk of composite outcome even after adjustment for clinical and echocardiographic factors including age, coronary artery disease, low gradient AS, greater than moderate MR and TR, TAPSE, and paravalvular leak[41]. The group also concluded on 1 month follow up that patients with no improvement in CT GLS had a higher risk of composite outcome compared to those with preserved GLS. No difference was observed between individuals who had a preserved GLS or improved GLS.

CT GLS is one marker that has been shown consistently across many studied to be of prognostic value in predicting outcomes of TAVR patients. ECG-gated CTA can also be used for quantification of myocardial extracellular volume (ECV). Although this is not the focus of this review, it is worth mentioning to emphasize that there are other tissue characterization markers that can be derived from CT besides strain. Tamarappoo *et. al.* in a single centre study of 150 patients with low flow low gradient aortic stenosis undergoing TAVR, demonstrated that a myocardial ECV >33% is associated with adverse clinical outcomes and provides incremental value to STS score, age, and LVEF for predicting death and heart failure hospitalization. Although CMR is routinely used for quantification of ECV, the ability to quantify ECV from CTA is very powerful as it is much faster and better tolerated in critically ill patients. Thus, CTA ECV and strain measurements could become a part of the routine TAVR CTA that helps physicians in risk stratifying patients preprocedurally[42].

Table 2: Predictive value of LV longitudinal strain in CT

Reference	Sample Size	LV GLS cut-off	Follow up period (months)	Main findings
Vach *et. al.* [15]	43	-	-	CT-derived myocardial strain measurements are feasible in patients with advanced cardiac valve disease. They are highly reproducible and correlate with established parameters of strain measurements.
Benetos *et. al.* [37]	123	-	875 ± 383 days	TAD and MAD are associated with heart failure hospitalization and clinical events respectively in patients undergoing TAVI with a self-expanding valve.
Gegenava *et. al.* [38]	214	-14%	45 month (median)	FT MDCT-derived LV GLS is independently associated with all-cause mortality

Fukui *et. al.* [39]	223	−20.5%	32 months (median)	Reduced CTA-GLS is independently associated with all-cause mortality and the risk of composite outcome
Marwan *et. al.* [40]	25	-	6 months	CT-derived parameters of global myocardial strain improves on short-term follow-up
Fukui *et. al.* [41]	431	-18.2	1 month	CTA-LVGLS > -18.2 is associated with the risk of composite outcome even after adjustment for clinical and echocardiographic factors including age, coronary artery. disease, low gradient AS, greater than moderate MR and TR, TAPSE, paravalvular leak
Tamarappoo *et al*[42]	150	33% (ECV cut off)	13.9 months (median)	ECV >33% is associated with increase in death and heart failure hospitalization.

2.4 PROGNOSTIC VALUE OF MAGNETIC RESONANCE IMAGING DERIVED LV STRAIN

The role of CMR has exploded in recent years, largely due to advances in scanner technology, software and accessibility. Its ability to identify, quantify, and discriminate between different disease entities is superior to many imaging modalities. This is equally important in aortic stenosis, where an understanding of myocardial health and function may be of clinical relevance, beyond the standard measurements of valve hemodynamics and obstruction. Currently, the use of CMR to detect myocardial fibrosis is the most studied application of myocardial tissue characterization in AS. However, there are other markers like strain, ECV, and T1 mapping that

can be applied to CMR images and serve with equal importance of tissue characterisation measure in the assessment of those patients.

As the TAVR procedure becomes more common, there will be an increase in the number of patients who cannot undergo CTA or stress echocardiography. Thus, a free radiation, non-contrast MR may have an important role to play in the pre-operative evaluation of TAVR patients. Patients with a history of allergic reaction to iodine contrast, impaired renal function, poor acoustic windows or low cardiac output are few examples of patients who will benefit from a CMR assessment. Post-gadolinium delayed enhancement imagining can also be used to assess severity of myocardial fibrosis in patients undergoing TAVR, which has been demonstrated as a marker for recovery of LVEF post TAVR[43].

There are many publications evaluating the usefulness of CMR both before and after implantation for the evaluation of TAVR. However, these publications have focused on few aspects of the increasingly complex assessment needed for the evaluation of TAVR patients, There are other set of publications that focused on myocardial strain as a prognostication marker obtained from pre-procedural MR scan and those will be outlined in this review.

LV strain can be measured with CMR[44]. Tissue tracking in a simple and practical method for assessing strain and predicting reverse remodeling in severe AS, especially in patients with sub-optimal echocardiography imaging quality. Most CMR protocols for assessing myocardial strain use the conventional protocols that are already in use to assess myocardial health. The standard steady-state free procession pulse sequences described earlier to image the entire left and right ventricle are used. There are many commercially available software used to perform CMR tissue tracking[45]. The two, three, four chamber and short axis images are used by the software to

reconstruct a 3D model that is used for analysis of 2D and 3D radial, circumferential and longitudinal LV strain. The tissue tracking relies on drawing endo and epicardial surface contours in the end-diastole phase (reference phase) using short axis stacked slices. A short axis reference point is marked at the anterior and posterior RV insertion point on the LV to allow for regional and global analysis of strain and to generate polar maps. Most software today, have the ability to track the myocardium voxel points through the cardiac cycle. The ability to track the endo and epicardial contours in reference to the end-diastolic contours allows for the computation of strain and outputting the delta in a 17 segment model for assessing regional and global myocardial strain.

In a multi-centre study involving 98 patients (52 TAVI, 46 SAVR), Musa *et. al*. has utilised this protocol in order to characterize pre-procedural strain in severe AS and determine whether abnormalities in strain were associated with outcome[46]. The group demonstrated on multivariable Cox analysis, baseline middle LV circumferential strain was significantly associated with all-cause mortality, independent of age, LVEF, and Society of Thoracic Surgeons (STS) mortality risk score. Receiver operating curve analysis indicated that a mid-LV circumferential strain > –18.7% was associated with significantly reduced survival. No significant change in basal or middle LV circumferential strain or diastolic strain rate was seen after either intervention. However, a significant and comparable decline in LV torsion and twist was observed in the TAVR and SAVR group, which likely reflects an improvement towards normal physiology after alleviation of AS. Higher circumferential strain in patients with preserved LVEF, and increased apical rotation in patients with mild LV dysfunction are thought to indicate compensatory mechanics serving to maintain radial strain. These compensatory mechanisms are reduced as LV

performance declines and their loss appears to occur at the time of symptom onset indicating their potential use for surveillance and timing of surgery.

In another study by Hwang *et. al.*, 63 patients with severe AS and normal LV systolic function (EF > 60%) were enrolled and underwent both CMR and transthoracic echocardiography before surgical aortic valve replacement (AVR) [47]. The group's aim was to evaluate the correlation between reverse remodeling as an outcome and left ventricular strain using CMR tissue tracking, and to evaluate prediction of reverse remodeling by myocardial deformation in patients with severe aortic stenosis (AS). LV mass regression had significantly improved after AVR. Statistically significant Pearson's correlations with LVMi regression were observed for longitudinal global strain, radial strain, and circumferential strain. A simple linear regression analysis showed that all strain parameters could predict the amount of LVMI regression as well as non-contrast T1 value and ECV. However, ECV had the lowest predictive power. Multiple regression analysis showed that strain could independently predict the amount of LVMI regression and the longitudinal global strain.

It is very clear that using a non-contrast MRI for pre-TAVR planning is going to play a pivotal role not only in the assessment of aortic root complex and thoracic access sites, but also in the prediction of outcomes of patients undergoing therapy. Many of the ongoing trails are likely to underscore the importance of CMR in managing this high-risk cardiac population. Nonetheless, further work will be needed to determine the role of tissue tracking for monitoring reverse remodeling and to aid in stratification of AS patients. The correlation of myocardial strain with other tissue characteristics like myocardial fibrosis, T1 mapping, and ECV need to be further studied to shed light on the behavior of the myocardium post-surgery.

Table 3: Predictive value of LV longitudinal strain in MRI

Reference	Sample Size	LV GLS cut-off	Follow up period (months)	Main findings
Al Musa *et. al*.[46]	98	-18.7 (mid LV circumferential strain)	6 years	Mid LV circumferential strain was significantly associated with all-cause mortality independent of age, LV ejection fraction and STS mortality risk score.
Hwang *et. al*.[47]	63	-	28.8 months median	Longitudinal global strain measured by CMR tissue tracking as a technique was correlated with reverse remodeling as LVMI regression and was predictive of this outcome

2.5 CONCLUSION

Assessment of LV function remains the most common reason for cardiac imaging because of its powerful ability to predict morbidity and mortality. However, the current routine methods to quality LVEF are not without limitations[48]. We have seen though this review that multi-modality LV derived strain imaging is feasible and offers a promise for quantifying LV function, particularly in patients with subclinical disease. This powerful tool offers the treating physicians with a unique opportunity to alter the course of the disease before the onset of overt LV dysfunction, which may improve prognosis. There is a significant amount of work that needs to be done to refine the role and usefulness of strain imaging despite the undoubtedly meaningful role many groups have demonstrated in echocardiography, computer tomography, and magnetic resonance imaging. Its wide acceptance and clinical adoption will be challenged with the analysis time and ease of use and therefore those are certain aspects that will require further

improvement. There is great optimism however, that strain analysis will be at the forefront of prognostic markers to assess TAVR patients and other cardiovascular disease.

2.6 REFERENCE

1. Omar AM, Bansal M, Sengupta PP. Advances in Echocardiographic Imaging in Heart Failure With Reduced and Preserved Ejection Fraction. *Circ Res.* 2016;119(2):357-374.
2. Inciardi RM, Galderisi M, Nistri S, Santoro C, Cicoira M, Rossi A. Echocardiographic advances in hypertrophic cardiomyopathy: Three-dimensional and strain imaging echocardiography. *Echocardiography.* 2018;35(5):716-726.
3. Chang A, Cadaret LM, Liu K. Machine Learning in Electrocardiography and Echocardiography: Technological Advances in Clinical Cardiology. *Curr Cardiol Rep.* 2020;22(12):161.
4. Lee WW. Recent Advances in Nuclear Cardiology. *Nucl Med Mol Imaging.* 2016;50(3):196-206.
5. Gomez J, Doukky R, Germano G, Slomka P. New Trends in Quantitative Nuclear Cardiology Methods. *Curr Cardiovasc Imaging Rep.* 2018;11(1).
6. Hamirani YS, Kramer CM. Advances in stress cardiac MRI and computed tomography. *Future Cardiol.* 2013;9(5):681-695.
7. Aziz W, Claridge S, Ntalas I, et al. Emerging role of cardiac computed tomography in heart failure. *ESC Heart Fail.* 2019;6(5):909-920.
8. Seetharam K, Lerakis S. Cardiac magnetic resonance imaging: the future is bright. *F1000Res.* 2019;8.
9. Ghosn MG, Shah DJ. Important advances in technology and unique applications related to cardiac magnetic resonance imaging. *Methodist Debakey Cardiovasc J.* 2014;10(3):159-162.
10. Bax JJ, Beanlands RS, Klocke FJ, et al. Diagnostic and clinical perspectives of fusion imaging in cardiology: is the total greater than the sum of its parts? *Heart (British Cardiac Society).* 2007;93(1):16-22.
11. Ross J, Jr., Braunwald E. Aortic stenosis. *Circulation.* 1968;38(1 Suppl):61-67.
12. Iung B, Baron G, Tornos P, Gohlke-Bärwolf C, Butchart EG, Vahanian A. Valvular heart disease in the community: a European experience. *Curr Probl Cardiol.* 2007;32(11):609-661.
13. Iung B, Vahanian A. Epidemiology of acquired valvular heart disease. *Can J Cardiol.* 2014;30(9):962-970.
14. Kodali SK, Williams MR, Smith CR, et al. Two-year outcomes after transcatheter or surgical aortic-valve replacement. *N Engl J Med.* 2012;366(18):1686-1695.
15. Vach M, Vogelhuber J, Weber M, et al. Feasibility of CT-derived myocardial strain measurement in patients with advanced cardiac valve disease. *Scientific Reports.* 2021;11(1):8793.
16. Vollema EM, Sugimoto T, Shen M, et al. Association of Left Ventricular Global Longitudinal Strain With Asymptomatic Severe Aortic Stenosis: Natural Course and Prognostic Value. *JAMA Cardiol.* 2018;3(9):839-847.

17. Povlsen JA, Rasmussen VG, Vase H, et al. Distribution and prognostic value of left ventricular global longitudinal strain in elderly patients with symptomatic severe aortic stenosis undergoing transcatheter aortic valve replacement. *BMC cardiovascular disorders.* 2020;20(1):506-506.
18. Vollema EM, Sugimoto T, Shen M, et al. Association of Left Ventricular Global Longitudinal Strain With Asymptomatic Severe Aortic Stenosis: Natural Course and Prognostic Value. *JAMA cardiology.* 2018;3(9):839-847.
19. Herrmann S, Störk S, Niemann M, et al. Low-gradient aortic valve stenosis myocardial fibrosis and its influence on function and outcome. *J Am Coll Cardiol.* 2011;58(4):402-412.
20. Magne J, Cosyns B, Popescu BA, et al. Distribution and Prognostic Significance of Left Ventricular Global Longitudinal Strain in Asymptomatic Significant Aortic Stenosis: An Individual Participant Data Meta-Analysis. *JACC Cardiovasc Imaging.* 2019;12(1):84-92.
21. Iwahashi N, Nakatani S, Kanzaki H, Hasegawa T, Abe H, Kitakaze M. Acute improvement in myocardial function assessed by myocardial strain and strain rate after aortic valve replacement for aortic stenosis. *J Am Soc Echocardiogr.* 2006;19(10):1238-1244.
22. Poulsen SH, Søgaard P, Nielsen-Kudsk JE, Egeblad H. Recovery of left ventricular systolic longitudinal strain after valve replacement in aortic stenosis and relation to natriuretic peptides. *J Am Soc Echocardiogr.* 2007;20(7):877-884.
23. Korinek J, Wang J, Sengupta PP, et al. Two-dimensional strain--a Doppler-independent ultrasound method for quantitation of regional deformation: validation in vitro and in vivo. *J Am Soc Echocardiogr.* 2005;18(12):1247-1253.
24. Dandel M, Hetzer R. Echocardiographic strain and strain rate imaging--clinical applications. *Int J Cardiol.* 2009;132(1):11-24.
25. Sitia S, Tomasoni L, Turiel M. Speckle tracking echocardiography: A new approach to myocardial function. *World J Cardiol.* 2010;2(1):1-5.
26. Nagata Y, Takeuchi M, Wu VC-C, et al. Prognostic Value of LV Deformation Parameters Using 2D and 3D Speckle-Tracking Echocardiography in Asymptomatic Patients With Severe Aortic Stenosis and Preserved LV Ejection Fraction. *JACC: Cardiovascular Imaging.* 2015;8(3):235-245.
27. Arbucci R, Lowenstein Haber DM, Rousse MG, et al. Long Term Prognostic Value of Contractile Reserve Assessed by Global Longitudinal Strain in Patients with Asymptomatic Severe Aortic Stenosis. *J Clin Med.* 2022;11(3):689.
28. Povlsen JA, Rasmussen VG, Vase H, et al. Distribution and prognostic value of left ventricular global longitudinal strain in elderly patients with symptomatic severe aortic stenosis undergoing transcatheter aortic valve replacement. *BMC Cardiovascular Disorders.* 2020;20(1):506.
29. Al-Rashid F, Totzeck M, Saur N, et al. Global longitudinal strain is associated with better outcomes in transcatheter aortic valve replacement. *BMC Cardiovascular Disorders.* 2020;20(1):267.
30. Tsampasian V, Panoulas V, Jabbour RJ, et al. Left ventricular speckle tracking echocardiographic evaluation before and after TAVI. *Echo Res Pract.* 2020;7(3):29-38.

31. Lozano Granero VC, Fernández Santos S, Fernández-Golfín C, et al. Sustained Improvement of Left Ventricular Strain following Transcatheter Aortic Valve Replacement. *Cardiology.* 2019;143(1):52-61.
32. Cimino S, Monosilio S, Luongo F, et al. Myocardial contractility recovery following acute pressure unloading after transcatheter aortic valve intervention (TAVI) in patients with severe aortic stenosis and different left ventricular geometry: a multilayer longitudinal strain echocardiographicanalysis. *The International Journal of Cardiovascular Imaging.* 2021;37(3):965-970.
33. Shiino K, Yamada A, Scalia GM, et al. Early Changes of Myocardial Function After Transcatheter Aortic Valve Implantation Using Multilayer Strain Speckle Tracking Echocardiography. *Am J Cardiol.* 2019;123(6):956-960.
34. Kim HJ, Lee SP, Park CS, et al. Different responses of the myocardial contractility by layer following acute pressure unloading in severe aortic stenosis patients. *Int J Cardiovasc Imaging.* 2016;32(2):247-259.
35. Suzuki-Eguchi N, Murata M, Itabashi Y, et al. Prognostic value of pre-procedural left ventricular strain for clinical events after transcatheter aortic valve implantation. *PLoS One.* 2018;13(10):e0205190.
36. Nagata Y, Takeuchi M, Wu VC, et al. Prognostic value of LV deformation parameters using 2D and 3D speckle-tracking echocardiography in asymptomatic patients with severe aortic stenosis and preserved LV ejection fraction. *JACC Cardiovasc Imaging.* 2015;8(3):235-245.
37. Benetos G, Delakis I, Charitos D, et al. Novel computed-tomography derived prognostic markers in patients undergoing TAVI with a self-expanding valve. *European Heart Journal.* 2021;42(Supplement_1):ehab724.0177.
38. Gegenava T, van der Bijl P, Vollema EM, et al. Prognostic Influence of Feature Tracking Multidetector Row Computed Tomography-Derived Left Ventricular Global Longitudinal Strain in Patients with Aortic Stenosis Treated With Transcatheter Aortic Valve Implantation. *Am J Cardiol.* 2020;125(6):948-955.
39. Fukui M, Xu J, Thoma F, et al. Baseline global longitudinal strain by computed tomography is associated with post transcatheter aortic valve replacement outcomes. *J Cardiovasc Comput Tomogr.* 2020;14(3):233-239.
40. Marwan M, Ammon F, Bittner D, et al. CT-derived left ventricular global strain in aortic valve stenosis patients: A comparative analysis pre and post transcatheter aortic valve implantation. *J Cardiovasc Comput Tomogr.* 2018;12(3):240-244.
41. Fukui M, Hashimoto G, Lopes BBC, et al. Association of baseline and change in global longitudinal strain by computed tomography with post-transcatheter aortic valve replacement outcomes. *Eur Heart J Cardiovasc Imaging.* 2021.
42. Tamarappoo B, Han D, Tyler J, et al. Prognostic Value of Computed Tomography-Derived Extracellular Volume in TAVR Patients With Low-Flow Low-Gradient Aortic Stenosis. *JACC Cardiovasc Imaging.* 2020;13(12):2591-2601.
43. Freixa X, Chan J, Bonan R, et al. Impact of coronary artery disease on left ventricular ejection fraction recovery following transcatheter aortic valve implantation. *Catheter Cardiovasc Interv.* 2015;85(3):450-458.
44. Scatteia A, Baritussio A, Bucciarelli-Ducci C. Strain imaging using cardiac magnetic resonance. *Heart Fail Rev.* 2017;22(4):465-476.

45. Schuster A, Stahnke VC, Unterberg-Buchwald C, et al. Cardiovascular magnetic resonance feature-tracking assessment of myocardial mechanics: Intervendor agreement and considerations regarding reproducibility. *Clin Radiol.* 2015;70(9):989-998.
46. Musa TA, Uddin A, Swoboda PP, et al. Cardiovascular magnetic resonance evaluation of symptomatic severe aortic stenosis: association of circumferential myocardial strain and mortality. *J Cardiovasc Magn Reson.* 2017;19(1):13.
47. Hwang J-w, Kim SM, Park S-J, et al. Assessment of reverse remodeling predicted by myocardial deformation on tissue tracking in patients with severe aortic stenosis: a cardiovascular magnetic resonance imaging study. *Journal of Cardiovascular Magnetic Resonance.* 2017;19(1):80.
48. Chester E, Pierpont G, Weir EK, Francis GS, Shafer R. Limitations of Echocardiography in Measuring Left Ventricular Ejection Fraction in Coronary Artery Disease. *American Journal of Noninvasive Cardiology.* 1987;1:166-170.

Chapter 3: Feasibility and Clinical Value of 3-Dimensional Myocardial Deformation Analysis by Computed Tomography in Transcatheter Aortic Valve Replacement Patients

A version of this chapter will be submitted for publication – JACC Imaging.

3.1 INTRODUCTION

Degenerative aortic stenosis (AS) has become the most prevalent valvular heart disease in developing countries with increasing annual incidence due to an aging population [1]. Transcatheter aortic valve replacement (TAVR) has been shown to reduce mortality compared to conservative medical treatment in patients with severe AS [2]. While initially introduced as an alternative to surgical aortic valve replacement (SAVR) in high or prohibitive surgical risk patients[3,4], both PARTNER 2[5] and SURTAVI[6,7] trials have now demonstrated TAVR to be non-inferior to SAVR in patients at intermediate risk, establishing strong momentum towards the expanded use of TAVR for management of severe AS across broader referral populations.

The routine clinical adoption of ECG-gated, multi-phase reconstructed computed tomography angiography (CTA) for the pre-procedural planning of TAVR has greatly assisted in reducing peri-procedural complications in this referral population[8]. However, following valve deployment, downstream heart failure (HF) hospitalization and mortality remains prevalent at intermediate periods of clinical follow-up. In the high-risk cohort of the PARTNER COHORT A Trial heart failure hospitalization and death were seen at 2-years with a respective prevalence of 47% and 34% [5]. By comparison, in the low-risk population of the SUTAVI trial 2-year heart failure hospitalization and mortality rates were lower, however, remained clinically relevant at 13% and 12%, respectively. Overall, rapidly expanding need exists for novel approaches aimed at

predicting future risk of these major cardiovascular outcomes following TAVR to assist in identifying those who may derive maximal benefit from targeted or personalized care strategies.

Risk scores play an important prognostic role and are used in the clinical setting for prediction of procedural and periprocedural outcomes after TAVR. The logistic EuroSCORE (European System for Cardiac Operative Risk Evaluation) and the Society of Thoracic Surgeons (STS) score are the most commonly used. However, both have their limitations in predicting outcomes[9]. The EurosSCORE was shown to overestimate the periprocedural risk in TAVR, especially in high-risk patients and was abandoned. The EuroSCORE II and STS score are more accurate for TAVR patients and are therefore currently in use to estimate risk of death in patients undergoing TAVR[10,11]. The current construct for assessing patients pre-TAVR emphasizes the evaluation of symptoms, hemodynamics, and reduced left ventricular ejection fraction as the main determinants for intervention. Recent work, however, has shown that structural and functional changes from left and right sided chambers relate to the clinical outcomes[12], which suggests that additional markers are needed to optimize selection of patients for TAVR and for earlier intervention.

Structural remodelling and alterations in contractile health of the cardiac chambers has been shown to be predictive of clinical outcomes following TAVR [12-25]. Of several investigated markers, strain of the ventricular tissue has emerged as a powerful non-invasive imaging marker with incremental value to LVEF for the prediction of adverse outcomes in patients with AS[13,26,27]. To date, studies have focussed on 2D-based approaches for estimating tissue deformations along pre-defined axes that are produced by visualizing the LV by its long and

short-axis views by either 2D echocardiography[28] or using similarly reconstructed 2D planes from multi-phase CT[29]. However, native deformations of the LV are recognized to be complex and multi-axial, representing the summation of forces delivered from helically-oriented myocardial fibres [30]. Multi-phase CTA provides a unique potential to assess these native, multi-axial deformations and represent them in their locally dominant orientation. This can be achieved through principal strain (PS) analysis, an approach describing the amplitude and timing of deformation along its local inherent axis of maximal deformation [31,32]. The value of this unique approach to assist in the prediction of clinical outcomes following TAVR from multi-phase CTA datasets has not been previously explored.

In this study, we sought to assess the feasibility and predictive value of 3D myocardial deformation analysis (3D-MDA) based principal strain from routinely performed multi-phase gated CTA for the prediction of HF hospitalization or all-cause mortality in patients undergoing TAVR. The incremental predictive value of 3D PS was assessed in the context of and adjusted for all baseline clinical and imaging variables currently available in routine clinical practice.

3.1.1 Research Questions

The following research questions were posed in conducting this study:

1. Is it feasible to compute global peak minimum principal strain (min-PS) from multiphase computed tomography (CT) images in both single source and dual source CT scanners?
2. Does 3D minPS improve risk stratification in the TAVR patients and what is the prognostic value it offers over the clinical and echocardiography characteristics?

Answering these research question will allow us to determine the utility of minPS in the TAVR population and plan future projects that will involve patients from multi-centres for the sake of

building a deep neural network for the prediction of patients' clinical outcomes from pre-procedural images regularly obtained pre-TAVR. This work may aid in guiding the clinical decisions and surgical plans of TAVR patients in the future.

3.2 METHODS

3.2.1 Study Population

This was a single centre, cohort study of retrospectively identified patients meeting inclusion criteria who underwent TAVR for severe AS at the Libin Cardiovascular Institute between January 1st, 2017 and August 30th, 2021 (**Figure 1**). For study enrolment, all patients were required to have had a retrospective ECG gated contrast enhanced CTA with 10 cardiac phase reconstruction within 90 days prior to TAVR and to have been followed for a minimum of 6 months post TAVR.

Inclusion criteria

1. Patient must be Age ≥18 years of age or older *(*There is no upper age limit for eligibility in this study)
2. Ability to provide informed consent
3. Patients underwent comprehensive clinical evaluation by the heart team and deemed appropriate to undergo TAVR in accordance with clinical guidelines[33,34].
4. Successfully completed a pre-procedural computed tomography with ECG gating at 10% interval within the 0-90% of the cardiac cycle with contrast enhancement of the left ventricle (10 phase reconstructed image).

5. Severe aortic stenosis, defined as mean trans-valvular gradient ≥40 mmHg and aortic valve area < 1 cm^2, as assessed by trans-thoracic echocardiography or invasive hemodynamics performed at the local institution.
6. Patients should be symptomatic as assessed by the heart team with primary dyspnea or having symptoms like angina pectoris or syncope associated with aortic stenosis.

Exclusion criteria

1. Patients in active cardiogenic shock or with recent myocardial infarction (≤3 months)
2. Inadequate CT data to perform strain analysis:
    a. CT image reconstructed into more or less than 10 phase reconstruction.
    b. Bad image quality.
    c. Left ventricle not captured fully by CT image.
    d. CT motion artifacts creating through plane discontinuity or cross-sectional stair stepping, blurring, or streaking.
3. Non-conditional cardiac pacemaker or implantable defibrillator
4. Contraindications to receiving iodinated contrast dye

3.2.2 Ethics Approval

The study design was approved by the Conjoint Health Research Ethics Board at the University of Calgary (REB13-0902) and all patients provided written informed consent. All research activities were performed in accordance with the Declaration of Helsinki.

Figure 1. Study flow chart.

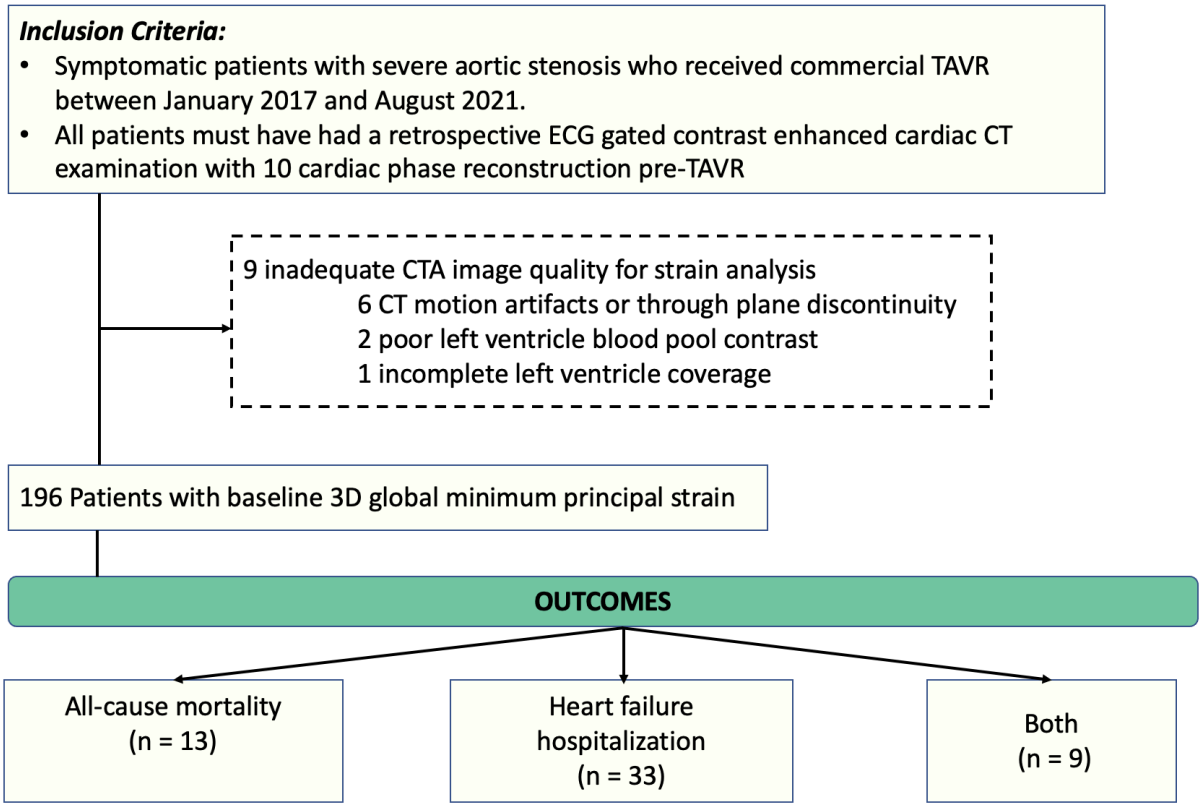

CTA, computed tomography angiography; TAVR, transcatheter aortic valve replacement, 3D, 3-dimentional, ECG, electrocardiogram.

3.2.3 Clinical Characteristics

Patient's demographic information, past medical history and cardiac risk factors were obtained from both the APPROACH (Alberta Provincial Project for Outcome Assessment in Coronary Heart Disease) Registry and the Cardiovascular Imaging Registry of Calgary (CIROC, NCT04367220). Electronic medical record were reviewed to adjudicate New York Heart Association (NYHA) functional status, Canadian Cardiovascular Society (CCS) angina grade, laboratory values, coronary catheterization data (significant coronary artery obstruction ≥2 vessels defined as ≥75% stenosis or left main ≥50%, peak and mean pulmonary artery systolic pressures), pre- and post-procedural echocardiography data, TAVR access route and valve type,

and other variables that permit for the calculation of the Society of Thoracic Surgeons (STS) scores.

3.2.4 Outcomes

The primary endpoint for the study was the composite outcome of all-cause mortality or hospitalization for heart failure after TAVR. Events were defined from date of procedure to last day of medical record interrogation on 24 April 2022. Occurrence of death was obtained from the municipal civil registries (Vital Statistics) and adjudicated through chart review. Heart failure hospitalization data was obtained using health ministry databases and ICD-10 codes. All heart failure hospitalizations were adjudicated by review of medical records. The definition of heart failure hospitalization was standardized in the examination of clinical events[35]. The first event of death or heart failure hospitalization during the follow-up period was used as the primary endpoint and analyzed.

3.2.5 Echocardiography Imaging Acquisition

Comprehensive transthoracic echocardiograph (TTE) examinations were performed as per institutional TAVR protocol at the time of initial referral (baseline assessment), immediately prior to discharge post-procedure and 3-months post procedure. Echocardiography was performed using a commercially available ultrasound system equipped with a 1-5 MHz transducer (iE33, Philips Medical Systems, Andover Massachusetts). Imaging acquisitions and measurements were performed according to current guidelines. Routine ECG-gated, 2D cine loops and Doppler imaging acquisitions from three consecutive beats in sinus rhythm and five in atrial fibrillation were obtained. Echocardiography variables were collected retrospectively for all patients. LV end-diastolic and end-systolic volumes were measured and used to calculate

ejection fraction (EF) using the biplane method of disks summation (Simpson's method). The aortic valve area was calculated using the continuity equation and indexed to body surface area, and the peak and mean systolic transvalvular pressure gradient was estimated using the modified Bernoulli equation[36]. Measured LV wall thickness was used to calculate LV mass and indexed to body surface area. LA volume was measured using the biplane method of disks in apical 2- and 4-chamber views[37], and indexed to body surface area (BSA) to calculate left atrial volume index (LAVi). Measured LV diastolic function parameters included left atrial volume index (LAVI), pulsed-wave Doppler early (E) and late (A) diastolic mitral inflow velocities, and averaged septal and lateral mitral annular e' tissue Doppler velocities. RA pressure estimation was based on interrogation of the inferior vena cava diameter and collapsibility and pulsed-wave Doppler interrogation of hepatic vein flow. Pulmonary artery (PA) systolic pressure (PASP) was estimated from the peak continuous-wave Doppler velocity of TR plus the estimated RA pressure. The severity of valvular regurgitation was determined on a qualitative scale (none, mild, moderate, and severe) according to the current guidelines[34].

3.2.6 Computed Tomography Imaging Acquisition

CT examination pre-TAVR were performed using three scanners over the course of the study period from January 2017 to August 2021. In the early phase of pre-TAVR planning at our institution 2017-2019, CTA imaging acquisition was performed using a wide detector CT scanner with single heartbeat acquisition (Revolution CT, GE Healthcare, Waukesha, Wisconsin, US) with 256 x 0.625 mm collimation; temporal resolution=140 ms; rotation time 0.28 sec or with multi-heartbeat acquisition (Discovery CT750 HD, GE Healthcare, Milwaukee Wisconsin) with 62 x 0.625 mm collimation; temporal resolution 228 ms; rotation time 0.35 sec. Later, CTA

acquisition using a dual-source CT scanner (Somatom Force, Siemens Medical Solutions, Forchheim, Germany) was added with 192 x 0.6 mm collimation; temporal resolution = 66 ms; rotation time 0.25 sec. The tube voltage was set at 100 or 120 kVp, and Smart-mA was used to determine the tube current. Prospective gating with axial acquisition was used to cover the entire cardiac cycle, with dose modulation commonly engaged to maximize tube current during systolic phase for aortic annulus measurements. Intravenous contrast (Optiray®, Ioversol injection, Guerbet, Villepinte, France) dose ranged from 60 – 100 mL at a rate of 5 – 6 mL/sec, depending on the body mass index (BMI) of the patient and renal function. Images were acquired craniocaudally, from the aortic arch to the diaphragm over the entire cardiac cycle with ECG gating. Functional datasets were reconstructed using a standard algorithm at 10% intervals within the 0% to 90% of the cardiac cycle resulting in 10 images per heart cycle with a slice thickness 0.625 mm. No additional radiation dose was needed to perform CTA-derived strain analysis. Data sets were anonymized and transferred offline to a stand-alone workstation for further analysis.

3.2.7 Multi-chamber CT Whole Heart Segmentation and Meshing

CT image analysis was initiated by the generation of a static 3D mesh cardiac model from phase 1 data of each multi-phase dataset. This was accomplished using a trained multi-chamber segmentation algorithm (Simpleware ScanIP Medical version S-2021.06, Bradninch Hall, Castle Street, Exeter, UK). A unique application dependent pipeline was personalized for the needs of this project **(Figure 2).** Briefly, the different aspect of this pipeline included: (1) Importing the 10 multiphase reconstructed CTA image and re-sampling the data for consistency and reducing analysis time. (2) Performing whole-heart segmentation of all cardiac structures and major

cardiac vessels to phase 1 of the multiphase CT image. The complexity of the heart is further increased by the presence on the endocardial layer, papillary muscles, and the trabeculae carneae, which make the inner part of the heart rough and irregular. Manual contouring of the endocardial surface excluding the papillary muscles was performed in all subjects (**Figure 3)**; (3) Whole-heart mesh generation for all cardiac structures and major cardiac vessels were created using 2 separate surface models. Model 1 included aorta, left atrium, epicardium (created through a Boolean function combining LV blood pool with myocardium), pulmonary artery, right atrium and right ventricle. Model 2 included endocardium. Meshes were setup to have an "image" coordinate system and exported; (4) Landmarks of interest important for the 3D- MDA performance were identified and labelled on the LV mesh model in a standardized fashion and then exported in image coordinate system. This included labelling the left ventricle apex, LV basal plane, and left aortic coronary cusp. On average, total contour time, mesh generation and landmarking took 15-20 min per patients.

Figure 2: Methodology explained – from multiphase CTA image to whole heart mesh generation

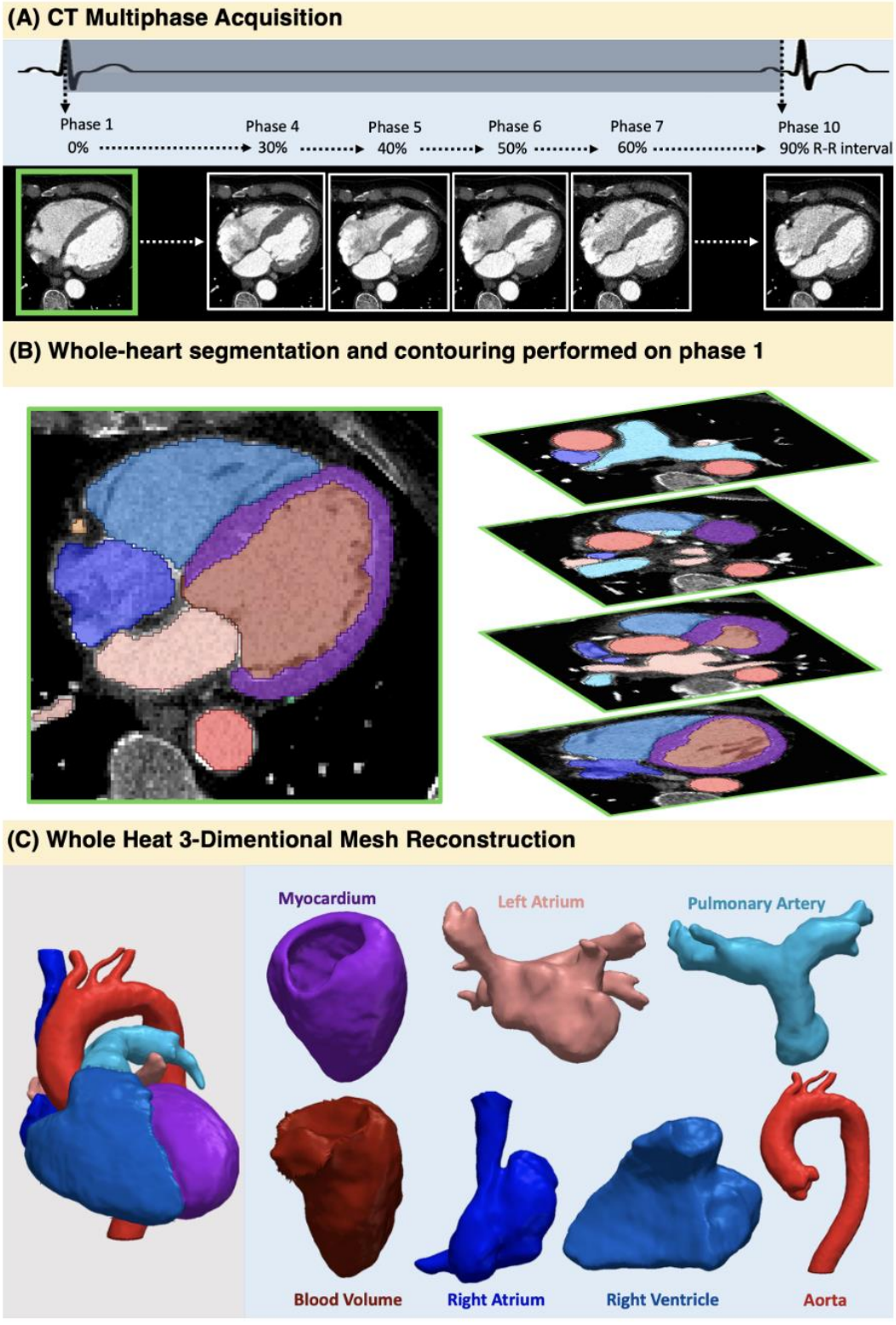

(A) Functional CT datasets are reconstructed using a standard algorithm at 10% intervals within the 0% to 90% of the cardiac cycle resulting in 10 images per heart cycle. **(B)** Phase 1 was used to perform active contouring of all cardiac chambers and major cardiac vessels. **(C)** Whole-heart mesh generation was computed on all chambers and major cardiac vessels.

Figure 3: Contour modification of the endocardial layer

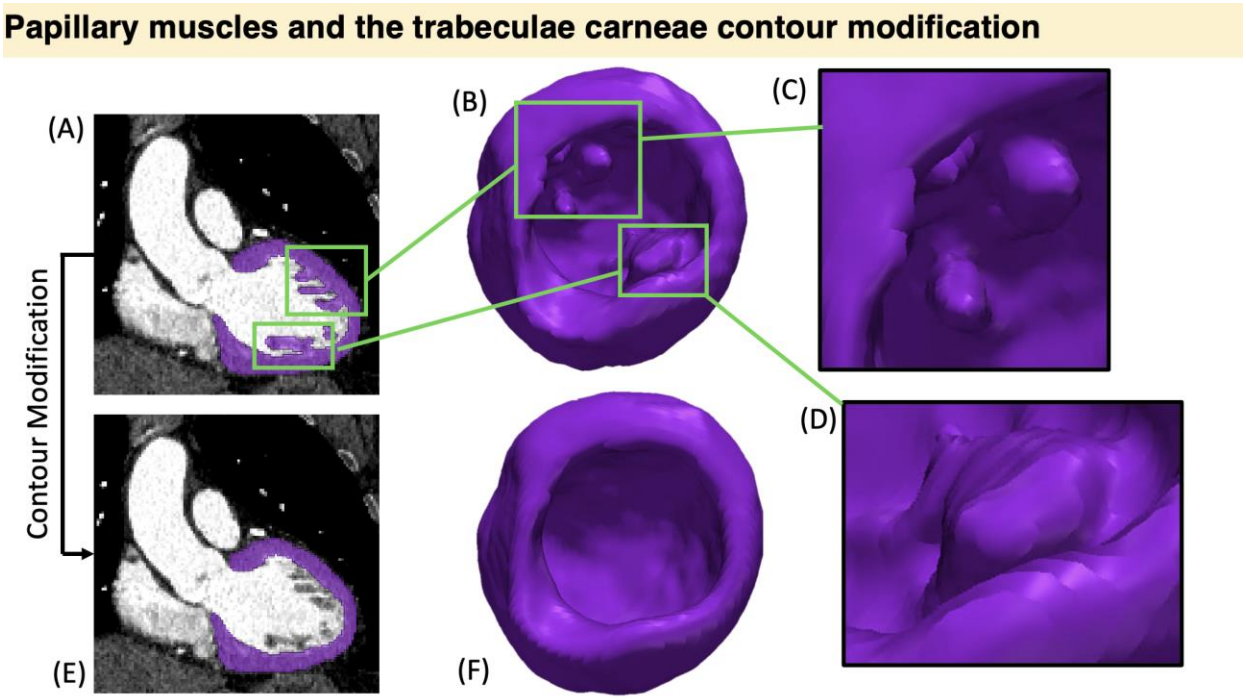

(A) CT image showing the endocardial contour including the papillary muscles and trabeculae as performed by AS Cardio. **(B-C)** A superior view of the LV cavity showing a highly irregular endocardial mesh layer generated with a rough inner surface difficult to track for strain analysis. **(E-F)** Manual contouring of the endocardial surface excluding the papillary muscles and trabeculae generated a smooth endocardial surface suitable for tracking and strain analysis.

3.2.8 3D Myocardial Deformation Analysis (3D-MDA)

3D-MDA analysis was executed from matched 3D single-phase segmentation and multi-phase DICOM data without need for user interaction. Mesh models of cardiac structures were trained

to deform in accordance with this 4D displacement field to deliver a dynamic mesh model upon which estimations of 3D deformation can be established. For the latter, principal strain is used as an axis-independent marker of strain between adjacent elements of the mesh model, this providing vector orientation, amplitude and time to peak amplitude of displacement in the dominant direction of tissue shortening (minimum PS), as previously described[38]. In our current study, global subendocardial, subepicardial and transmural peak-systolic minimum principal strain amplitude values were estimated and reported. Minimum PS represents the maximal shortening of tracked tissue features and is reported as negative strain.

3.3 STATISTICAL ANALYSIS

Descriptive statistics were performed using mean ± standard deviation (SD) for normally distributed continuous variables and median (interquartile range (IQR)) for non-normally distributed variables. Skewness and normality were assessed using the Kolmogorov–Smirnov test. Differences between groups were assessed using the t-test and Chi-squared test for continuous and discrete variables, respectively. A random sample of 10 patients from the study cohort were chosen to determine intraobserver and interobserver variability of global minimum principal strain (endo, epi, and transmural) measurements using intraclass correlation (ICC). Univariable and multivariable Cox proportional hazards analyses were performed to identify predictors of all-cause mortality or heart failure hospitalization. Linearity and proportionality of each covariate in the multivariable model are assessed using the supremum test. Estimated hazard ratios (HR) are reported together with their 95% confidence intervals (CI) and p-values.

Three models were built with covariates selected based on a backward stepwise model that identified variables associated with the primary end-point ($p<0.1$). Covariates in Model 1 were age, atrial fibrillation or flutter, CCS class II and above, STS score, baseline LA volume index, baseline aortic valve peak gradient, global peak endocardial minimum principal strain. Model 2 and Model 3 replaced global peak endocardial minimum principal strain with global peak epicardial minimum principal strain and global peak transmural minimum principal strain respectively. Goodness-of-fit statistics were computed using a 2-Log Likelihood and Akaike information criterion (AIC). The time varying performance of each model was estimated using time-dependent receiver operative characteristics (ROC) approach at 1- and 2- years post TAVR to derive the survival concordance index (c-index) and time specific AUC(t).

Cox proportional hazards models were used to estimate the association between global peak endocardial minimum principal strain and risk of composite outcome. The threshold cut off value for strain was estimated as the relative HR was equal to 1. Survival after TAVR above and below the threshold are displayed using Kaplan-Meier curves and comparison between the two groups via the log-rank test. A two-sided p-value < 0.05 was considered statistically significant. Statistical analyses were performed by using SAS Enterprise Guide 8.3 (SAS Institute, Cary, NC, USA) and R version 4.1.0.

3.4 RESULTS

3.4.1 Baseline Clinical and Non-CTA Imaging Characteristics

A total of 205 consecutive patients met the inclusion criteria with 9 (4%) having inadequate CTA image quality for strain analysis, resulting in 196 subjects**.** Baseline clinical and imaging characteristics are summarized in **Tables 1 and 2**. The cohort had a median age (IQR) of 85

(79.5-88) years and a slight male predominance (55%). Baseline median TTE-LVEF was 60 (55.9-65.0)% with 89% of patients having an LVEF ≥50%. The median STS-PROM score was 3.10 (2.10- 4.55)%. TAVR was successfully performed in all subjects using balloon-expandable (77%) or self-expandable (23%) valves. Baseline TTE's were performed at a median (IQR) of 219 (103–381) days prior to TAVR, while multi-phase CTA was performed a median of 72 (34–134) days prior to the procedure.

Table 1: Demographic and baseline characteristics of all TAVR patients, patients with and patients without occurrence of composite outcome.

	All (n=196)	**With Primary Outcome (n=55)**	**Without Primary Outcome (n=141)**	**p-value**
Age	85 (79.5-88)	85 (78-88)	85 (80-88)	0.47
Male	107 (54.6)	27 (49.1)	80 (56.7)	0.33
Height (m)	167 (157-175)	168 (155-175)	167 (158-175)	0.54
Weight (kg)	76.4 ± 16.6	74.1 ± 17.2	77.2 ± 16.4	0.24
Body surface area (m^2)	1.87 (1.7-2.0)	1.90 (1.6-2.0)	1.85 (1.7-2.0)	0.25
Body mass index(kg/m^2)	26.7 (24.0-30.4)	26.6 (23.0-29.7)	26.8 (24.3-30.7)	0.31
Systolic BP (mmHg)	135.4 ± 20.6	131.5 ± 20.6	136.8 ± 20.5	0.11
Diastolic BP (mmHg)	72.7 ± 11.9	72.0 ± 12.7	73.0 ± 11.6	0.58
Heart Rate (bpm)	69 (61-79)	68 (60-90)	69 (62-78)	0.47
Diabetes	48 (24.5)	15 (27.3)	33 (23.4)	0.57
Hypertension	155 (79.1)	46 (83.6)	109 (77.3)	0.33
Hyperlipidemia	136 (69.4)	40 (72.7)	96 (68.1)	0.53
Smoker				0.10
Never	112 (57.1)	25 (45.5)	87 (61.7)	
Current	12 (6.1)	5 (9.1)	7 (5)	
Past	72 (36.7)	25 (45.5)	47 (33.3)	
Prior myocardial infarction	20(10.2)	7 (12.7)	13 (9.2)	0.47
Prior PCI	39 (19.9)	12 (21.8)	27 (19.1)	0.67
Prior CABG	37 (18.9)	12 (21.8)	25 (17.7)	0.51
Prior stroke or TIA	24 (12.2)	10 (18.2)	14 (9.9)	0.11
Peripheral Vascular Disease	**35 (17.9)**	**17 (30.9)**	**18 (12.8)**	**0.003**
Pulmonary hypertension	48 (24.5)	18 (32.7)	30 (21.3)	0.09
COPD	42 (21.4)	12 (21.8)	30 (21.3)	0.93
Home O_2 dependent	4 (2)	1 (1.8)	3 (2.1)	0.89
Creatinine (µmol/L)	89.5 (71.0-112.5)	88 (74-124)	90 (68-111)	0.35
eGFR (ml/min/1.73 m^2)	64.0 ± 21.7	59.4 ± 22.8	65.8 ± 21.0	0.06

Renal insufficiency (eGFR <45)	63 (32.1)	23 (41.8)	40 (28.4)	0.07
Dialysis	2 (1)	2 (3.6)	0 (0)	**0.02**
Atrial fibrillation or flutter	**38 (19.4)**	**20 (36.4)**	**18 (12.8)**	**<0.001**
NYHA functional class II and above	**156 (79.6)**	**49 (89.1)**	**107 (75.9)**	**0.04**
CCS class II and above	19 (9.7)	8 (14.5)	11 (7.8)	0.15
Syncope	12 (6.1)	2 (3.6)	10 (7.1)	0.36
STS-PROM Score (%)	**3.10 (2.10-4.55)**	**3.6 (2.6-5.2)**	**2.7 (2.0-4.3)**	**0.002**
Obstructive coronary artery disease ≥ 2 vessels[a]	51 (26)	17 (30.9)	34 (24.1)	0.33
Peak PASP (mmHg)	36 (31-46)	39 (32-49)	36 (31-44)	0.18
Mean PASP (mmHg)	23 (19-29)	23 (19-31)	23 (19-28)	0.34
Access route				0.09
Transfemoral	182 (92.9)	50 (90.9)	132 (93.6)	
Transaortic	4 (2)	3 (5.5)	1 (0.7)	
Transaxillary	10 (5.1)	2 (3.6)	8 (5.7)	
Valve type[b]				0.12
Balloon-expandable	150 (76.5)	38 (69.1)	112 (79.4)	
Self-expandable	46 (23.5)	17 (30.9)	29 (20.6)	

Data in bold $p < 0.05$

Numbers are shown as number (%) or mean ± SD or median (Q1-Q3)

BP, blood pressure; PCI, percutaneous coronary intervention, CABG, coronary artery bypass grafting; TIA, transient ischemia attack; COPD, chronic obstructive pulmonary disease; eGFR, estimated glomerular filtration rate; NYHA, New York Heart Association; CCS, Canadian Cardiovascular Society grading of angina pectoris; STS-PROM, Society of Thoracic Surgeons Predicted Risk of Mortality; PASP, pulmonary artery systolic pressure;

[a] Obstructive coronary artery disease defined as narrowing of ≥75 in more than 2 coronary vessels or LM ≥ 50%.

[b] All 150 patients with balloon-expandable received Sapien 3 valves. Among patients with self-expandable valve, 35 Evolute R, 6 Evolute Pro, 5 ACURATE neo

Table 2: Baseline and post procedural Echocardiography and multiphase CTA derived 3-Dimensional Myocardial Deformation (3D-MDA) values of all TAVR patients, patients with and patients without occurrence of composite outcome.

	All (n=196)	With Primary Outcome (n=55)	Without Primary Outcome (n=141)	p-value
Baseline 2D Transthoracic Echocardiography				
Left ventricle ejection fraction (%)	**60 (55.9-65.0)**	**60 (45.0-62.0)**	**60 (57.0-65.0)**	**0.03**
LV mass index (g/m^2)	**102.6 (86-118.5)**	**107 (95-125)**	**99 (82-117)**	**0.01**
LA volume index (ml/m^2)	**36 (28.0-44.0)**	**39 (32-46.3)**	**34 (27-43)**	**0.003**
Aortic valve peak gradient (mmHg)	67 (54.1-80)	62.7(50-75.9)	70 (57-81)	0.06
Aortic valve mean gradient (mmHg)	38.8(30.7-46.1)	37.0 (27.9-46.0)	39.0 (31.8-46.1)	0.16
Aortic valve area index (cm^2/m^2)	0.44 (0.36-0.51)	0.41 (0.35-0.52)	0.45 (0.36-0.51)	0.17
TAPSE (cm)	**2.0 ± 0.5**	**1.9 ± 0.5**	**2.1 ± 0.5**	**0.002**
Mitral regurgitation ≥ moderate	22 (11.2)	9 (16.4)	13 (9.2)	0.15
Tricuspid regurgitation ≥ moderate	22 (11.2)	10 (18.2)	12 (8.5)	0.05
Post-Procedural 2D Transthoracic Echocardiography				
Post-procedural aortic insufficiency				0.53
None/trivial	173 (88.3)	46 (83.6)	127 (90.1)	
Mild	16 (8.2)	7 (12.7)	9 (6.4)	
Moderate	7 (3.6)	2 (3.6)	5 (3.5)	
Severe	0 (0)	0 (0)	0 (0)	
Post-procedural aortic peak gradient (mmHg)	20.75 (15.45-25.90)	21.0 (15.5-26.0)	20.4 (15.0-25.8)	0.71
Post-procedural aortic mean gradient (mmHg)	9.65 (7.45-12.25)	9.3 (7.0-12.0)	9.7 (7.5-12.6)	0.99
3D CT-Derived Strain Markers				
Global peak endocardial minimum principal strain (%)	**-23.7 (-26.6 to -20.4)**	**-21.6 (-23.9 to -16.0)**	**-24.5 (-26.7 to -21.5)**	**<0.001**
Global peak epicardial minimum principal strain (%)	**-11.6 (-13.2 to -9.9)**	**-10.4 (-12.2 to -8.8)**	**-12.0 (-13.3 to -10.2)**	**<0.001**
Global peak transmural minimum principal strain (%)	**-18.7 (-21.1 to -15.9)**	**-17.6 (-19.8 to -14.3)**	**-19.1 (-21.5 to -16.7)**	**0.002**

Data in bold $p < 0.05$

Numbers are shown as number (%) or mean ± SD or median (Q1-Q3)

LV, left ventricle; LA, left atrium; TAPSE, Tricuspid annular plane systolic excursion.

3.4.2 Intra-observer and Inter-observer Variability

Intra-observer and inter-observer reliability were assessed for 3D-CT minPS assessment given user interaction still required for initial 3D segmentation adjustments. This showed strong respective agreements with ICC's of 0.98 (95% CI, 0.91-0.99) and 0.97 (95% CI, 0.89-0.99) for minPS measured at the endocardial layer. Similar findings were observed for epicardial and transmural strain values (**Table 3**).

Table 3: Intra-observer repeatability and inter-observer reliability among different strain parameters

Parameter	**Intra-observer repeatability**	**Inter-observer reliability**
	ICC (95% CI)	**ICC (95% CI)**
Endocardial minPS	0.98 (0.91-0.99)	0.97 (0.89-0.99)
Epicardial minPS	0.96 (0.82-0.99)	0.84 (0.60-0.96)
Transmural minPS	0.97 (0.88-0.99)	0.95 (0.82-0.98)

3.4.3 Primary Composite Clinical Outcome

Over a median (IQR) follow up of 25 (11–36) months, 55 patients (28%) experienced a composite outcome (13 all-cause death, 33 heart failure hospitalization, 9 both). As shown in Table 1, patients experiencing the primary outcome were more likely to have peripheral vascular disease, atrial fibrillation or flutter, NYHA class ≥2, and higher STS scores. Numerous echocardiographic parameters were also associated with the primary outcome, inclusive of LV mass index, LA volume index, LV EF and TAPSE.

Patients experiencing the primary outcome demonstrated significantly reduced minPS amplitudes compared to those without the primary outcome. Consistent and significant

differences in minPS amplitude was observed across sub-endocardial, transmural, and sub-epicardial derived measures of minimum PS. Peak endocardial minPS amplitude (%) was -21.6% (-23.9 to -16.0%) in event positive patients vs -24.5% (-26.7 to -21.5) in event negative (p<0.001). Corresponding values for transmural minPS were -17.6% (-19.8 to -14.3%) vs -19.1% (-21.5 to -16.7%) (p=0.002) while sub-epicardial minPS (%) was -10.4 (-12.2 to -8.8) vs -12.0 (-13.3 to -10.2) (p<0.001**) (Figure 4**).

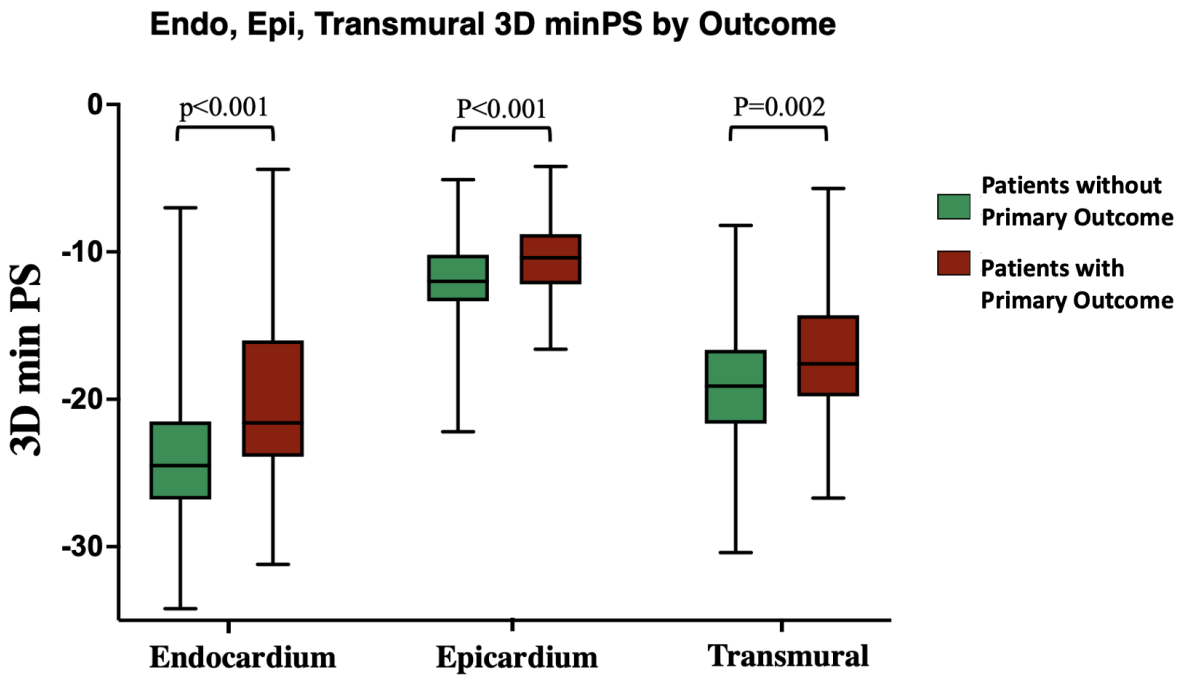

Figure 4: Box plots of endocardial, epicardial and transmural 3D min PS comparing patients with and without the primary composite outcome.

3.4.4 CT 3D-MDA and Associations with the Composite Clinical Outcome

To assess for the independent prognostic value of endocardial, transmural and epicardial 3D minPS from routine multi-phase CTA versus conventional risk markers, univariable and separate multivariable models inclusive of all relevant baseline clinical and echocardiographic variables with separate entry of each layer-specific global PS marker were constructed (**Table 4**). In all

three models, age, atrial fibrillation, CCS class ≥II, STS-PROM score, and baseline LA volume index consistently maintained independent associations with the primary composite outcome (TTE-derived LVEF not independently associated with the primary outcome). Adjusting for these variables, peak endocardial minPS, peak transmural minPS and peak epicardial minPS each showed independent prognostic value with adjusted hazards per 1% change of 1.09 (1.05-1.15, p<0.001), 1.21 (1.09-1.36, p<0.001), and 1.11 (1.03-1.19, p=0.004), respectively. The performance of the three models was further compared using time-dependent statistics to identify the prognostic value of each model. While all models performed well, endocardial min-PS showed greater improvement in C-index and AUC suggesting best risk prediction among the three models (**Table 5**).

Table 4: Cox regression analysis for a composite outcome of all-cause mortality or heart failure hospitalization

	Univariable		**Multivariable**					
			Model 1		**Model 2**		**Model 3**	
	HR (95% CI)	**p -value**	**HR (95% CI)**	**p -value**	**HR (95% CI)**	**p -value**	**HR (95% CI)**	**p -value**
Age (per 1 year)	0.97 (0.94-1.00)	0.08	0.96 (0.93-1.00)	0.04	0.96 (0.93-1.00)	0.04	0.96 (0.93-1.00)	0.04
Male	0.82 (0.72-2.07)	0.47						
Diabetes	1.32 (0.42-1.38)	0.36						
Hypertension	1.34 (0.36-1.52)	0.42						
Hyperlipidemia	1.27 (0.44-1.43)	0.44						
PVD	**2.24 (0.25-0.79)**	**0.006**						
PHTN	1.54 (0.37-1.14)	0.13						
COPD	0.96 (0.55-1.97)	0.91						
Creatinine (per 10 mmol/L)	**1.03 (1.01- 1.06)**	**0.01**						
Dialysis	**4.83 (0.05-0.86)**	**0.03**						
Atrial fibrillation or flutter	**3.08 (0.19-0.57)**	**<0.001**	2.33 (1.24-4.36)	0.008	2.54 (1.36-4.74)	0.003	2.3 (1.23-4.30)	0.009
NYHA class II and above	2.29 (0.19-1.02)	0.06						
CCS class II and above	1.91 (0.25-1.11)	0.09	2.54 (1.17-5.51)	0.02	2.26 (1.05-4.87)	0.04	2.37 (1.10-5.123)	0.03

STS- PROM Score (per 1%)	1.11 (1.00-1.23)	0.05	1.15 (1.04-1.28)	0.008	1.13 (1.02-1.25)	0.02	1.14 (1.03-1.27)	0.012
Obstructive CAD	1.32 (0.43-1.34)	0.34						
Peak PASP (per 1 mmHg)	**1.03 (1.01-1.05)**	**0.02**						
LVEF (per 1%)	**0.96 (0.94-0.98)**	**<0.001**						
LVMi (per 1 g/m^2)	**1.01 (1.01-1.02)**	**0.03**						
LAVi (per 1 ml/m^2)	**1.03 (1.01-1.05)**	**0.003**	1.03 (1.00-1.05)	0.02	1.02 (1.00-1.05)	0.03	1.03 (1.00-1.05)	0.02
Baseline AV peak gradient (per 1 mmHg)	0.99 (0.98-1.00)	0.09	0.99 (0.98-1.00)	0.06	0.99 (0.97-1.00)	0.02	0.99 (0.98-1.00)	0.04
Baseline AV mean gradient (per 1 mmHg)	0.98 (0.96-1.00)	0.12						
TAPSE (per 0.1 cm)	**0.90 (0.85-0.96)**	**<0.001**						
Degree of TR (Moderate and Above)	**2.12 (0.24-0.94)**	**0.03**						
Endocardial minPS (per 1%)	**1.10 (1.05-1.15)**	**<0.001**	1.09 (1.04-1.15)	<0.001				
Epicardial minPS (per 1%)	**1.20 (1.08-1.33)**	**<0.001**			1.21 (1.09-1.36)	<0.001		
Transmural minPS (per 1%)	**1.12 (1.05-1.19)**	**<0.001**					1.11 (1.03-1.19)	0.004

Data in bold $p < 0.05$

Model 1variable are age, atrial fibrillation or flutter, CCS class, STS score, baseline LAVi, baseline aortic valve peak gradient and global peak endocardial minimum principal strain.

Model 2 replaces global peak endocardial minimum principal strain with Global peak epicardial minimum principal strain.

Model 3 replaces Global peak endocardial minimum principal strain with Global peak transmural minimum principal strain.

PVD, peripheral vascular disease; PHTN, pulmonary hypertension; COPD, chronic obstructive pulmonary disease; NYHA, New York Heart Association; CCS, Canadian Cardiovascular Society grading of angina pectoris; STS-PROM, Society of Thoracic Surgeons Predicted Risk of Mortality; CAD, coronary artery disease; PASP, pulmonary artery systolic pressure; LVEF, left ventricle ejection fraction; LVMi, left ventricle mass index; LAVi; Left atrial volume index; AV, aortic valve; TAPSE, tricuspid Annular Plane Systolic Excursion; TR, tricuspid regurgitation; minPS, minimum principal strain.

Table 5: Prognostic value of 3D CT- derived minimum principal strain

	Model 1	Model 2	Model 3
Model fit statistics			
Global Chi-square test	44.9	44.3	40.9
AIC	497.2	498.2	501.6
Performance of the models			
C-index (95% CI)	0.76 (0.55-0.88)	0.75 (0.55-0.87)	0.74 (0.52-0.86)
AUC (*t*) at *t*=1 year (95% CI)	0.76 (0.49-0.89)	0.74 (0.51-0.88)	0.72 (0.47-0.87)
AUC (*t*) at *t*=2 years (95% CI)	0.77 (0.53-0.88)	0.75 (0.54-0.87)	0.73 (0.50-0.86)

Model 1 variable are age, atrial fibrillation or flutter, CCS class, STS score, baseline LAVi, baseline aortic valve peak gradient and global peak endocardial minimum principal strain.
Model 2 replaces global peak endocardial minimum principal strain with Global peak epicardial minimum principal strain.
Model 3 replaces Global peak endocardial minimum principal strain with Global peak transmural minimum principal strain.
AIC, Alkaike's an information criterion; AUC, area under curve.

3.4.5 Survival Free of Composite Outcome Based on Principal Strain Threshold

Optimal threshold values were determined by performing cubic-spline-based analyses of relative hazards for the composite outcome adjusted for age and gender (**Supplementary Figure 1**). As shown in **Figure 5**, using a threshold of -23.7%, Kaplan–Meier analysis revealed significant differences in composite outcomes for patient with endocardial minPS above versus below this value. Patients with lower strain (values above -23.7%) experienced a 3-fold higher rate of heart failure hospitalization or death (HR = 2.97; 95% CI, 1.63,5.39; p<0.001) with respective cumulative event rates of 32% vs 20% at 1 year, and 49% vs 39% at 2 years. Similar observations were seen for epicardial minPS (Model 2) and transmural min-PS (Model 3) (**Supplementary Figures 2**).

Figure 5: Relative hazard of death or heart failure hospitalization by baseline 3D CT endocardial minPS.

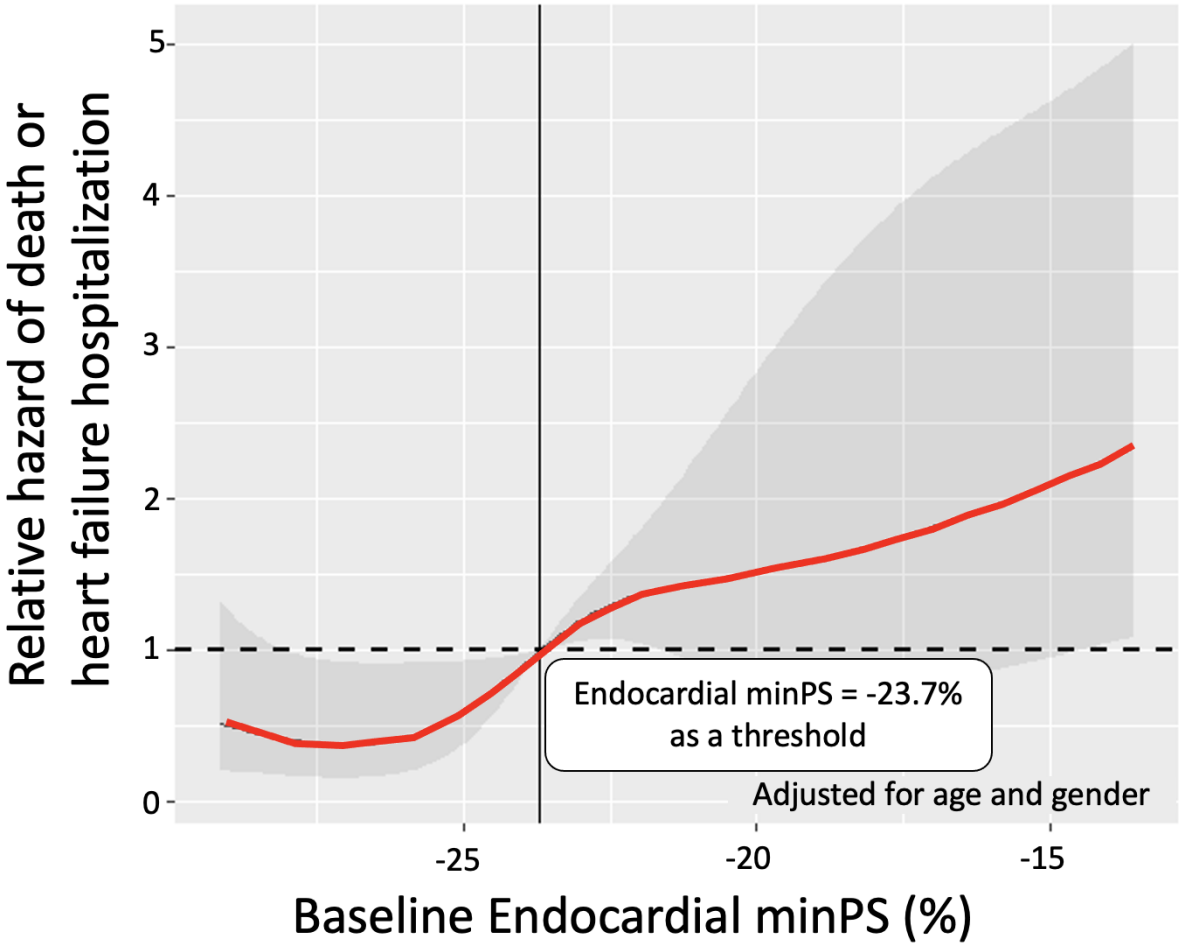

As baseline endocardial minPS worsens, the relative hazard of composite outcome of all cause death or heat failure hospitalization after TAVR adjusted for age and gender also increases with -23.7% as threshold of endocardial minPS.

Figure 6: Event Free Survival Curves Based on Left Ventricle 3D Myocardial Deformation Analysis

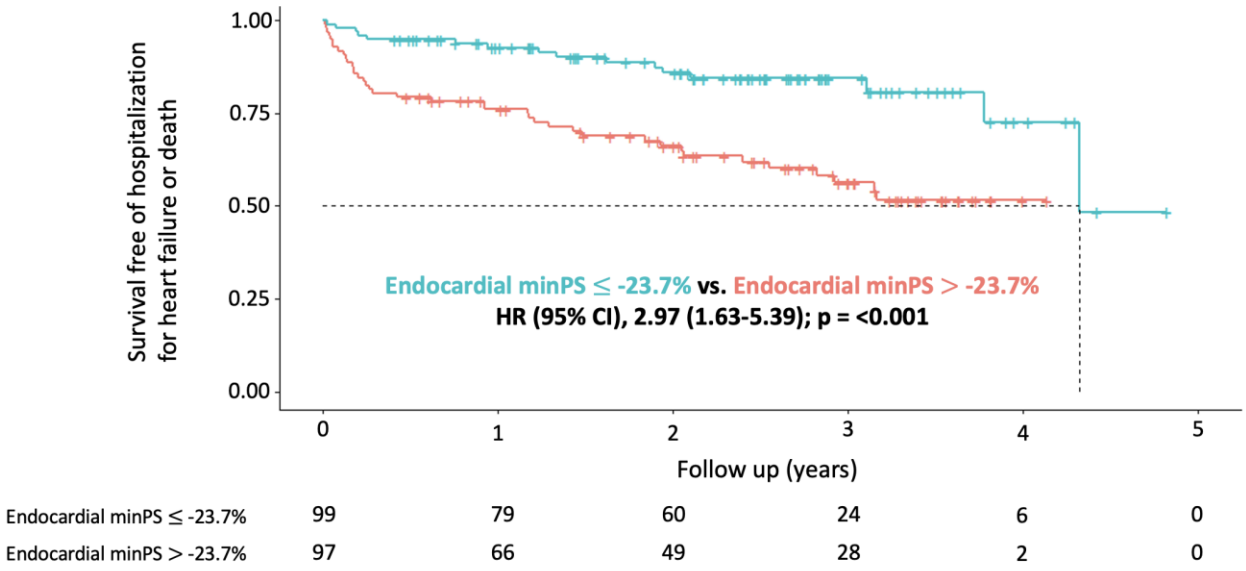

Patients with baseline endocardial minPS> −23.7% had higher risk of composite outcome than those with endocardial minPS ≤ −23.7%

3.5 DISCUSSION

In this study we demonstrated the feasibility and prognostic value of 3D principal strain analysis from multi-phase CTA to predict future heart failure hospitalization or death in patients referred for TAVR. We identified CTA minPS to be an independently predictive marker of future clinical outcomes following adjustment for all baseline clinical and echocardiographic variables. To our knowledge, this is the first study to evaluate the role of 3D CTA-derived PS to predict future clinical outcomes in patients referred for TAVR.

3.5.1 Three-dimensional Myocardial Deformation Analysis Highly Feasible in TAVR

Several prior retrospective cohort studies have evaluated CT-derived strain analysis using 2D techniques among patients undergoing TAVR, accomplished through the reconstruction of multi-phase 3D datasets into standard long and/or short axis 2D imaging planes. In a study with 214

patients by Gegenava *et. al.* [39], over a median follow up of 45 months, 2D LV GLS was independently associated with all cause mortality with hazard ratio of 0.85 and an identified threshold of -14%. A more recently published study by Fukui *el. al.* estimated 2D global longitudinal strain (2D-GLS) from multi-phase CTA datasets obtained in 431 patients undergoing TAVR [40]. Over a median follow up period of 19 months, patients with a GLS below -18.2% experienced a 1.77 fold increased risk of all-cause death or heart failure hospitalization. This was independent of age, LVEF, TAPSE, degree of mitral or tricuspid regurgitation, coronary artery disease and AV mean gradient. While both studies looked at 2D LV strain, the results remain consistent with the current study where we have also identified 3D minPS below −23.7% to be independently associated with the outcome with a 3 fold higher rate in mortality and heart failure hospitalization.

In addition, the work performed by Fukui *el. al.* [40] has demonstrated a high feasibility up to 97% of obtaining global longitudinal strain using only dual source CT scanners. In another study however, that looked at the use of single source CT scanners a much lower feasibility was reported (23%) [41]. What is novel about the present study is the ability to compute 3D geometry independent markers of LV deformation using both single source and dual source CT technology with feasibly up to 96%. This is also a much higher feasibility when compared to other modalities such as echocardiography where it is reported to be as low as 60% due to the high dependence on adequate echocardiographic windows [42].

3.5.2 Left Ventricle Minimum Principal Strain is Highly Predictive of Clinical Outcomes

In a third study, Fukui *et. al.* [23] looked at 223 consecutive patients with pre-TAVR retrospective gated acquisition CT study to evaluate the prognostic value of CT GLS with all-cause mortality and hospitalization for heart failure after TAVR. Patients with normal LVEF (≥50%) but reduced CT GLS (> -20.5%) had higher rate of all-cause mortality and risk of composite outcome when compared to patients with normal LVEF and preserved CT GLS (≤-20.5%). The results held true even for patients with impaired LVEF. In a multi-variable Cox regression analysis, reduced CT GLS was independently associated with all-cause mortality and the risk of composite outcome despite adjustment for multiple clinical and echocardiographic characteristics. In the present study, LV EF, which is usually central in clinical assessment of TAVR patients, only predicted mortality in the univariate analysis. The loss of LVEF as an independent predictor in the multivariable analysis can be explained by the deferential response of the left ventricle with concentric remodeling or hypertrophy in this patient population. Our results demonstrate that 3D LV minPS is a powerful marker and its inclusion in any of the three-models created superseded LV EF in the prognostication of patients.

3.5.3 Prognostic Value of 3D Left Ventricle Principal Strain

In the present study, endocardial minPS (Model 1) provides the best prediction of the composite outcome at 1 and 2 years post-TAVR with an AUC of 0.76 and 0.77 respectively. When looking at epicardial minPS (Model 2) and transmural minPS (Model 3), the models performance remains comparably high with an AUC of 0.75 and 0.73 respectively at 2 years. This is consistent with previous work performed in 3D CMR by Tanacli *et. al.* and colleagues [43] that revealed LV GLS measured selectively at the epicardial layer has an increasing potential to diagnose HFpEF and discriminate early phases of contractile impairment. One potential

explanation takes into consideration that the pericardium is a rigid membrane that contains movement of the heart towards the exterior and therefore the confounding effect of shear strain is absent at the epicardial level which may explain the good performance of epicardial strain in our study when compared to endocardial strain [44]. In addition, the PARTNER Cohort B study indicated standard medical treatment was associated with a cardiovascular mortality of 63% and repeat hospitalisation of 73% at two-year follow up [45]. The lack of effective medical management emphasizes the importance of timing of aortic intervention to reverse the functional deterioration and remodeling; ultimately restoring prognosis. This present study demonstrates that in a TAVR cohort with severe aortic stenosis and mostly preserved ejection fraction, a sub-group of patients can be identified to have a higher risk of composite outcome simply by analysing their pre-existing CT datasets in a process that takes less than 20 minutes. This novel technique holds the potential to greatly improve the current treatment algorithms in TAVR.

3.5.4 Transition to Using Novel CT Derived 3D Axis Independent Markers of Tissue Deformation

Incremental to these studies, we demonstrate capacity of strain markers to be derived leveraging the complete 3D representation of a chamber throughout its cardiac cycle, and to describe its tissue deformations using 3D PS. There is a growing body of evidence supporting an incremental value of 3D PS over 2D-based descriptions of strain to deliver improved descriptors of myocardial health [31,32,46], with expanding use seen in both CMR [47-50] and 3D-echocardiography[51-54]. However, the expanded clinical use of multi-phase 3D CTA presents a novel and clinically relevant target for this technique. Inherently suited for the study of natively 3D datasets, PS-based analyses are ubiquitously applicable across geometrically complex structures that fail to

conform to pre-defined axes. The latter, such as the atria and right ventricle, are of increasing interest for the prediction of cardiovascular outcomes post TAVR [55-57].

3.5.5 Left Atrial Contribution to Clinical Outcomes

Interestingly our study also identifies LAVi to be an independent predictor of clinical outcomes. This is in agreement with previous studies that have been conduction in the aortic stenosis population where LAVi was identified as an independent predictor of mortality[58]. In TAVR patients, LA enlargement is the reflection of chronically elevated LV filling pressures necessary to maintain adequate LV filling and cardiac output. In addition, the occurrence of symptoms in severe AS is associated with impairment in diastolic function, LV hypertrophy, concentric remodelling and LA dilation[59]. Taken together, future work will need to assess LA volume and LA strain profiles which is of great importance as multiple obstacles are acting on the LA including increased LA filling pressure, valvular obstacles, and LV remodelling. Our study shows a signal for those markers, and further work will need to be carried to verify those observations. Accordingly, 3D PS may offers a foundational approach to the delivery of multi-chamber phenotyping and prediction modelling in this patient population. Several prior studies have explored capacity to execute 3D PS-based analysis from multi-phase CTA [31,32,46,55-57]. However, to date none have focused on its role to predict clinical outcomes in patients undergoing TAVR like demonstrated in the current study.

3.5.6 Clinical Implications

There are several clinical implications of this cohort study. Our study highlights the potential of CT derived functional assessment in patients undergoing TAVR. Treatment with TAVR in

recent years has shifted from being offered to high-risk patients, to include intermediate and low risk patients many of which have normal LV function. The defined AHA/ ESC guidelines for undergoing TAVR will be challenging to apply in a population where in most cases LV EF remains normal [60,61]. Therefore, evaluating a more sensitive marker like 3D minPS may offer more insight into patients' suitability for surgery.

The capacity to leverage routinely performed pre-procedural multi-phase CTA for the delivery of post-procedural outcome prediction offers an elegant and cost-effective strategy for improved decision making and personalized care strategies in patients referred for TAVR. The accurate identification of patients with high likelihood of post-procedural freedom from heart failure or death may provide valuable assistance in decision making for both patients and clinicians. Further, patients at higher likelihood of such events may directly benefit from targeted surveillance or personalized care pathways to reduce the risk of re-admission for heart-failure related complications. Accordingly, future studies aimed at assessing the impact of such prediction tools on clinical decision making and their capacity to support personalized care strategies are required.

3.6 LIMITATIONS

Several limitations are recognized in this study. Our results reflect those of a single-center study, and therefore external validation in a unique clinical setting is required. Our study did not compare 3D-based strain analyses to 2D-based analyses given lack of availability of software used to derive the latter. Based on prior work 3D-based strain analyses deliver unique descriptions of deformation that, for axis-dependent strain markers, are typically of lower amplitude[62]. Accordingly, direct comparison is not advised. This acknowledged, a comparison of

the predictive value delivered by these respective techniques is of importance for future work. Normal reference values for CTA-derived strain are inherently lacking due to challenges surrounding use of ionizing radiation in healthy volunteers. Accordingly, we were not able to provide reference values for health. However, for the described role of discriminating risk of future cardiovascular events in a target referral population this is not inherently required.

3.7 CONCLUSITONS

This is the first study to assess the prognostic value of 3D principal strain from pre-procedural multi-phase CTA for the prediction of future cardiovascular outcomes in patients undergoing TAVR. We identified high feasibility and reproducibility with strong predictive utility for the identification of patients at elevated risk of future heart failure admission or death. The unique capacity of 3D principal strain to deliver a ubiquitous descriptor of contractile health across all chamber architectures presents unique opportunity for its expansion toward multi-chamber phenotyping in this referral population.

3.8 SUPPLEMENTARY FIGURES

Supplementary figure 1: Relative hazard of death or heart failure hospitalization by baseline 3D CT minPS (epicardial and transmural)

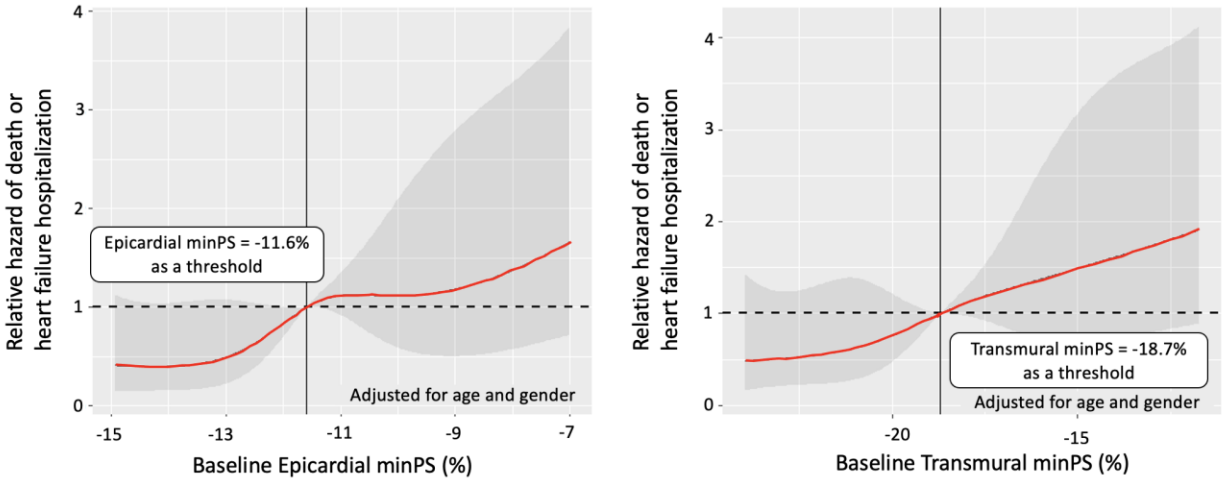

As baseline epicardial and transmural minPS worsen, the relative hazard of composite outcome of all cause death or heat failure hospitalization after TAVR adjusted for age and gender also increases with -11.6% and -18.7% as threshold, respectively.

Supplementary figure 2: Event Free Survival Curves Based on Left Ventricle 3D Myocardial Deformation Analysis for Epicardial and Transmural Strain

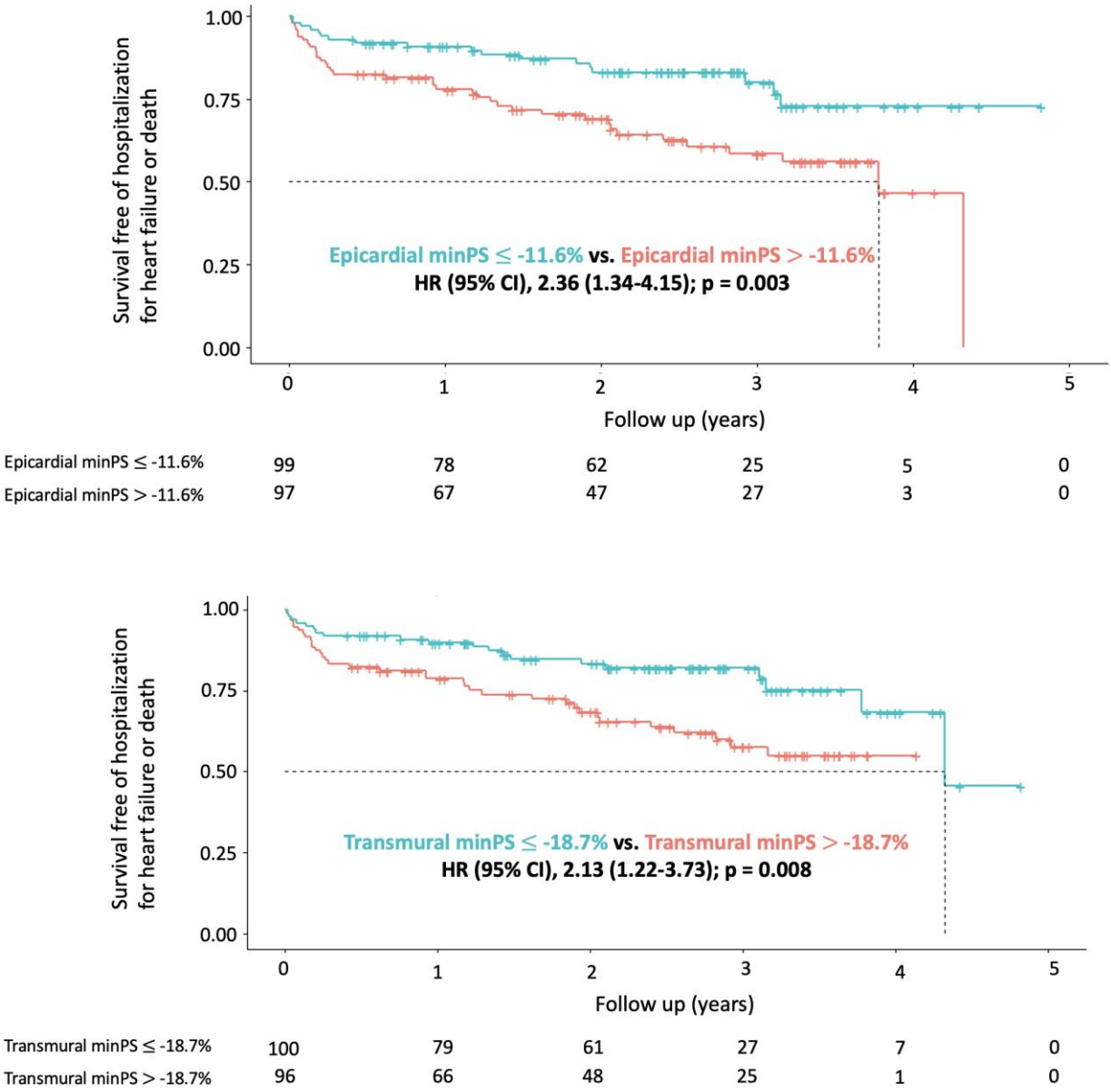

(Top) Patients with baseline epicardial minPS $> -11.6\%$ had higher risk of composite outcome than those with epicardial minPS $\leq -11.6\%$. **(Bottom)** Patients with baseline transmural minPS $> -18.7\%$ had higher risk of composite outcome than those with transmural minPS $\leq -18.7\%$

3.8 REFERENCE

1. Carabello BA, Paulus WJ. Aortic stenosis. *The Lancet.* 2009;373(9667):956-966.
2. Takeji Y, Taniguchi T, Morimoto T, et al. Transcatheter aortic valve implantation versus conservative management for severe aortic stenosis in real clinical practice. *PLoS One.* 2019;14(9):e0222979-e0222979.
3. Leon MB, Smith CR, Mack M, et al. Transcatheter aortic-valve implantation for aortic stenosis in patients who cannot undergo surgery. *N Engl J Med.* 2010;363(17):1597-1607.
4. Smith CR, Leon MB, Mack MJ, et al. Transcatheter versus surgical aortic-valve replacement in high-risk patients. *N Engl J Med.* 2011;364(23):2187-2198.
5. Leon MB, Smith CR, Mack MJ, et al. Transcatheter or Surgical Aortic-Valve Replacement in Intermediate-Risk Patients. *N Engl J Med.* 2016;374(17):1609-1620.
6. Reardon MJ, Van Mieghem NM, Popma JJ, et al. Surgical or Transcatheter Aortic-Valve Replacement in Intermediate-Risk Patients. *N Engl J Med.* 2017;376(14):1321-1331.
7. Barbanti M, Petronio AS, Ettori F, et al. 5-Year Outcomes After Transcatheter Aortic Valve Implantation With CoreValve Prosthesis. *JACC Cardiovasc Interv.* 2015;8(8):1084-1091.
8. Ina Tamburino C, Barbanti M, Tamburino C. Transcatheter aortic valve implantation: how to decrease post-operative complications. *European Heart Journal Supplements.* 2020;22(Supplement_E):E148-E152.
9. Holinski S, Jessen S, Neumann K, Konertz W. Predictive Power and Implication of EuroSCORE, EuroSCORE II and STS Score for Isolated Repeated Aortic Valve Replacement. *Ann Thorac Cardiovasc Surg.* 2015;21(3):242-246.
10. Stähli BE, Tasnady H, Lüscher TF, et al. Early and late mortality in patients undergoing transcatheter aortic valve implantation: comparison of the novel EuroScore II with established risk scores. *Cardiology.* 2013;126(1):15-23.
11. Piazza N, Wenaweser P, van Gameren M, et al. Relationship between the logistic EuroSCORE and the Society of Thoracic Surgeons Predicted Risk of Mortality score in patients implanted with the CoreValve ReValving system--a Bern-Rotterdam Study. *Am Heart J.* 2010;159(2):323-329.
12. Fukui M, Gupta A, Abdelkarim I, et al. Association of Structural and Functional Cardiac Changes With Transcatheter Aortic Valve Replacement Outcomes in Patients With Aortic Stenosis. *JAMA Cardiol.* 2019;4(3):215-222.
13. Fukui M, Hashimoto G, Lopes BBC, et al. Association of baseline and change in global longitudinal strain by computed tomography with post-transcatheter aortic valve replacement outcomes. *Eur Heart J Cardiovasc Imaging.* 2022;23(4):476-484.
14. Al-Rashid F, Totzeck M, Saur N, et al. Global longitudinal strain is associated with better outcomes in transcatheter aortic valve replacement. *BMC Cardiovascular Disorders.* 2020;20(1):267.
15. Tsampasian V, Panoulas V, Jabbour RJ, et al. Left ventricular speckle tracking echocardiographic evaluation before and after TAVI. *Echo Res Pract.* 2020;7(3):29-38.
16. Lozano Granero VC, Fernández Santos S, Fernández-Golfín C, et al. Sustained Improvement of Left Ventricular Strain following Transcatheter Aortic Valve Replacement. *Cardiology.* 2019;143(1):52-61.

17. Cimino S, Monosilio S, Luongo F, et al. Myocardial contractility recovery following acute pressure unloading after transcatheter aortic valve intervention (TAVI) in patients with severe aortic stenosis and different left ventricular geometry: a multilayer longitudinal strain echocardiographicanalysis. *The International Journal of Cardiovascular Imaging.* 2021;37(3):965-970.
18. Shiino K, Yamada A, Scalia GM, et al. Early Changes of Myocardial Function After Transcatheter Aortic Valve Implantation Using Multilayer Strain Speckle Tracking Echocardiography. *Am J Cardiol.* 2019;123(6):956-960.
19. Suzuki-Eguchi N, Murata M, Itabashi Y, et al. Prognostic value of pre-procedural left ventricular strain for clinical events after transcatheter aortic valve implantation. *PLoS One.* 2018;13(10):e0205190.
20. Vach M, Vogelhuber J, Weber M, et al. Feasibility of CT-derived myocardial strain measurement in patients with advanced cardiac valve disease. *Scientific Reports.* 2021;11(1):8793.
21. Benetos G, Delakis I, Charitos D, et al. Novel computed-tomography derived prognostic markers in patients undergoing TAVI with a self-expanding valve. *European Heart Journal.* 2021;42(Supplement_1):ehab724.0177.
22. Gegenava T, van der Bijl P, Vollema EM, et al. Prognostic Influence of Feature Tracking Multidetector Row Computed Tomography-Derived Left Ventricular Global Longitudinal Strain in Patients with Aortic Stenosis Treated With Transcatheter Aortic Valve Implantation. *Am J Cardiol.* 2020;125(6):948-955.
23. Fukui M, Xu J, Thoma F, et al. Baseline global longitudinal strain by computed tomography is associated with post transcatheter aortic valve replacement outcomes. *J Cardiovasc Comput Tomogr.* 2020;14(3):233-239.
24. Marwan M, Ammon F, Bittner D, et al. CT-derived left ventricular global strain in aortic valve stenosis patients: A comparative analysis pre and post transcatheter aortic valve implantation. *J Cardiovasc Comput Tomogr.* 2018;12(3):240-244.
25. Fukui M, Hashimoto G, Lopes BBC, et al. Association of baseline and change in global longitudinal strain by computed tomography with post-transcatheter aortic valve replacement outcomes. *Eur Heart J Cardiovasc Imaging.* 2021.
26. Fukui M, Thoma F, Sultan I, et al. Baseline Global Longitudinal Strain Is Associated With All-Cause Mortality After Transcatheter Aortic Valve Replacement. *JACC Cardiovasc Imaging.* 2020;13(4):1092-1094.
27. Ng ACT, Prihadi EA, Antoni ML, et al. Left ventricular global longitudinal strain is predictive of all-cause mortality independent of aortic stenosis severity and ejection fraction. *Eur Heart J Cardiovasc Imaging.* 2018;19(8):859-867.
28. Dandel M, Lehmkuhl H, Knosalla C, Suramelashvili N, Hetzer R. Strain and strain rate imaging by echocardiography - basic concepts and clinical applicability. *Curr Cardiol Rev.* 2009;5(2):133-148.
29. Buss SJ, Schulz F, Mereles D, et al. Quantitative analysis of left ventricular strain using cardiac computed tomography. *Eur J Radiol.* 2014;83(3):e123-130.
30. Voigt J-U, Cvijic M. 2- and 3-Dimensional Myocardial Strain in Cardiac Health and Disease. *JACC Cardiovasc Imaging.* 2019;12(9):1849-1863.
31. Tanabe Y, Kido T, Kurata A, et al. Three-dimensional maximum principal strain using cardiac computed tomography for identification of myocardial infarction. *Eur Radiol.* 2017;27(4):1667-1675.

32. Pedrizzetti G, Sengupta S, Caracciolo G, et al. Three-Dimensional Principal Strain Analysis for Characterizing Subclinical Changes in Left Ventricular Function. *Journal of the American Society of Echocardiography.* 2014;27(10):1041-1050.e1041.
33. Baumgartner H, Falk V, Bax JJ, et al. 2017 ESC/EACTS Guidelines for the management of valvular heart disease. *Eur Heart J.* 2017;38(36):2739-2791.
34. Otto CM, Nishimura RA, Bonow RO, et al. 2020 ACC/AHA Guideline for the Management of Patients With Valvular Heart Disease: A Report of the American College of Cardiology/American Heart Association Joint Committee on Clinical Practice Guidelines. *Circulation.* 2021;143(5):e72-e227.
35. Kappetein AP, Head SJ, Généreux P, et al. Updated standardized endpoint definitions for transcatheter aortic valve implantation: The Valve Academic Research Consortium-2 consensus document∗. *The Journal of Thoracic and Cardiovascular Surgery.* 2013;145(1):6-23.
36. Baumgartner HC, Hung JC-C, Bermejo J, et al. Recommendations on the echocardiographic assessment of aortic valve stenosis: a focused update from the European Association of Cardiovascular Imaging and the American Society of Echocardiography. *Eur Heart J Cardiovasc Imaging.* 2017;18(3):254-275.
37. Lester SJ, Ryan EW, Schiller NB, Foster E. Best method in clinical practice and in research studies to determine left atrial size. *Am J Cardiol.* 1999;84(7):829-832.
38. Satriano A, Afzal Y, Sarim Afzal M, et al. Neural-Network-Based Diagnosis Using 3-Dimensional Myocardial Architecture and Deformation: Demonstration for the Differentiation of Hypertrophic Cardiomyopathy. *Front Cardiovasc Med.* 2020;7:584727-584727.
39. Gegenava T, van der Bijl P, Vollema EM, et al. Prognostic Influence of Feature Tracking Multidetector Row Computed Tomography-Derived Left Ventricular Global Longitudinal Strain in Patients with Aortic Stenosis Treated With Transcatheter Aortic Valve Implantation. *The American Journal of Cardiology.* 2020;125(6):948-955.
40. Fukui M, Hashimoto G, Lopes BBC, et al. Association of baseline and change in global longitudinal strain by computed tomography with post-transcatheter aortic valve replacement outcomes. *European Heart Journal - Cardiovascular Imaging.* 2022;23(4):476-484.
41. Fukui M, Xu J, Abdelkarim I, et al. Global longitudinal strain assessment by computed tomography in severe aortic stenosis patients - Feasibility using feature tracking analysis. *Journal of Cardiovascular Computed Tomography.* 2019;13(2):157-162.
42. Macron L, Lairez O, Nahum J, et al. Impact of acoustic window on accuracy of longitudinal global strain: a comparison study to cardiac magnetic resonance. *Eur J Echocardiogr.* 2011;12(5):394-399.
43. Tanacli R, Hashemi D, Neye M, et al. Multilayer myocardial strain improves the diagnosis of heart failure with preserved ejection fraction. *ESC Heart Fail.* 2020;7(5):3240-3245.
44. Lee JM, Boughner DR. Mechanical properties of human pericardium. Differences in viscoelastic response when compared with canine pericardium. *Circ Res.* 1985;57(3):475-481.
45. Kodali SK, Williams MR, Smith CR, et al. Two-year outcomes after transcatheter or surgical aortic-valve replacement. *N Engl J Med.* 2012;366(18):1686-1695.

46. Yoshida K, Tanabe Y, Kido T, et al. Characteristics of the left ventricular three-dimensional maximum principal strain using cardiac computed tomography: reference values from subjects with normal cardiac function. *Eur Radiol.* 2020;30(11):6109-6117.
47. Spath NB, Gomez M, Everett RJ, et al. Global Longitudinal Strain Analysis Using Cardiac MRI in Aortic Stenosis: Comparison with Left Ventricular Remodeling, Myocardial Fibrosis, and 2-year Clinical Outcomes. *Radiology: Cardiothoracic Imaging.* 2019;1(4):e190027.
48. Satriano A, Heydari B, Narous M, et al. Clinical feasibility and validation of 3D principal strain analysis from cine MRI: comparison to 2D strain by MRI and 3D speckle tracking echocardiography. *Int J Cardiovasc Imaging.* 2017;33(12):1979-1992.
49. Satriano A, Afzal Y, Sarim Afzal M, et al. Neural-Network-Based Diagnosis Using 3-Dimensional Myocardial Architecture and Deformation: Demonstration for the Differentiation of Hypertrophic Cardiomyopathy. *Front Cardiovasc Med.* 2020;7:584727.
50. Liu B, Dardeer AM, Moody WE, et al. Reference ranges for three-dimensional feature tracking cardiac magnetic resonance: comparison with two-dimensional methodology and relevance of age and gender. *Int J Cardiovasc Imaging.* 2018;34(5):761-775.
51. Nagata Y, Takeuchi M, Wu VC, et al. Prognostic value of LV deformation parameters using 2D and 3D speckle-tracking echocardiography in asymptomatic patients with severe aortic stenosis and preserved LV ejection fraction. *JACC Cardiovasc Imaging.* 2015;8(3):235-245.
52. Vitarelli A, Mangieri E, Capotosto L, et al. Assessment of Biventricular Function by Three-Dimensional Speckle-Tracking Echocardiography in Secondary Mitral Regurgitation after Repair with the MitraClip System. *J Am Soc Echocardiogr.* 2015;28(9):1070-1082.
53. Schueler R, Sinning JM, Momcilovic D, et al. Three-dimensional speckle-tracking analysis of left ventricular function after transcatheter aortic valve implantation. *J Am Soc Echocardiogr.* 2012;25(8):827-834.e821.
54. Broch K, de Marchi SF, Massey R, et al. Left Ventricular Contraction Pattern in Chronic Aortic Regurgitation and Preserved Ejection Fraction: Simultaneous Stress-Strain Analysis by Three-Dimensional Echocardiography. *J Am Soc Echocardiogr.* 2017;30(4):422-430.e422.
55. Aquino GJ, Decker JA, Schoepf UJ, et al. Computed tomographic assessment of right ventricular long axis strain for prognosis after transcatheter aortic valve replacement. *Eur J Radiol.* 2022;149:110212.
56. Fukui M, Sorajja P, Hashimoto G, et al. Right ventricular dysfunction by computed tomography associates with outcomes in severe aortic stenosis patients undergoing transcatheter aortic valve replacement. *J Cardiovasc Comput Tomogr.* 2022;16(2):158-165.
57. Aquino GJ, Decker JA, Schoepf UJ, et al. Utility of Functional and Volumetric Left Atrial Parameters Derived From Preprocedural Cardiac CTA in Predicting Mortality After Transcatheter Aortic Valve Replacement. *AJR Am J Roentgenol.* 2022;218(3):444-452.
58. Rusinaru D, Bohbot Y, Kowalski C, Ringle A, Maréchaux S, Tribouilloy C. Left Atrial Volume and Mortality in Patients With Aortic Stenosis. *Journal of the American Heart Association.*6(11):e006615.

59. Dahl JS, Christensen NL, Videbæk L, et al. Left Ventricular Diastolic Function Is Associated With Symptom Status in Severe Aortic Valve Stenosis. *Circulation: Cardiovascular Imaging.* 2014;7(1):142-148.
60. Nishimura RA, Otto CM, Bonow RO, et al. 2014 AHA/ACC Guideline for the Management of Patients With Valvular Heart Disease: executive summary: a report of the American College of Cardiology/American Heart Association Task Force on Practice Guidelines. *Circulation.* 2014;129(23):2440-2492.
61. Vahanian A, Beyersdorf F, Praz F, et al. 2021 ESC/EACTS Guidelines for the management of valvular heart disease: Developed by the Task Force for the management of valvular heart disease of the European Society of Cardiology (ESC) and the European Association for Cardio-Thoracic Surgery (EACTS). *European Heart Journal.* 2021;43(7):561-632.
62. Amzulescu MS, Langet H, Saloux E, et al. Improvements of Myocardial Deformation Assessment by Three-Dimensional Speckle-Tracking versus Two-Dimensional Speckle-Tracking Revealed by Cardiac Magnetic Resonance Tagging. *Journal of the American Society of Echocardiography.* 2018;31(9):1021-1033.e1021.

Chapter 4: Proposal for Validation study

4.1 INTRODUCTION

The next phase of this project is to validate the work that has been done against another imaging modality. In this section, we will discuss the planned proposal that is underway to accomplish this goal. We have been able so far to perform 3D-MDA on computed tomography images to compute LV principal strain with a plan to apply this to multi-chamber analysis from multi-phase CT. The retrospective study discussed here with 196 patients who successfully undergone TAVR and subsequently followed for a minimum of 6 months combined with other centres TAVR populations will help achieve a deep neural network able to identify features from combined data resources, inclusive of raw mesh-based data, chamber-specific principal strain, and electronic health information to predict the future occurrence of heart failure admission or death at 1, 2 and 3 years after the successful results at our institution.

This validation study aims to demonstrate i) cross-modality validation for CT- derived 3D-MDA measures of principal strain (PS), ii) correlation of CT-derived PS measures to MRI-based measures of myocardial fibrosis, iii) estimation of influence from valvular obstruction on myocardial deformation, and iv) among patients completing TAVR, describe preliminary associations between 3D-MDA based chamber markers and 3-month improvement in patient health.

4.2 STUDY OBJECTIVES

- **Primary objectives**
  - Validate and compare multi-phase CT-derived 3D-MDA and echocardiography 3D-MDA techniques as a surrogate of MRI-derived 3D-MDA (reference standard technique) in a cohort of patients referred for TAVR.
- **Secondary objectives**
  - Identify associations between 3D-MDA based markers of LV tissue deformation and MRI-based markers of tissue health using T1-mapping.
  - Identify associations between 3D-MDA markers of LA, LV and Aortic deformation with hemodynamic measures of valvular disease using 4D Flow MRI.
  - Describe associations between imaging-based markers of disease and standardized assessments of cardiovascular and global patient health, adjusting for frailty.

4.3 METHODS

This is a prospective cohort study aimed at recruiting a total of 20 patients referred for multi-phase CT imaging as part of a routine pre-procedural assessment for TAVR.

Patients will be approached for informed consent to undergo a 2.5-hour in-person visit at the Stephenson Cardiac Imaging Centre within 30 days of planned CT study. Inclusion and exclusion criteria are listed below. The baseline research assessment includes: i) standardized patient health questionnaires, ii) 6-minute hall walk test (6-MHWT), iii) Edmonton Frailty Assessment, iv) quality of life and Seattle angina questionnaire, v) Contrast-enhanced cardiac MRI study, vi) 3D-echocardiography acquisition added to the pre-operative echocardiogram done before surgery.

Clinically ordered laboratory blood work and 12-lead ECGs will be captured from the electronic health record. Patients will be seen in-person at 3-months in the TAVR follow-up clinic for repeat questionnaires, 6MHWT and Frailty assessments. Patients may be contacted for up to 5 years for the documentation of clinical health complications and vital status.

All patients will be booked to undergo clinical imaging on a Siemens Force CT. A routine clinical TAVR imaging protocol will be followed with HR and BP recorded at time of imaging. Images will be reconstructed and digitally stored at 5% intervals for optimal multi-phased reconstruction to conduct 3D-MDA. A 3D echocardiograph will be organized to occur either during the planned pre-procedural echo or shortly after CT performance. A 60-minute cardiac MRI imaging protocol will be completed, as described below. Image analyses will be performed according to standardized operational procedures (SOPs), inclusive of matched 3D-MDA analyses of the left ventricle and left atrium.

For all patients completing TAVR, a follow-up research visit will be conducted and coordinated with time of clinic follow-up in the TAVR clinic, this being scheduled for 3-months post-procedure. Patients will undergo repeat clinical assessments, questionnaires, frailty and 6-minute hall walk test. In addition, a repeat MRI study will be performed to evaluate for alterations in cardiac function, myocardial health and flow.

Beyond the 3-month research visit, patients will be tracked remotely for a period of 5 years using electronic health records to document admissions to hospital and occurrence of death. The latter will be achieved in conjunction with data provided by Vital Statistics Alberta as well as by telephone contact, as required.

4.3.1 Study Population

- **Inclusion Criteria:**
  1) Age ≥18 years of age
  2) Ability to provide informed consent
  3) NYHA class ≥II or CCS class ≥II
  4) Severe aortic stenosis, defined as mean trans-valvular gradient ≥40 mmHg and aortic valve area < 1 cm^2, as assessed by trans-thoracic echocardiography or invasive hemodynamics performed at the local institution
  5) Referred for multi-phase CT TAVR imaging protocol, regardless of LVEF.

- **Exclusion Criteria**
  1) Permanent or persistent atrial fibrillation.
  2) Paroxysmal atrial fibrillation with history of sustained atrial fibrillation (>24 hours) in the 6 months prior to recruitment.
  3) Severe mitral valve disease (stenosis or insufficiency)
  4) Concurrent obstructive epicardial coronary disease, defined as ≥70% lesion in ≥1 epicardial vessel on left main disease >50% (*eligible if successful PCI ≥4 weeks prior to baseline imaging procedures).
  5) Severe kidney disease (eGFR<30 mL/min/1.73m^2).
  6) Known hypersensitivity or contraindication to gadolinium contrast
  7) Non-conditional cardiac pacemaker or implantable defibrillator
  8) Standard contra-indications to MRI
  9) Pregnant women

4.3.2 Study Subject Recruitment

Patients will be *recruited* from outpatient and in-patient clinical cardiology services upon decision to refer patients for pre-procedural CT imaging. Recruitment will be performed in coordination with the TAVR clinic and coordinators of both the Interventional cardiology and Cardiac Surgery programs.

4.3.3 Imaging Protocols

- **Echocardiography 3D-STE Protocol**

Speckle tracking echocardiography (STE) analyzes LV deformation by tracking cardiac motion from image intensities. Features being tracked can include image contours and image textures, more specifically looking at the natural specked pattern of the myocardium when it is imaged by ultrasound. Using the conventional B-mode images, 3D-STE can be performed. The most common approach used is block matching which is dependent on the local tissue motion and can extract the displacement of the speckle pattern from one frame to another. 3D images will be acquired in the full volume mode with the focus on the LV chamber from a single cardiac cycle during coordinated breath holds. Frame rate will be optimized to >20 frames/s by focusing imaging sector size. Volumetric strain analysis of the 3D images will be performed using a commercially available software system (4D LV-Analysis version 3.0; TomTec Imaging Systems, Unterschleissheim, Germany). Endocardial border is contoured in three standard LAX views, the software then uses a speckle tracking algorithm to generate a 3D LV endocardial surface mesh model throughout the cardiac cycle. Epicardial contours can also be applied. The left ventricle is divided into 16 segments and a right ventricle insertion point is identified. This will allow for the computation of regional longitudinal, circumferential, and radial strain.

- **Cardiac MRI Protocol**

All patients will undergo a standardized Cardiac MRI protocol on a 3 Tesla Siemens scanner (Prisma or Skyra, Siemens Healthineers, Germany). A summary of the CMR imaging protocol is as follows:

Imaging Protocol (estimated duration 60 minutes):

- Scout images / localizers
- Cine imaging (30 phases): Short axis, 2, 3 and 4 chamber views, RV 2 chamber view
- Axial cine stack of ascending / descending thoracic aorta (15 slices)
- Non-contrast T1 mapping (MOLLI): Basal, Mid and Apical short axis + 4 chamber
- Non-contrast T2 mapping (T2-prep SSFP): Basal, Mid and Apical short axis + 4 chamber
- 0.1 mmol/L Gadolinium macrocyclic chelate agent (Gadovist®, Bayer Inc.) given
- intravenously by 18-guage peripheral intravenous cannula
- IR-GRE Late Gadolinium Enhancement LGE): Short axis, 2, 3 and 4 chamber
- 15-minute T1 mapping (MOLLI): Basal, Mid and Apical short axis + 4 chamber
- 2D Phase contrast flow imaging of the aortic and mitral valves
- 4D Flow Whole Heart (respiratory navigated): VENC 250 cm/sec

4.4 PLANNED ANALYSIS

4.4.1 Cardiac MRI Analysis

Standard core laboratory analyses will be performed in accordance to Stephenson Core Laboratory SOPs. This will include routine volumetric analysis of cine MR images using commercial software (cvi[42], Circle Cardiovascular Imaging Inc, Calgary, Canada) to determine LV end-diastolic volume (LVEDV), LV end-systolic volume (LVESV), LV ejection fraction

(LVEF), LV mass and LA maximal volume. Left atrial volumes will be measured at the LV end-systolic phase prior to mitral valve opening using the bi-plane area-length method from temporally matched 4- and 2-chamber cine views. Where appropriate, volume and mass measurements will be indexed to body surface area (BSA), calculated using the Mosteller formula.

4.4.2 3D-MDA

3D feature tracking-based strain analysis will be performed using locally developed and previously validated software[1]. For cardiac MRI-based datasets, an end-diastolic 3D mesh of the LV and LA will be created from long axis views followed by automated slice-based alignment to perpendicular imaging planes. Feature tracking is performed for all pixels on each cine slice throughout the cardiac cycle[1]. A 3D velocity field will be generated, for MRI this considering slice orientation, in-plane resolution, and distance from each node from the 3D LV mesh. Each node of the mesh is instructed on its motion throughout the cardiac cycle by the 3D velocity field. Using a finite-element approach, deformation for each element will be projected in radial, circumferential and longitudinal, as well as local principal directions, in order to compute corresponding strain amplitudes, peak-systolic timing and rate[1]. CT-based segmentation will be delivered through the same method used in chapter 3 using (Simpleware™ AS Cardio module, Synopsys) and the in house 3D-MDA developed software for CTA images.

4.4.3 4D Flow Analysis

4D flow MRI data is aimed at providing objective evaluations of valvular disease severity for both aortic and mitral valves with exploratory evaluations of aortic wall shear stress in this patient population. 4D Flow image datasets will undergo pre-processing to execute corrections for Maxwell terms, eddy current-induced phase offset and velocity aliasing (when necessary) [2]. A 3D PC MR angiogram (MRA) will be generated as previously described[2-4]. This 3D PC MRA will be used to manually perform a 3D segmentation (Matlab, Mathworks, Natick, Massachusetts, USA) of the LV, RV, Left atrium and ascending aorta. The 4D flow MRI data set will be masked according to each of these 3D segmentations for final computational analysis. The masked time-resolved velocity field will be used to calculate velocity magnitude for all included voxels (i.e. $V_{mag} = \sqrt{V_x^2 + V_y^2 + V_z^2}$). Flow visualization will be performed using task-optimized local software (Ensight, CEI, Apex, North Carolina, USA). 4D flow outputs for the quantification of peak aortic valve pressure gradients, transvalvular pressure drop and regurgitant volume will be obtained. Exploratory analyses of wall shear stress of the ascending thoracic aorta will be obtained for comparison to CT-derived regional strain values.

4.4.4 Tissue Mapping Analysis

Tissue mapping analyses are aimed at providing objective insights into tissue health for the LV, this to allow for associations between observed strain values identified by CT-3D-MDA and MRI-based measures of ECV. Short-axis (SAX) pre and post-contrast T1 mapping data will be analyzed using a dedicated analysis module to obtain segmental measures of native T1 and ECV, according to the AHA segmental model. Segments with visible artifact crossing the myocardium will be excluded from analysis. For patients with both native and post-contrast T1 measurements, partition coefficient can be used as a surrogate marker of ECV, and is calculated as [5,6]:

$$\lambda = \frac{1/T_{1myo\_post} - 1/T_{1myo\_pre}}{1/T_{1blood\_post} - 1/T_{1blood\_pre}}$$

where T_{1myo_pre} and T_{1myo_post} are native and post-gadolinium measures of myocardial T1, respectively, and T_{1blood_pre} and T_{1blood_post} are native and post-gadolinium measures of T1 in the blood pool.

4.4.5 Sample Size

Given the unique and exploratory nature of this study no sample size calculations are provided (i.e. convenience sample of 20 patients).

4.5 STATISTICAL ANALYSIS

Standard statistical analytic techniques will be undertaken as appropriate for the different proposed analyses. Categorical variables will be presented as counts with percentages, while continuous variables will be expressed as means ± standard deviation or as median values with interquartile range depending on normality of distributions. Categorical variables will be compared using the Fisher's exact test, while comparisons for continuous data will be performed using 2-sample Student t test or Wilcoxon rank-sum test, where appropriate. Serial changes in strain parameters, 4D flow and tissue characteristics will be evaluated by ANOVA. All analyses will be performed using commercial statistical software (SPSS Statistics Version 24).

4.6 EXPECTED RESULTS AND SIGNIFICANCE

The primary objective of the study is to validate and compare multi-phase CT-derived 3D-MDA data and echo-derived 3D data to MRI-derived 3D-MDA (our reference standard technique). In

the case of CT and MRI, we will compare 3D-MDA-dervied assessments of LV, LA, RV and Aorta: these being those structures adequately visualized by both techniques. In the case of echocardiography, the comparison will be focused on the LV.

We expect that carrying this proposed project will allow us to achieve our proposed primary and secondary objectives. Validation of our work is essential in this patient population to be able to carry more extensive analysis and prognostication in the future using deep neural networks. We expect that there will be a good correlation between chamber specific CT derived principal strain when compared to echocardiography and MRI-derived strain measurements. The strength of this correlation is yet to be determined, but our prediction is it would be in strong agreement based on previous work done in this field[1]. Second, we expect that in our segmental analysis, we will find a correlation between MRI based markers such at T1 mapping and CT/Echo derived 3D-MDA. In a regional analysis of strain, we expect that segments with high T1 values will show a reduction in strain value. Previous work and clinical studies in the field of echocardiography revealed that strain imaging enabled the discrimination between myocardium with non-transmural (viable) and transmural scar tissue[7]. We expect that comparing CT-derived strain with MRI tissue markers will reveal a similar conclusion. This is powerful as it highlights the potential for CT derived strain imaging to be used for viability assessment. Thirdly, a 4D flow analysis combined with strain parameters obtained from LV, LA and aorta, will allow for a comprehensive hemodynamic analysis of this patient population. This may help elucidate new markers correlated with the outcome. The results of this analysis will be essential for our understanding of preload, afterload, and contractility in this patient population. Combined with the hemodynamic valve gradients, this will allow for investigating markers such as atrial-ventricular coupling and ventricular-arterial coupling. The potential applicating of those markers

in the clinical practice is large as it can be applied to different settings including the field of hypertension, heart failure, coronary artery disease and valvular heart disease.

4.7 REFERENCES

1. Satriano A, Heydari B, Narous M, et al. Clinical feasibility and validation of 3D principal strain analysis from cine MRI: comparison to 2D strain by MRI and 3D speckle tracking echocardiography. *Int J Cardiovasc Imaging.* 2017;33(12):1979-1992.
2. Markl M, Harloff A, Bley TA, et al. Time-resolved 3D MR velocity mapping at 3T: improved navigator-gated assessment of vascular anatomy and blood flow. *J Magn Reson Imaging.* 2007;25(4):824-831.
3. Garcia J, van der Palen RLF, Bollache E, et al. Distribution of blood flow velocity in the normal aorta: Effect of age and gender. *J Magn Reson Imaging.* 2018;47(2):487-498.
4. Garcia J, Barker AJ, Collins JD, Carr JC, Markl M. Volumetric quantification of absolute local normalized helicity in patients with bicuspid aortic valve and aortic dilatation. *Magn Reson Med.* 2017;78(2):689-701.
5. Salerno M, Janardhanan R, Jiji RS, et al. Comparison of methods for determining the partition coefficient of gadolinium in the myocardium using T1 mapping. *J Magn Reson Imaging.* 2013;38(1):217-224.
6. Diesbourg LD, Prato FS, Wisenberg G, et al. Quantification of myocardial blood flow and extracellular volumes using a bolus injection of Gd-DTPA: kinetic modeling in canine ischemic disease. *Magn Reson Med.* 1992;23(2):239-253.
7. Migrino RQ, Zhu X, Pajewski N, Brahmbhatt T, Hoffmann R, Zhao M. Assessment of segmental myocardial viability using regional 2-dimensional strain echocardiography. *J Am Soc Echocardiogr.* 2007;20(4):342-351.

Chapter 5: Future Prospective from a Cardiac Surgery Point of View

We have seen in this thesis the powerful use of multimodality imaging and the ability to provide cardiac surgeons and interventional cardiologists alike with both anatomical and functional assessment of patients undergoing TAVR. We have also seen the prognostic advantage that imaging can provide to patients undergoing revolutionary cardiac procedures. Technology will always be two steps ahead of us and therefore it is our responsibility to maintain strong knowledge of the diagnostic modalities and their interconnect to surgical use. Cardiac surgeons must stay at the forefront of technological advancement by actively participating in emerging new innovations and maintaining an ability to evolve with time as this field continues to change. It is clear from this thesis that the scope of practice in cardiac surgery has evolved because of the development of new surgical procedures, techniques, devices, and treatment options. As a result, a cardiac surgeon equipped with multi-modality imaging skills will become necessary to advance cardiovascular care in the future.

The medical field is witnessing an explosive expansion in the non-invasive and invasive technologies that can provide detailed information about the structure and function of the heart. A single scan produces an abundance of clinical and operational data which is becoming increasingly more complex as technology advances[1]. Often this big data is generated with countless, nonlinear associations that exceed the capability of conventional statistical methods. Although they are the gold standard in current research, this may not hold in the near future. Machine learning and artificial intelligence have emerged as a far more dynamic method. With larger datasets, a brain like neural network that can enable reasoning and interpretation can be

created[2]. This convention is based on the fact that there are larger datasets and the algorithm will use several layers of connection to analyze and interpret. These algorithms within deep learning are called conventional neural networks (CNN) that are widely used for numerous applications.

Cardiac surgery should be at the forefront of utilizing those neural networks as the stakes and risk of mortality is very high in our patient population and complications are not forgiving. A surgical patient should be thought of as several layers that encompass patient information, diagnostic workup, pharmacological interventions, and treatment plans. Future neural networks should be directed towards carefully selected tasks that align with the topics mentioned in this thesis. A mutually beneficial relationship needs to be built between surgeon and neural networks. One where surgeons can trust a neural network to provide the best surgical option for a patient, and surgeons provide the neural network with accumulated data and outcomes needed to learn to make accurate predictions and choices. We believe that multimodality cardiac imaging will be the segway to this neural network and play a very important role in guiding management of patients.

Cardiac surgery is moving away from the tradition operating room and the complexity of the procedure is requiring a hybrid OR. The use of hybrid OR is expected to grow with the evolution of technology. The increasing number of transcatheter based procedures and minimally invasive surgery will require more utilization of hybrid OR to accommodate its demand. For cardiac surgery to continue to flourish in the field of valvular heart disease, surgery needs to move to a less invasive method of delivery. Therefore, operating will become difficult to rely on visual assessment. Pre-operative image planning and intra-operative imaging guidance will be the

solution to many of the minimally invasive techniques in cardiac surgery today. Visualization, automation, and execution in a minimal number of surgical steps will be needed as part of the general workflow of a surgeon to be able to excel in the field of minimally invasive surgery.

REFERECE

1. Kharat AT, Singhal S. A peek into the future of radiology using big data applications. *Indian J Radiol Imaging.* 2017;27(2):241-248.
2. Liu D, Jia Z, Jin M, et al. Cardiac magnetic resonance image segmentation based on convolutional neural network. *Comput Methods Programs Biomed.* 2020;197:105755.

Appendix

Publishing License (Permission to Reuse Figures)

ELSEVIER LICENSE
TERMS AND CONDITIONS

May 26, 2022

This Agreement between Dr. Mohamad Rabbani ("You") and Elsevier ("Elsevier") consists of your license details and the terms and conditions provided by Elsevier and Copyright Clearance Center.

License Number	5316580183010
License date	May 26, 2022
Licensed Content Publisher	Elsevier
Licensed Content Publication	JACC: Cardiovascular Imaging
Licensed Content Title	Prognostic Value of LV Deformation Parameters Using 2D and 3D Speckle-Tracking Echocardiography in Asymptomatic Patients With Severe Aortic Stenosis and Preserved LV Ejection Fraction
Licensed Content Author	Yasufumi Nagata,Masaaki Takeuchi,Victor Chien-Chia Wu,Masaki Izumo,Kengo Suzuki,Kimi Sato,Yoshihiro Seo,Yoshihiro J. Akashi,Kazutaka Aonuma,Yutaka Otsuji
Licensed Content Date	Mar 1, 2015
Licensed Content Volume	8
Licensed Content Issue	3
Licensed Content Pages	11
Start Page	235
End Page	245
Type of Use	reuse in a thesis/dissertation
Portion	figures/tables/illustrations
Number of figures/tables/illustrations	1
Format	electronic
Are you the author of this Elsevier article?	No
Will you be translating?	No
Title	Feasibility and Clinical Value of 3-Dimensional Myocardial Deformation Analysis by Computed Tomography in Transcatheter Aortic Valve Replacement (TAVR) Patients
Institution name	Western University
Expected presentation date	Jun 2022
Portions	Fig 1
Requestor Location	Dr. Mohamad Rabbani [redacted]

SPRINGER NATURE LICENSE
TERMS AND CONDITIONS

May 26, 2022

This Agreement between Dr. Mohamad Rabbani ("You") and Springer Nature ("Springer Nature") consists of your license details and the terms and conditions provided by Springer Nature and Copyright Clearance Center.

License Number	5316560653788
License date	May 26, 2022
Licensed Content Publisher	Springer Nature
Licensed Content Publication	Current Cardiology Reports
Licensed Content Title	Role of Cardiac CT Before Transcatheter Aortic Valve Implantation (TAVI)
Licensed Content Author	Mohamed Marwan et al
Licensed Content Date	Jan 28, 2016
Type of Use	Thesis/Dissertation
Requestor type	academic/university or research institute
Format	electronic
Portion	figures/tables/illustrations
Number of figures/tables/illustrations	5
Will you be translating?	no
Circulation/distribution	1 - 29
Author of this Springer Nature content	no
Title	Feasibility and Clinical Value of 3-Dimensional Myocardial Deformation Analysis by Computed Tomography in Transcatheter Aortic Valve Replacement (TAVR) Patients
Institution name	Western University
Expected presentation date	Jun 2022
Portions	Fig. 1, Fig. 2, Fig. 3, Fig.5
Requestor Location	Dr. Mohamad Rabbani [redacted] [redacted] Attn: Dr. Mohamad Rabbani
Total	**0.00 USD**
Terms and Conditions	

Springer Nature Customer Service Centre GmbH
Terms and Conditions

BMJ PUBLISHING GROUP LTD. LICENSE TERMS AND CONDITIONS

May 26, 2022

This Agreement between Dr. Mohamad Rabbani ("You") and BMJ Publishing Group Ltd. ("BMJ Publishing Group Ltd.") consists of your license details and the terms and conditions provided by BMJ Publishing Group Ltd. and Copyright Clearance Center.

License Number	5316550759202
License date	May 26, 2022
Licensed Content Publisher	BMJ Publishing Group Ltd.
Licensed Content Publication	Heart
Licensed Content Title	Transcatheter aortic valve implantation: the procedure
Licensed Content Author	Stefan Stortecky,Lutz Buellesfeld,Peter Wenaweser,Stephan Windecker
Licensed Content Date	Nov 1, 2012
Licensed Content Volume	98
Licensed Content Issue	Suppl 4
Type of Use	Dissertation/Thesis
Requestor type	Individual Account
Format	Electronic
Portion	Figure/table/extract
Number of figure/table/extracts	1
Descriptionof figure/table/extracts	Figure 1 Treatment selection algorithm for patients with symptomatic, severe aortic stenosis.
Will you be translating?	No
Circulation/distribution	1
Title	Feasibility and Clinical Value of 3-Dimensional Myocardial Deformation Analysis by Computed Tomography in Transcatheter Aortic Valve Replacement (TAVR) Patients
Institution name	Western University
Expected presentation date	Jun 2022
Portions	Figure 1 Treatment selection algorithm for patients with symptomatic, severe aortic stenosis.
Requestor Location	Dr. Mohamad Rabbani [redacted] [redacted] Attn: Dr. Mohamad Rabbani
Publisher Tax ID	GB674738491
Total	**0.00 CAD**

Curriculum Vitae

Mohamad Rabbani, M.D., C.M.

Education and Training

Institution	Description	Start—End
Western University	Cardiac Surgery Residency	2019-2025 (Expected)
Western University	Master in Surgery	2021-2022 (Expected)
McGill University	Doctor of Medicine	2015-2019
McGill University	Honours in Physiology	2011-2015

Related Experience

Title	Dept./ Supervisor	Description	Start—End
Cardiac Magnetic Resonance Study	Department of Cardiology McGill University (Montreal, QC) Dr. Matthias Friedrich	This project focused on the use of strain analysis in CMR imaging as a method for the detection of coronary artery disease. It also focused on the use of non-invasive voluntary breathing maneuvers instead of the use of pharmacologic vasoactive drugs.	2016- 2019
Pulmonary Thromboendarterectomy Study	Department of Cardiac Surgery McGill University (Montreal, QC) Dr. Jean-Francois Morin	This study looked at the operative and functional outcomes of patients after pulmonary endarterectomy procedure. It also looked at the quantity of excised obstructive tissue and correlation to CT-image prediction.	2018-2019

Related Publications

Published Refereed Papers

Mohamad Rabbani, Jonathan Kanevsky, Kamran Kafi, Florent Chandelier, Francis J. Giles. *Role of artificial intelligence in the care of patients with non-small cell lung cancer.* European journal of clinical investigation. 2018;48(4).

Conference Abstracts/ Poster Presentation

Mohamad Rabbani, Elizabeth Hillier, Kady Fischer, Giulia Vinco, Matthias G. Friedrich. *CMR Analysis During Breathing Maneuvers for the Detection of Single Vessel Coronary Artery Disease.* Cardiac Magnetic Resonance Imaging 2018 Conference, Barcelona, Spain.